Universidad Autónoma de San Luis Potosí

Facultad de Ingeniería

Centro de Investigación y Estudios de Posgrado

CONCEPTUALIZATION AND DESIGN OF A FORMULA-STYLE RACING CAR FOR FSAE

THESIS

Submitted for the degree of:

MAESTRO EN INGENIERÍA MECÁNICA

Presented by:

ING. JUAN JAIME CARMONA RAMÍREZ

Advisor:

DR. HUGO IVÁN MEDELLÍN CASTILLO

San Luis Potosí, S.L.P. August 2025

UASLP
Universidad Autónoma de San Luis Potosí
FACULTAD DE INGENIERÍA

20 de marzo de 2025

ING. JUAN JAIME CARMONA RAMÍREZ
P R E S E N T E.

En atención a su solicitud de Temario, presentada por el **Dr. Hugo Iván Medellín Castillo**, Asesor de la Tesis que desarrollará Usted, con el objeto de obtener el Grado de **Maestro en Ingeniería Mecánica**. Me es grato comunicarle que en la sesión del H. Consejo Técnico Consultivo celebrada el día 20 de marzo del presente, fue aprobado el Temario propuesto:

TEMARIO:

"Conceptualización y diseño de un vehículo de carreras estilo fórmula para FSAE"

Introducción.
1. Automovilismo y la competencia de la Formula SAE.
2. Modelo para la simulación inicial de la dinámica del vehículo.
3. Desarrollo conceptual del vehículo de carreras.
4. Diseño a nivel sistema del vehículo de carreras.
5. Diseño a detalle del vehículo de carreras.
6. Simulación final y pruebas del vehículo de carreras.

Conclusión.
Referencias.
Apéndice.

"MODOS ET CUNCTARUM RERUM MENSURAS AUDEBO"

A T E N T A M E N T E

UNIVERSIDAD AUTONOMA DE SAN LUIS POTOSI FACULTAD DE INGENIERIA DIRECCION

DR. EMILIO JORGE GONZÁLEZ GALVÁN
DIRECTOR

Copia. Archivo
*etn.

www.uaslp.mx

Av. Manuel Nava 8
Zona Universitaria • CP 78290
San Luis Potosí, S.L.P.
tel. (444) 826 2330 al 39
fax (444) 826 2336

UASLP Universidad Autónoma de San Luis Potosí | FACULTAD DE INGENIERÍA | CENTRO DE INVESTIGACIÓN Y ESTUDIOS DE POSGRADO

UNIVERSIDAD AUTÓNOMA DE SAN LUIS POTOSÍ
FACULTAD DE INGENIERÍA
Área de Investigación y Estudios de Posgrado

D E C L A R A C I Ó N

El presente trabajo que lleva por título:

Conceptualización y diseño de un vehículo de carreras estilo fórmula para FSAE

se realizó en el periodo 02 de 2023 a 08 de 2025 bajo la dirección del Dr. Hugo Iván Medellín Castillo

Originalidad

Por este medio aseguro que he realizado el trabajo reportado, y la escritura de este documento de tesis para fines académicos sin ayuda indebida de terceros y sin utilizar otros medios más que los indicados.

Las referencias e información tomadas directa o indirectamente de otras fuentes se han definido en el texto como tales y se ha dado el debido crédito a las mismas.

El autor exime a la UASLP de las opiniones vertidas en este trabajo escrito y asume la responsabilidad total del mismo.

Este trabajo no ha sido sometido como tesis o trabajo terminal a ninguna otra institución nacional o internacional en forma parcial o total, exceptuando el caso cuando existe un convenio específico de doble titulación celebrado entre ambas instituciones.

Se autoriza a la UASLP para que divulgue este documento para fines académicos.

El autor del trabajo escrito,
Juan Jaime Carmona Ramírez

Abstract

On a global scale, the automotive industry demands prominent levels of scientific and technological innovation as well as development to achieve safer, more efficient and more compliant with environmental regulations. To promote innovation and development, the Society of Automotive Engineers (SAE) organizes the Formula SAE competition, which is an automotive design competition with a focus on formula-type racing cars. Every university or institute willing to participate must develop a competition vehicle that meets the guidelines defined by the Formula SAE coordinators. Since their origins back in the eighties to actuality, the Formula SAE competition has expanded. Nowadays, in many countries such as Germany, Italy, Japan or Mexico hold annual competitions in a similar fashion of the Formula SAE format and under the label of Formula Student or even other denominations with supervision of the Formula World Council.

This thesis project covers the conceptual design and the detailed design of a race car in compliance with the requirements and guidelines emitted by the Formula SAE organizers. The main objective is to develop the first Formula SAE race car for UASLP (Autonomous University of San Luis Potosi) that can be used as a platform for innovation and continuous improvement in the future, as well as the debut of the university in these student competitions. To achieve this, the thesis project is set to formulate the vehicle´s engineering to guarantee a high performance on track.

The race car evolved within a structured process in this thesis project, which is marked with a design process that starts with the establishment of the design requirements by means of an initial dynamic simulation of the vehicle and the recognition of the current Formula SAE rules in effect. Based on those design requirements, the next step in the design process is the conceptual design phase, the configuration design phase and the detailed design phase. At the end of the phase of detailed design and in order to determine the performance of the designed race car, a set of final simulations of the complete race car are executed. Finally, the designed vehicle is presented with the list of materials and relevant manufacturing drawings.

Resumen

La industria automotriz a nivel global demanda altos niveles de desarrollo e innovación científica y tecnológica para lograr vehículos automotores eficientes, seguros y amigables con el medio ambiente. Para promover la innovación y desarrollo automotriz, la Sociedad de Ingenieros Automotrices (SAE, por sus siglas en inglés), organiza la Fórmula SAE, la cual es una competencia de diseño automotriz de vehículos de carreras tipo fórmula. Cada universidad o institución participante debe desarrollar un vehículo de competencia de acuerdo con los lineamientos definidos por la Fórmula SAE. Desde sus orígenes en la década de los ochenta a la fecha, la Fórmula SAE se ha expandido. En la actualidad, se desarrollan a nivel internacional competencias de Fórmula Student en países como Estados Unidos, Alemania, Japón y Austria bajo la organización de la SAE International y otras competencias similares bajo la supervisión del Formula World Council.

El presente proyecto de tesis comprende el diseño conceptual y el diseño de detalle de un vehículo de carreras en base al cumplimiento de los requisitos y lineamientos definidos por la Fórmula SAE. El objetivo es desarrollar un primer vehículo Fórmula SAE que sirva como plataforma para la mejora e innovación continua a lo largo de los años, así como la participación de la UASLP en estas competencias estudiantiles. Para lograr lo anterior, se desarrollará toda la ingeniería del vehículo que garantice un alto desempeño en las pistas de carreras.

En el presente proyecto de tesis, el desarrollo del vehículo de carreras se estructura a partir de un proceso de diseño que comienza con la definición de los requerimientos de diseño mediante un modelo de simulación dinámica del vehículo de carreras y los lineamientos definidos por la Fórmula SAE. Con base a los requerimientos de diseño definidos, se continúa con las fases de diseño conceptual, diseño de configuración y diseño a detalle. Al término de la fase de diseño a detalle, se realiza una serie de simulaciones al vehículo de carreras para predecir el rendimiento del vehículo en los eventos de la competencia. Finalmente, se presenta la lista de materiales, así como los planos de fabricación del vehículo diseñado.

Acknowledgements

I would like to express my deepest gratitude to all those who supported and motivated me throughout the course of my academic lectures, my research and the writing of this thesis.

First and foremost, I am profoundly grateful to my advisor, Dr. Hugo Iván Medellín Castillo, for his invaluable guidance, professional advice and constant encouragement throughout this project. His expertise, insight and patience were instrumental in shaping the direction and quality of this work.

I would also like to thank the members of my thesis committee, Dr. Gilberto Mejía Rodríguez, Dr. Juan Carlos Arellano González and Dr. Emilio Jorge González Galván, for their constructive feedback, time invested and thoughtful suggestions that helped the clarity and depth of my research.

My sincere thanks to all my colleagues and fellow researchers for the collaboration and camaraderie that made this journey enjoyable, to the Mechanical Engineering program coordinator M.Sc. José Adrián Chiquito Cruz for his trust, as well as the academic and professional opportunities he made available to me throughout the development of this work, and to the administrative staff at UASLP for their logistical and technical support.

On a personal note, I am forever grateful and indebted to my family, my friends and my girlfriend for their unwavering support. To my parents, Mrs. María del Rosario and Mr. Juan Manuel, thank you for your unconditional love and belief in me. Once again, thank you for your patience and understanding, specially during the most challenging times.

Table of contents

Abstract III
Resumen IV
Acknowledgements V
Table of contents VI
List of figures VIII
List of tables X
Nomenclature XII
Symbols XII
Abbreviations XIV
Introduction 1
Problem statement 2
General objective 2
Specific objectives 3
Structure of the thesis 3
Chapter 1: Motor racing and the Formula SAE competition 4
1.1. Formula SAE competition 4
1.2. Automotive design 6
1.3. Design specifications of the racing car 10
Chapter 2: Model for initial vehicle dynamics simulation 14
2.1. Dynamic model of a vehicle 14
2.2. Preliminary calculations 17
2.3. Linear acceleration of the racing car 18
2.4. Vehicle behavior in curved segments 22
2.5. Model and validation for the IVDS 24
Chapter 3: Conceptual development of the racing car 28
3.1. Functional requirements 28
3.2. Selection of key components for IVDS 30
3.3. Criteria for the generation and evaluation of conceptual alternatives 37
3.4. Analysis of conceptual alternatives 47
Chapter 4: System-level design of the racing car 55
4.1. Architecture of the racing car 55

4.2. Material selection 57
4.3. Configuration of parts and systems for the racing car 60
Chapter 5: Detail design of the racing car 103
5.1. Technical specifications and documentation 103
5.2. Numerical simulations 104
Chapter 6: Final simulation and testing of the racing car 114
6.1. Simscape vehicle virtual prototype model 114
6.2. Vehicle virtual prototype simulation 120
Conclusion 122
Contributions of the study 123
Future work 123
References 124
Appendix A 129
Appendix B 130
Appendix C 131

List of figures

Figure 1.1. Acceleration event test course layout and dimensions....5
Figure 1.2. Skidpad event test course layout, guidance and dimensions. 6
Figure 1.3. Proposed design methodology for the formula-style racing car. 7
Figure 1.4. QFD for the design of the formula-style racing car. 11
Figure 2.1. Technical design dimensions of the vehicle in (a) the top view and (b) the rear view.15
Figure 2.2. Longitudinal mass distribution for the vehicle (a) in static conditions and (b) under acceleration....20
Figure 2.3. Lateral view of the vehicle in ascent of a slope. 21
Figure 2.4. Top view of the vehicle while taking a corner. 22
Figure 2.5. Rear view of the vehicle (a) in static conditions and (b) taking a corner. 24
Figure 2.6. ICE performance curves for the engine associated with the RC. 25
Figure 2.7. RC data plot for (a) vehicle performance curves and (b) engine frequency against vehicle speed. 25
Figure 2.8. IVDS results of the acceleration event in relation to elapsed time for (a) speed, (b) longitudinal acceleration, (c) gear shifted and (d) displacement. 26
Figure 2.9. IVDS results of skidpad event in relation to elapsed time for (a) speed, (b) lateral acceleration, (c) gear shifted and (d) displacement....27
Figure 3.1. Wheel rim geometry and dimensional parameters. 36
Figure 3.2. Driver template positioned in relation to front bulkhead and roll hoops....44
Figure 3.3. Quarter car SMD system model....50
Figure 3.4. Braking forces and parameters of the racing car....52
Figure 3.5. Conceptual chassis geometry for the racing car....53
Figure 4.1. Module breakdown structure diagram for the formula-style racing car. 56
Figure 4.2. Sketch interaction diagram for the formula-style racing car....57
Figure 4.3. Standard roller chain for the powertrain of the racing car. 61
Figure 4.4. Geometry of the aftermarket LSD. 63
Figure 4.5. Wheel stud and lug nut clamping wheel hub and wheel rim. 71
Figure 4.6. Geometry of the wheel hub....73
Figure 4.7. Side view of the wheel assembly and knuckle dimensions. 77
Figure 4.8. Air intake sequence for naturally aspirated ICE for the racing car. 78
Figure 4.9. Block diagram for the electrical cluster of the racing car. 87
Figure 4.10. Front view of the suspension geometry for the (a) front axle and (b) rear axle. 89
Figure 4.11. Side view of the suspension mounting points for the (a) rear axle and the (b) front axle. 90
Figure 4.12. Mesh convergence study for the conceptual chassis geometry....98
Figure 4.13. FEA of the conceptual chassis geometry submitted to longitudinal torsion....99
Figure 4.14. Relative vehicle stiffness as a function of chassis stiffness. 100
Figure 5.1. Numerical simulation methodology flowchart. 104
Figure 5.2. Mesh convergence study results for the CFD simulation of the nosecone. 106
Figure 5.3. Results of the CFD simulation of the nosecone for (a) pressure distribution and (b) velocity field....106

Figure 5.4. Mesh convergence study results for the FEA simulation of the wheel hub. 108
Figure 5.5. Results of FEA simulation of the wheel hub for (a) equivalent stress and (b) fatigue safety factor. 108
Figure 5.6. Mesh convergence study results for the FEA simulation of the wheel knuckle. 109
Figure 5.7. Results of FEA simulation of the wheel knuckle for (a) equivalent stress and (b) fatigue life...110
Figure 5.8. Mesh convergence study results for the FEA simulation of the chassis and suspension. 112
Figure 5.9. Results of FEA longitudinal torsion simulation of chassis and suspension for (a) combined stress and (b) total displacement..112
Figure 5.10. Results of FEA acceleration test simulation of chassis and suspension for (a) combined stress and (b) total displacement. 112
Figure 5.11. Results of FEA cornering test simulation of chassis and suspension for (a) combined stress and (b) total displacement. 113
Figure 6.1. Engine model subsystem at Simscape. 115
Figure 6.2. Powertrain model at Simscape for (a) gearshift control unit and (b) powertrain unit. 116
Figure 6.3. Vehicle model subsystem at Simscape...118
Figure 6.4. Results of Simscape simulation for (a) acceleration test and (b) acceleration and braking test. 120

List of tables

Table 1.1. Static and dynamic events of the Formula SAE events [8]. 5
Table 1.2. Comparison of race cars participating in Formula SAE competitions and spin-offs [7], [9]. 8
Table 1.3. Key performance indicators for the race car vehicle. 8
Table 1.4. Systems and components of the formula-style racing car. 9
Table 1.5. Design specifications for the formula-style racing car. 12
Table 2.1. Results comparation and approximation error of the RC. 27
Table 3.1. Usage-disposure method for the formula-style racing car. 29
Table 3.2. FBM method for the formula-style racing car. 30
Table 3.3. Rating scale for the WREM for the selection process. 31
Table 3.4. Alternatives for the ICE and transmission group selection. 31
Table 3.5. Analysis parameters for the ICE and transmission group selection. 32
Table 3.6. WREM for the ICE and transmission group selection. 33
Table 3.7. Technical specification data for the ICE and transmission group for the formula-style racing car. 33
Table 3.8. Alternatives for tire selection of the formula-style racing car. 34
Table 3.9. WREM for the tire selection. 35
Table 3.10. Alternatives for wheel rim selection of the formula-style racing car. 35
Table 3.11. WREM for the wheel rim selection. 36
Table 3.12. Conceptual alternatives for the power transmission cluster. 38
Table 3.13. Technical data of the ICE systems from the KNZ. 39
Table 3.14. Conceptual alternatives for the ICE systems cluster. 40
Table 3.15. Technical data of the electrical system from the KNZ. 40
Table 3.16. Sensor scrutiny for the electrical cluster of the formula-style racing car. 41
Table 3.17. Conceptual alternatives for the electrical cluster. 41
Table 3.18. Conceptual alternatives for the dynamic control cluster. 43
Table 3.19. Conceptual alternatives for the enclosure cluster. 46
Table 3.20. Criteria for evaluation for conceptual alternatives of the formula-style racing car. 47
Table 4.1. Criteria for evaluation for material selection of the special-purpose parts for the racing car. 58
Table 4.2. Boundary and continuity conditions for LSD slope and deflection analysis. 65
Table 4.3. Results of the analysis of available torque at the tires of the racing car. 68
Table 4.4.Wheel assembly loads under critical conditions. 69
Table 4.5. Results of the fatigue analysis of the geometry of the wheel hub. 76
Table 4.6. Alternatives for radiator selection for the cooling system. 83
Table 4.7. Technical specification of the shutdown circuit switches. 85
Table 4.8. Results of the FEA for the conceptual chassis geometry. 99
Table 5.1. Simulation data for the CFD analysis of the nosecone. 105
Table 5.2. Simulation data for the FEA of the wheel hub. 107
Table 5.3. Simulation data for the FEA of the wheel knuckle. 109
Table 5.4. Simulation data for the FEA of the chassis and suspension. 111

Table 6.1. Engine model subsystem simulation parameters..115
Table 6.2. Powertrain model subsystem simulation parameters. 117
Table 6.3. Vehicle model subsystem simulation parameters. 119
Table 6.4. Acceleration event simulation results benchmark. 121

Nomenclature

Symbols

A	Area, dimensional parameter.
a	Acceleration, aerodynamic, axial, allowable, application, alternating, air.
B	Dimensional parameter.
BFD	Brake force distribution.
b	Braking parameter, Weibull parameter, length.
C	Center-to-center distance, coefficient, dimensional parameter, viscous damping, index.
CCA	Cold cranking amps.
c	Centripetal, curvature, viscous damping, speed of sound.
cg	Center of gravity.
cr	Compression ratio.
D	Diameter, dimensional parameter.
d	Diameter, drag, driven, design, length.
dl	Percentage location of the driver´s mass relative to the wheelbase.
dm	Driver´s mass.
E	Modulus of elasticity, energy, engine, dimensional parameter.
e	Engine, external, effective.
F	Force.
f	Frontal axle of the vehicle, factor, fatigue, frequency.
$fvsa$	Front view swing arm.
g	Gravity acceleration, grip.
H	Horsepower, height.
h	Height, hydraulic.
I	Moment of inertia, current.
i	Index, input, instantaneous, interval.
K	Spring rate, factor, coefficient.
k	Marin endurance limit modifying factors, spring rate, factor, coefficient, kingpin, kinetic.
L	Length, longitudinal dimension, life.
LT	Load transfer.
l	Length, lift, limit.
lat	Lateral.
$long$	Longitudinal.
M	Bending moment.
m	Mass, midrange, mounting.
md	Mass distribution.
mr	Motion ratio.
N	Number.
NCV	Net calorific value.

n	Number, factor of safety, nominal.
o	Output, offset.
P	Mechanical power, load.
p	Pitch, pressure, percentage.
Q	Heat, flow rate.
q	Notch sensitivity.
R	Ratio, reaction force, reliability, resistance.
r	Radius, resistance, rear axle of the vehicle, rim, rolling, length.
S	Strength.
s	Service, shear, steering.
spl	Sound pressure level.
sr	Scrub radius.
$svsa$	Side view swing arm.
T	Torque.
t	Tangential, thrust, time, traction, tabulated, thickness, travel, length.
tw	Track width.
tcr	Average tire compression ratio.
tmd	Total mass distribution.
U	Overall heat transfer coefficient.
V	Volume, shear force, voltage.
v	Linear velocity, vehicle, vertical, von Mises.
W	Wheel, weight.
w	Wheel.
wb	Wheelbase.
x	Coordinate, variable, Weibull parameter.
y	Coordinate, variable, deflection, yield.
Z	Gear number of teeth.
α	Angular acceleration, angle.
β	Coefficient, angle.
Δ	Change, displacement.
ζ	Damping ratio.
η	Efficiency.
θ	Weibull parameter, angle.
λ	Slenderness ratio.
μ	Friction coefficient.
ρ	Density, resistivity.
σ	Normal stress.
τ	Shear stress.
ω	Angular speed, circular frequency.

Abbreviations

AC	Alternative current.
BOTS	Brake overtravel switch.
CAD	Computer-aided design.
CFD	Computational fluid dynamics.
DNA	Does not apply.
DNF	Do not finished.
ECU	Engine control unit.
FEA	Finite element analysis.
FBM	Function-behavior and function-structure matrix.
FSAE	Formula SAE.
ICE	Internal combustion engine.
IVDS	Initial vehicle dynamics simulation.
KPI	Key performance indicator.
LSD	Limited slip differential.
MBS	Module breakdown structure.
NHV	Noise, harshness and vibration
QFD	Quality function deployment.
RC	Code for race car as reference.
RON	Research octane number.
rpm	Revolutions per minute.
RWD	Rear wheel drive.
SAE	Society of Automotive Engineers
SMD	Spring-mass-damper.
TPS	Throttle position sensor.
UARM	Uniformly accelerated rectilinear motion.
WREM	Weighted rating evaluation matrix.

Introduction

In the current context, the automotive industry represents one of the most critical sectors in the global economy and it keeps adapting to meet the growing demand for transportation at different levels worldwide. The automotive production statistics show a consistent enhance year by year at many countries, most of them being part of the main countries at automotive production. As a reference, the International Organization of Motor Vehicles Manufacturers (OICA) places Mexico on the list of countries with a higher volume of production. Mexico is near a production of 3.5 million units of commercial vehicles and had over a 14% of incremental production when compared to the previous year considering the 2023 statistics [1].

In response to the demands requested by the national and international laws and standards, as well as the achievement of specific objectives of some of the automotive sector enterprises, at this time most of the research and technological improvements that revolve around the automobile are centered on the efficiency, security and sustainability of these vehicles. This in turn presents a challenge for the refinement of vehicles both in terms of design and manufacturing, in addition to the imperatives for the automotive sector to create, enhance or expand the research and development departments with highly qualified personnel. Based on the need for highly qualified personnel to approach the automotive industry, there must be a relationship and communication between students and these innovative departments. One way to establish a relationship is through student design and manufacture competitions.

There are some aspects that are already covered massively in relation to vehicles, both commercial and for competence. Nevertheless, there are still opportunity areas to refine existing ideas, suggest new ideas and bring solutions to different issues. As demonstrated by Mayyas et al. [2], although models have been proposed for analyzing the sustainability of commercial vehicle production, much of the vehicle manufacturing still relies on processes developed in the early 20th century. This represents a significative incentive for contemporary engineers to idealize, test and incorporate new strategies and technologies at automotive industry service.

To establish a fluid sequence between the academic phase and the experience of working at the automotive industry, the student design and manufacturing competitions are currently an important opportunity for students to enhance skills, test ideas and get involved in many tasks related to the automotive sector. A recent study by Gadola and Chindamo states that student design and manufacturing competitions offer to the participants a platform for learning and experimentation at solving real life problems by means of a creative, smart and innovative exercise [3]. Of course, this activity implies establishing an automobile or motorsport club to advance in the tasks that are required to compete with and must imply collaborative experience among the participants. As stated by Abhinav and Prasad, a university motorsport club significantly impacts in the students [4]. This is because of the participation and presentation of the students in the competition implies a great team of designers, manufacturers, managers and leaders. Likewise, an automobile club represents an important contribution for the university or institution that host the club because of all that the club can suppose for the students that decide to get involved in its activities.

On the other hand, focusing engineering knowledge into an application niche represents quite a challenge for universities and industries in many aspects. The case of motorsport is not exempted from this. As demonstrated by Hylton and Russomanno [5], the objective of the study programs for university education is to prepare students with the necessary skills and knowledge to find a place and sustain a professional career in the industry that closely matches their field of study. Considering this, developing and incorporating projects related to topic of interest is supposed as a timely activity to relate the students with the automotive application niche.

Problem statement

Considering the contribution and benefits that establishing a motorsport club can suppose for a university, the UASLP has expressed interest in participating in the Formula SAE competition. As referred by Ulrich and Eppinger [6], the design of a race car is governed by the design process passing through the planning phase, conceptual development, system-level design, detail design and the testing and refinement phase; although for the purpose of this thesis project the design process is limited excluding the testing and refinement phase. Following this, the design of the race car goes through the design process phases in a sequential manner.

As mentioned previously in this section, the vehicle must adjust to a series of constraints and guidelines delivered by the Formula SAE organizers. However, the designer must define the problem statement through technical specifications that can be used as a basis for other phases of the design process. Both guidelines and technical specifications must be listed in a clear and concise manner.

On the other hand, when consulting previous works in the literature related to racing cars for student competitions, it is possible to observe that there are only a few studies that are centered in the vehicle as a system and that, with that focus on mind, attend to design the vehicle within the main system and the subsystems concurrently. A vast majority of the race cars presented in the literature are subjected only to be compliant with the guidelines that the current Formula Student rules in effect state for.

For all of the above reasons, an opportunity to design a formula-style racing car for FSAE as a system is identified. The design of the racing car must take into account all the possible data that may serve as a basis for the decision-making process across the product development. For instance, defining a starting point for the design of the racing car is highlighted as one crucial step in order to achieve high performance.

General objective

This thesis project covers the conceptual design and the detailed design of a race car in compliance with the requirements and guidelines emitted by the Formula SAE organizers. The main objective is to develop a Formula SAE racing car that can be used as a platform for innovation and continuous improvement in the future. To achieve this, the project is set to formulate the vehicle´s engineering to guarantee a high performance on track.

Specific objectives

- Discern the status of the automotive industry in relation to competitive vehicles and specifically formula-style racing cars for FSAE.
- Discern the requirements and guidelines emitted by the organizers of the events related to the Formula SAE competition.
- Formulate and apply a model for initial vehicle dynamics simulation of the formula-style racing car for FSAE.
- Conceptualize the formula-style racing car for FSAE.
- Develop the detailed engineering of the formula-style racing car for FSAE.
- Simulate and evaluate the performance of the formula-style racing car for FSAE.

By achieving the specific objectives listed above, it is assumed that the general objective of this thesis project will be satisfied.

Structure of the thesis

The rest of the thesis is structured as follows. In Chapter one the theoretical framework is presented together with the establishment of the first pair of specific objectives listed above. The theoretical framework embraces the Formula SAE competition, the fundamental concepts regarding automotive design, the state of the art of the reported works in the literature related to systems and components of the race car, the requirements and guidelines emitted in the current Formula SAE in effect, in addition to the design specifications for the race car. Chapter two provides the formulation of the model for initial vehicle dynamics simulation (IVDS). The model initiates with the physical principles that act on the vehicle and that are considered in the limits defined by the initial approximation of vehicle dynamics. To model a vehicle, a set of parameters are defined inside the IVDS model. Later, the IVDS model algorithm is presented in addition to the results of simulation ability. Finally, for model validation a set of data corresponding to a reference race car is used with the IVDS model and the results of this simulation are compared towards the results of the reference race car in a Formula Student specific participation. In Chapter three the conceptualization of the formula-style racing car for FSAE is developed. Chapter four aims to advance the formula-style racing car design with the configurative design phase. In Chapter five the detailed engineering of the formula-style racing car for FSAE is presented. Finally, Chapter six conveys the performance of the designed vehicle with the results of final simulations for the formula-style racing car for FSAE.

Chapter 1: Motor racing and the Formula SAE competition

This chapter introduces the fundamental concepts related to the Formula SAE competition, the components that integrate a race car vehicle subjected to the guidelines of the organizers, in addition to the related works, in particular, the design of competition vehicles that are reported in the literature. Moreover, a resume of the labor of apprehending the requirements and guidelines demanded by the organizers of the Formula SAE competition for any racing car, which is willing to compete in the events of the student contest.

1.1. Formula SAE competition

The main student competition related to automotive design and manufacture on a global scale is Formula SAE, or Formula Student for general labeling around the world. The Formula SAE competition is organized by SAE International and started in the early decade of 1980 when Ron Mathews, assistant professor at the University of Texas, set in motion the student branch of SAE. Soon after this, Mathews and other officers decided to participate in a SAE competition related to asphalt racing. Even though this early SAE competition did not happen, the idea was conceived, and it was only a matter of time for an asphalt racing contest to take place. Under the label of Formula SAE, coined by Mathews and approved by SAE, a new competition with a new set of rules emerged. In the current time, the Formula SAE competition continues to expand not only in United States, but also in many countries around the world in the form of spin-off events. The expansion of Formula Student brand reaches over twenty competitions currently hosted by engineering societies or private businesses [7].

SAE International established that Formula SAE competitions represent a challenge for the teams formed by undergraduate and graduate students to conceive, design, manufacture, develop and compete with formula-style scaled vehicles. Even though it is considered as a multidisciplinary challenge, the Formula SAE competition is still an engineering education contest that requires a performance demonstration of vehicles designed in a series of tests, both on track and out of track with a certain number of chances and time available. Based on the information of SAE International, every competition provides the teams with the opportunity to demonstrate their creativity, and the engineering skills compared to other teams of other universities around the world.

To participate in the Formula SAE events it is necessary to adjust the design into a series of constraints, parameters and regulations provided by SAE International [8]. Nevertheless, the competition encourages and invites participants to enhance their vehicle with creative and innovative suggestions. Consequently, vehicle design at the contest becomes a challenge in order to remain within the limits of the regulations, achieve the best performance in the events and adequately document the development of the design and manufacture stages.

As established by the Formula SAE guidelines [8], the competition is qualified based on the participation in static and dynamic events. Static events and the score are indicated in Table 1.1. At the static events of the competition, the race car only participates and a project in which the design, costs and manufacture of the vehicle will be assessed along with an executive presentation by the coordinators of the events.

On the other hand, dynamic events involve the participation of a manufactured prototype of the designed vehicle in two different stages: inspection and initial tests stage and track testing stage. At the inspection and initial tests stage, it is mandatory to complete a set of scrutiny and related activities that accredit the vehicle as eligible to participate in the next stage. Later, the vehicles are prepared by the teams for the track testing stage, in which the race car and a collective of licensed drivers from the teams take part in the acceleration, skidpad, endurance, efficiency and autocross events. These events have their own protocol and the score for these is listed at Table 1.1.

Table 1.1. Static and dynamic events of the Formula SAE events [8].

Static events		**Dynamic events**	
Cost event	100 points	Acceleration event	100 points
Design event	150 points	Skidpad event	75 points
Presentation	75 points	Endurance event	275 points
		Efficiency event	100 points
		Autocross event	125 points
Subtotal	325 points	**Subtotal**	675 points
Total		1000 points	

Within the dynamic events in which eligible race cars participate in the Formula SAE competition, there are two specific events that can be considered as standardized events because the protocols apply for all Formula SAE events and spin-off competitions. Those are acceleration and skidpad events, which remain with no track relevant modification among the protocol from edition year by year.

1.1.1. Acceleration event

The acceleration event of the Formula SAE competition consists of a straight-line path. The event protocol is the same every year for each competition or spin-offs. Due to this, this event is considered as a standard event for this student contest. The acceleration event aims to evaluate the vehicle´s acceleration performance for the participant single seaters along a flat road surface or at least very close to being flat. The acceleration event test course layout is illustrated in Figure 1.1.

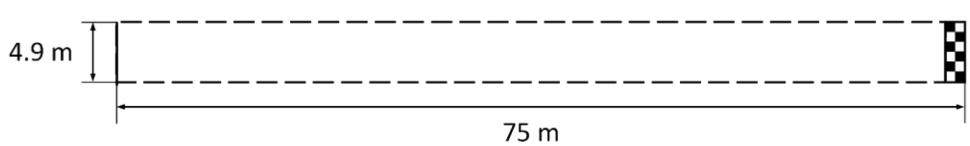

Figure 1.1. Acceleration event test course layout and dimensions.

As a standard and based on the Formula SAE regulations [8], the track layout for the acceleration event must have a distance of 75 m in a straight-line path from the starting line until the finish line set for the test. Additionally, the test course layout must have a minimum width of 4.9 m, this is based on the inner edges of the base of the cones used for track limits at the zone where the dynamic events take place. These cones are placed along the edges of the track at intervals of 6 m within the width of the course.

1.1.2. Skidpad event

The skidpad event of the Formula SAE competition consists of a course that includes turns to the right and to the left forming an eight track from a top view. The event protocol is the same every year for each competition or spin-offs. Due to this, this event is considered as a standard event for this student contest. The skidpad event aims to evaluate the ability of the participant single seaters to turn and handle in corners. The skidpad event test course layout is illustrated in Figure 1.2.

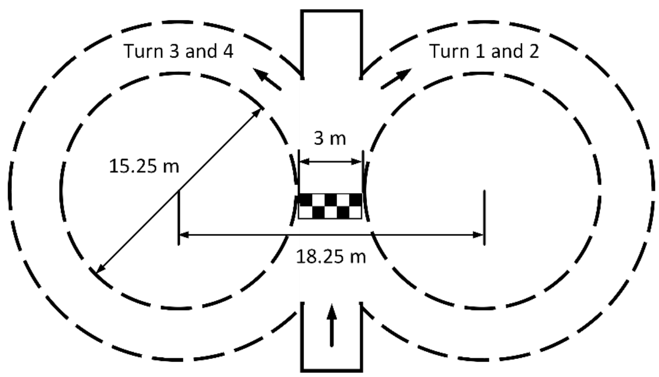

Figure 1.2. Skidpad event test course layout, guidance and dimensions.

As a standard, and based on the Formula SAE regulations [8], the design of the track for the skidpad event corresponds to a pair of arc segments that intersect in a tangent point in order to permit the access of the vehicles driving by a straight-line, which extends to provide an exit line form the track. The form is like an eight track with a line that sections the eight forms by the center. To establish the course of the skidpad event, an arrange of cones are placed forming two circumferences with a 15.25 m diameter and with a distance between centers of 18.25 m. Subsequently, an arrangement of cones forms concentric arc segments from the center of the previous circumferences in a way that the inside width for the track is about 3 m. Finally, at the middle of the distance between the centers of the circumferences, a set of cones are placed to form the starting and finishing straight-line path. The race car must take the starting straight line and take two turns to the right and immediately two turns to the left, finishing with the straight-line path away from the track, see Figure 1.2.

1.2. Automotive design

1.2.1. Design process

In this project, the product design and development methodology proposed in [6] is used to develop the formula-style racing car. This methodology comprises the following phases: planning, concept development, system-level design and detail design, which have been customized for the automotive design by incorporating an intermediate phase named as vehicle dynamics simulation. The proposed design methodology for the racing car is illustrated in Figure 1.3.

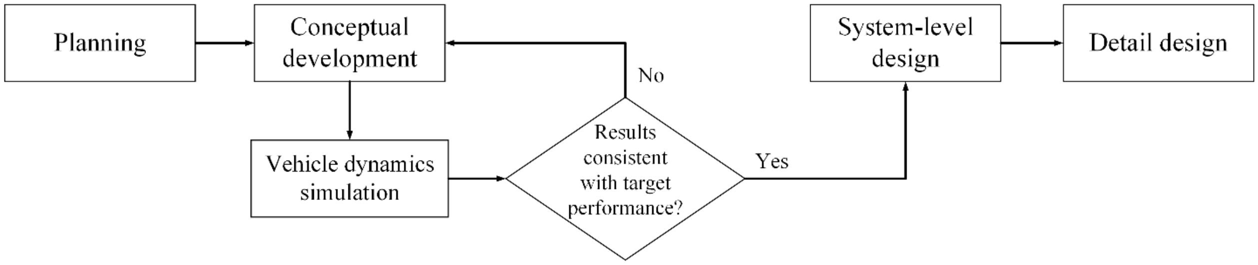

Figure 1.3. Proposed design methodology for the formula-style racing car.

During the planning phase, the scope and limitations of the design project for the vehicle are used in conjunction with the requirements and specifications. The design process phases are used to compile the research by different information sources related to automotive design of vehicles with similar characteristics, to the guidelines emitted by the Formula SAE organizers and in relation to the competitor's analysis from the participants that attend previous editions of the Formula SAE competitions and spin-offs. Additionally, the Quality function deployment (QFD) diagram is used to identify the key aspects regarding the customer requirements, technical characteristics, and development priorities of the vehicle.

In the conceptual development phase, a general concept for the race car vehicle is constructed. Upon this general concept, many specific concepts are established in relation to the systems and components that are going to form the single-seater vehicle. The concepts consider the requirements and design specifications, the principles of operation and the feasibility for the provision of alternatives, as well as the subsequent selection based on a group of evaluation criteria.

At the system-level design phase, the vehicle architecture is defined in accordance with the elements established on the conceptual development phase. In this phase, the material selection procedure is performed to select the materials for the components of the vehicle. In a similar way, the general and specific configuration for the systems, components and the race car vehicle are determined. The configuration for the single-seater vehicle is designed based on the selected concept, and the feasibility for the concept is reviewed within the characteristics, dimensions and geometry of various elements planned to integrate the car.

Finally, in the detail design phase the architecture of the vehicle and the components established on the system-level design phase are related in order to determine the adequate operation of the race car. This phase mainly involves the use of CAE tools to analyze the proposed design and validate the previous configuration of both individual parts and complete subsystems. For the specific case of the racing car, the process ends at this phase and the assembly and manufacturing drawings can be established.

1.2.2. Competitor's analysis and opportunity areas

As part of the planning phase of the design process of the race car, a competitor's analysis is performed. The information presented in this analysis considers data related to the technical specifications, the results, the reliability and the costs of several single-seater vehicles that participated in at least one of the Formula SAE competitions or spin-offs. The objective of the analysis is to provide relevant information for the decision-making procedure that will take place further on the design process in relation to the requirements and design specifications, the expectations for the performance of the car at the competition, along with the different opportunity areas that exists concerning the participant race cars on the contest.

Table 1.2 summarizes data from several single-seater vehicles that participated in at least one of the Formula SAE or spin-off competitions and makes a classification of this data into different aspects. Compiled data enables a comparison among similar designs with different characteristics and results. The information listed corresponds to public nature data and are straight from the competition reports related to Internal combustion engine (ICE) single-seater cars [7], [9]. As a reference, DNF stands for "do not finished", and it is a result when the team's performance do not allow the car to complete a test in the events of the competition. In a similar way, DNA stands for "does not apply" and it is used for those attributes in which no further information is known, or the aspect does not match the participant car results.

Table 1.2. Comparison of race cars participating in Formula SAE competitions and spin-offs [7], [9].

Score	Cylinders	Displacement	Weight (kg)	Cost (USD)	Time (acceleration)	Time (skidpad)	DNF
892.4	4	600	173.7	15,027	4.313 s	5.030 s	DNA
885.1	1	510	155.1	19,966	4.261 s	5.085 s	DNA
790.3	4	600	204.1	18,520	4.849 s	5.321 s	1
771.3	1	450	147.4	14,098	4.329 s	4.865 s	DNA
762.0	4	600	196.4	14,564	4.109 s	5.412 s	DNA
578.4	3	675	197.3	13,433	4.552 s	5.085 s	DNA
348.8	4	630	219.1	15,349	5.143 s	5.740 s	DNA
168.2	4	600	255.4	8,808	DNA	DNA	DNA
143.5	1	440	240	8,485	DNA	DNA	DNA
138.7	4	600	205.9	18,377	DNA	DNA	DNA

Based on the data listed in Table 1.2, a benchmark is performed for the design of the race car and the Key performance indicators (KPI) that define the performance of the vehicle are defined. The main KPI for the single seater cars participating in Formula SAE competitions are indicated in Table 1.3. The information shown in Table 1.3. is used to propose the requirements and technical specifications for the race car. These KPIs are set as the scope and limitations for the formula-style racing car for FSAE.

Table 1.3. Key performance indicators for the race car vehicle.

Category	KPI	Target
Performance	Engine maximum power	100 HP
	Vehicle total mass	250 kg
	Acceleration time	4.5 s
Fuel efficiency	Fuel consumption	20 km/L
Comfort	Maximum noise level	110 dB

1.2.3. Systems and components of the racing car

The formula-style racing car is integrated by a group of systems and components, from which their interaction determines the performance of the single-seater race car in the series of tests that correspond to dynamic events. As part of the planning phase of the vehicle design, it is required the selection of each system and component that must consolidate the car. To perform the design of the race car, the clusters listed in Table 1.4. are considered, which are based on the guidelines marked by the Formula SAE competition regulations along with vehicle operation.

Table 1.4. Systems and components of the formula-style racing car.

Cluster	Systems and components
Power transmission cluster	ICE and transmission group Powertrain Wheels and tires
ICE systems cluster	Intake system Injection system Exhaust system Cooling system Lubrication system
Electrical cluster	Charging system Ignition system Electric starter system Engine control system
Dynamic control cluster	Suspension system Steering system Braking system
Enclosure cluster	Cockpit and driver controls Chassis Bodywork

In a competitive environment, the power transmission cluster groups the most fundamental elements that can give the driver the adequate tools and the possibility to extract the maximum performance from the car on track. Since the power generation at the ICE, is passed through the transmission and delivered to the wheels and tires, the elements from the power transmission cluster must operate and couple properly to enable a high performance of the vehicle on the events. As demonstrated by Ayres et al. [10], there is a trend on the racing cars student competition to incorporate internal combustion engines with lower displacement or less number of cylinders due to modifications made to the scoring method in certain tests of the competition. It is important to note that maximum usable mechanical power and fuel consumption of an ICE are key performance indicators, as listed in Table 1.3., and finding a trade-off between these two indicators is a useful step in order to select the ICE unit for the racing car. On the other hand, the transmission plays a significant role in the power control provided by the engine. For instance, highest acceleration can be seen in manual transmission compared to other transmissions [11].

Conversely, to permit that the ICE operates correctly and to enable the performance extraction of the racing car by the means of the ICE, a series of systems must be provided to assist the engine operation. Whether for the continuous supply of fuel and air for the engine's charge cycle or for keeping lubrication or temperature controlled inside the engine, the ICE systems participate directly in the engine's ability to generate power. Kennedy et al. [12] explore the analysis and manufacture of elements pertaining to the intake and exhaust systems of the internal combustion engine of a race car. For these two systems, aspects such as the materials and the geometry used have a relevant influence on the intake and exhaust flow of the engine. On a similar way, there are many aspects and parameters to be considered for the design of the ICE systems.

Electrical installation in the participant vehicles are involved in different tasks within the activities that are marked by the requirements set by the Formula SAE regulations. Notwithstanding, it is necessary to define the elements that incorporate the installation in a way that these elements are functional in compliance with the guidelines that other components selected can establish.

The racing car must include elements that enable both the driver and the vehicle to have the ability to remain stable, change travel direction and gradually reduce the speed of the vehicle when participating in the events of the competition. These elements are grouped in the dynamic control cluster. Previous studies, such as the work of Gupta et al. [13], have highlighted the relation between the car security and some of the dynamic control cluster systems, including the braking system. The impact of these systems on the racing car security is relevant for the design of the formula-style racing car for FSAE.

The enclosure cluster includes the chassis, bodywork and driver controls, which are elements that are going to be close by at the layout of the car but still are equipped to accomplish different functions on the assembly. On the one hand, inside the cockpit the driver is meant to be located together with a group of control devices to fulfill some functions to manipulate the operation of the vehicle. Melvin and Gideon [14] highlighted the importance of the protection against lateral impacts, which is related to the location of the seat within the required ergonomic position to a comfort place of the driver. As marked previously, there is always a relation between the cockpit and the security enhanced by the chassis. With respect to the structure of the vehicle, the chassis is designed among a vast series of guidelines in conjunction with the regulations of the competition to provide a standard in the vehicles' design, and to ensure adequate conditions to be operated. For instance, Kaya and Ozyurt [15] noted the use of impact attenuators with reduced mass, slots on the lateral side and circular sections to implement a more efficient design and higher deformation in the case of a frontal impact. Considering this information, it can be stated that the design of structural elements has a significant influence on vehicle safety. Meanwhile, the main priority in the design of the bodywork is the effectiveness of the geometry to generate aerodynamic charge, since this effect translates into a higher traction capacity threshold in the tires of the racing car.

1.3. Design specifications of the racing car

The establishment of the design specifications is part of the planning phase of the design process of the car. To do this, the first step is to realize the quality function deployment (QFD) to ensure that the requirements for the car are translated into technical specifications during the design process.

1.3.1. Quality function deployment (QFD)

The formula-style racing car is designed within the regulations emitted in the current Formula SAE rules, which are separated into the following categories: general standards, administrative regulations, required documentation, vehicle requirements, technical aspects referred to the use of internal combustion engines or traction electric motors, static events, dynamic events, technical inspection and the driver and vehicle equipment. Based on the regulations and the KPIs defined previously at Table 1.3., the necessities for the racing car design are defined.

Figure 1.4. shows the house of quality of QFD for the single seater racing car on a general perspective. In one side of the matrix, the customer requirements are defined among a list of priorities with the scale located at the left. Meanwhile, the functional requirements are defined at the top of the matrix. The correlation between customer and functional requirements is illustrated at the center of the matrix with a scale that sets symbology to determine whether these requirements have a strong, moderate or weak relationship. In a similar way, at the top of the matrix the signs indicate whether a functional requirement is set to minimize, maximize or target. Based on the information in Figure 1.4., the functional requirements to highlight are mainly the material selection, scale and dimensions and the number of original equipment elements to integrate into the racing automobile.

				Column #	1	2	3	4	5	6	7	8	9	10	Competitive Analysis (0=Worst, 5=Best)					
				Direction of Improvement: Minimize (▼), Maximize (▲), or Target (x)		▼			▼	▲	▼		▼							
Row #	Max Relationship Value in Row	Relative Weight	Weight / Importance	Quality Characteristics (a.k.a. "Functional Requirements" or "Hows") / Demanded Quality (a.k.a. "Customer Requirements" or "Whats")	Material selection	Scale and dimensions	Forms and geometry	Vehicle layout and architecture	Number of assembly elements	Adjustability and operation range	Manufacturability	Number of original equipment elements	Budget	Performance powertrain elements	892.4	885.1	790.3	771.3	348.8	Vehicle used as reference for the IVDS
1	9	3.8	2.0	Aesthetics of the vehicle		▲	Θ	O			▲	O	▲		5	4	4	5	3	3
2	9	18.9	10.0	Regulations compliant vehicle	O	Θ	▲	▲	▲		▲	Θ	O	▲	5	4	4	5	3	3
3	9	11.3	6.0	Budget adjusted vehicle	Θ	O	▲		O	▲	O	Θ	Θ	Θ	3	3	4	4	2	4
4	9	13.2	7.0	Reliable vehicle	Θ	Θ	▲	▲	▲		▲	O	▲	▲	5	5	5	4	4	1
5	9	17.0	9.0	High-performance vehicle	O	Θ	Θ	O	▲	O	▲		▲	Θ	4	5	5	5	3	2
6	9	7.5	4.0	Practical vehicle	▲	O	▲	O	Θ	O	Θ	Θ	O	▲	5	4	4	5	3	3
7	9	5.7	3.0	Resource managed vehicle	O			▲	O		O	Θ	O		4	5	5	4	2	2
8	9	15.1	8.0	Safe vehicle	Θ	Θ		O	O	▲	O	Θ	▲		5	5	5	4	4	3
9	9	5.7	3.0	Ergonomic vehicle	▲	O	Θ	Θ		Θ		O	▲		4	5	5	5	3	3
10	9	1.9	1.0	Easy handling vehicle		O				Θ				▲	3	3	3	3	3	2

Figure 1.4. QFD for the design of the formula-style racing car.

1.3.2. List of design specifications for the racing car

The formula-style racing car represents a multidisciplinary challenge that involves an array of engineering principles to fulfill the specific objectives of security and performance. To enable that the single seater vehicle is in accordance with the regulations of the competition and the planned objectives to make a high-performance car, in this section of the project some of the design specifications for the racing automobile are listed. These design specifications are divided and located into categories with the aim of bringing structure to the presentation of this segment.

Table 1.5. Design specifications for the formula-style racing car.

Category	Design requirement	Details and target
Architecture	General architecture	Open wheeled and open cockpit with four wheels.
	Powertrain configuration	Engine location and traction axle: Rear mid-engine, rear wheel drive.
	Chassis type	Fabricated structural assembly to support all functional systems: Tubular spaceframe with correctly triangulated sections.
	Tire characteristics	Racing slicks for dry conditions and weather tires for wet conditions.
Project	Budget	The budget for the racing car must be under $20,000 USD and preferably near $15,000 USD
	Useful life	Projected lifespan for the car is about a year.
Performance	Vehicle total mass	Upper limit for the vehicle mass: 300 kg Goal for the vehicle mass: 200 kg.
	Acceleration time	Goal time from 0 to 100 kph: 4.0 seconds
	Fuel consumption	Upper limit for fuel efficiency: 20 km/L
	Torque capacity	Enable the capacity of traction in relation to the weight of the vehicle with driver.
Engine and transmission	Engine type	4-stroke ICE Upper limit for displacement: 710 cc.
	Engine power	Lower limit for maximum output power: 100 HP.
	Transmission type	Power control by means of a transmission: Manual or similar.
Cockpit	Cockpit opening	Lower limits for cockpit opening are defined by the template in the Formula SAE regulations.
	Cockpit interior space	Lower limits for cockpit internal cross section are defined by the template in the Formula SAE regulations.
	Driver seating position	The driver seating position must permit drivers of sizes ranging within 5th percentile female and 95th percentile male.
	Seat harness	Compliant specification 6-point harness mounted in double shear.
Noise, harshness and vibration (NHV)	Maximum noise level	The upper limit of noise level at competition: 110 dB at 0.5 m from the exhaust.
	Structural rigidity	Chassis torsional rigidity upper limit: 300 kNm/rad Chassis torsional rigidity lower limit: 50 kNm/rad

The categories listed are related to the architecture of the car, the design project, the performance of the car, the engine and transmission group, the cockpit and noise, harshness and vibration. The design requirements, details and targets are listed below in Table 1.5. Some of the design requirements listed in Table 1.5. directly came from the KPIs noted in Table 1.3.

On the other hand, some other design requirements are related to the Formula SAE regulations [8]. Architecture, engine and transmission group and cockpit requirements are mainly based on the guidelines emitted by the organizers of the competition. However, there are still some of the design requirements that come directly from customer or functional requirements from the QFD for the formula-style racing car, such as the project requirements. Ones of the most relevant design requirements listed in Table 1.5. are the performance requirements. These requirements include but are not limited to vehicle total mass, acceleration time, fuel consumption and torque capacity.

With the proposed design specifications, now it is possible to continue with the next phase of the design process. Nevertheless, to have a complement of these design specifications listed, an analysis of the vehicle dynamics for the design of the car must be carried out. This vehicle dynamics analysis at the initial stages of the design of the racing car is performed with a simplified model, as developed in Chapter two.

Chapter 2: Model for initial vehicle dynamics simulation

The design of the motorsport vehicle must take into account aspects such as ergonomics, aesthetics, practicality, applicable standards, among various others. However, the vehicle dynamics are more relevant when a high performance is sought. As mentioned by Anbazhagan et al. [16], the vehicle dynamics is defined as the study of the dynamic behavior of the vehicle, mainly in relation to the forces developed in the interface between the tires and the road surface. The design of the vehicle depends on the decision-making procedure made by the designer. Balena et al. [17] explore the behavior of a formula style vehicle and demonstrated that this behavior is dependent on a series of parameters, which many of them are defined at the initial design stage and are difficult to change later on. Considering this, it can be noted that vehicle dynamics play a significant role in the design process, especially at early phases when the results of the analysis may serve as a reference for decision making.

2.1. Dynamic model of a vehicle

The dynamic model of a vehicle can be as extensive and complete as needed. In this work, the dynamic model is defined to be part of an initial simulation, located at early stages of the design process of the car. At this specific point in the design process, most of the parameters are clearly not defined and this can complicate the vehicle's dynamic analysis. To create guidance within this stage of the design process, a simplified model of the motorsport vehicle is developed. This model contains the most relevant parameters to analyze the overall dynamics of the car. These parameters are separated into different modules: a technical design dimensions module, a static mass distribution module, a wheels and tires data module, an aerodynamic data module and an engine and transmission group module.

2.1.1. Technical design dimensions module

In the technical design dimensions module, the four main specific dimensions of the vehicle are defined. These dimensions are [18], [19], [20]: wheelbase (wb), track width of the front axle (tw_f), track width of the rear axle (tw_r), and center of gravity (h_{cg}), which are shown in Figure 2.1. These dimensions are very important because they define the general performance of the racing car in different driving situations, such as the acceleration, braking or taking a corner. Moreover, these dimensions are used in the vehicle dynamics analysis, particularly in the load transfer equations and the corner handling behavior of the vehicle.

As stated by Gaffney and Salinas [18], the wheelbase is defined as the distance between the center lines of the front axle and the rear axle. The wheelbase (wb) is a relevant dimension to determine, this is because of the influence of this parameter on the static mass distribution or the load transfer in the vehicle in a longitudinal perspective, having a compromise between the loads at the wheels in the front axle and the rear axle.

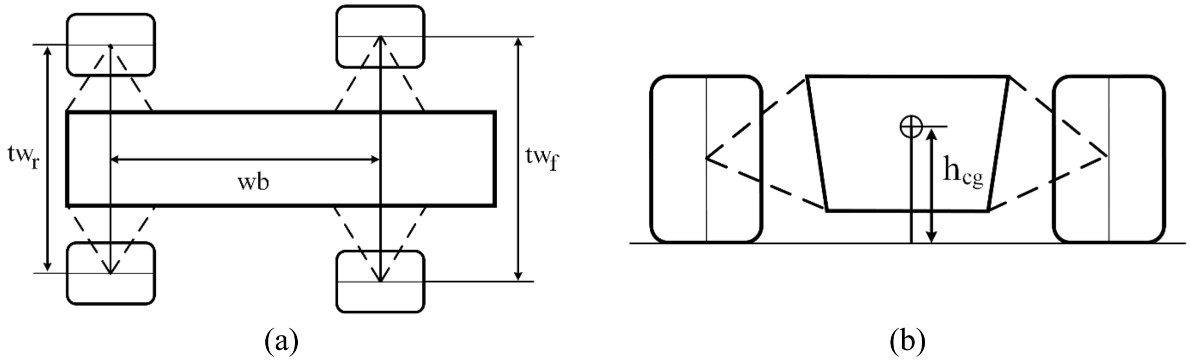

Figure 2.1. Technical design dimensions of the vehicle in (a) the top view and (b) the rear view.

The track width is the distance between the center lines of the left wheel and the right wheel of one of the axles of the vehicle, as cited by Gaffney and Salinas [18]. The track width (*tw*) as well has an influence on the lateral load transfer of the vehicle. In a Formula SAE racing car, typically the track width of the front axle (tw_f) and the track width of the rear axle (tw_r) are different. According to Meywerk [19], having a greater front track width than the rear track width in a vehicle is used in order to increase the traction in the rear axle at the exit of a corner. This is especially useful in an automobile with a rear wheel drive.

The location of the center of gravity has an influence on the stability of the car and the load transfer among the wheels of the car. In the literature, the rolling stability of the car has been associated to the compromise between the track width and the height of the center of gravity [20]. In other words, having a reduced height for the center of gravity (h_{cg}) translates into a greater stability for the vehicle.

2.1.2. Static mass distribution module

The static mass distribution (*md*) is developed based on the location of the center of gravity, particularly along the longitudinal location. The static mass distribution is given by providing the location of the center of gravity within the wheelbase of the vehicle. This percentage corresponds to the mass distribution at the front axle (md_f) and to the mass distribution at the rear axle (md_r). As a convention, the mass of the vehicle is used instead of the weight of the vehicle. An approximate location of the mass of the driver (*dm*) must be included in the model for better approximation for the static mass distribution. To include this in the model, it is required to introduce the total mass of the vehicle without the driver (*vm*) and the mass of the driver to eventually calculate the static mass distribution for each of the axles of the vehicle with an approximated location of the mass of the driver in relation to the wheelbase (*dl*).

2.1.3. Wheels and tires data module

Probably, the wheels and tires are the most crucial and complex parts in a model related to the dynamics of the vehicle. However, at this stage of the design process, most of the parts are not yet selected or some are partially selected. For the tires, the selection is arguably a difficult step. The parameters to consider into this model related to the tires are the most general parameters. The size of the wheels and tires have a significant impact on the performance of the vehicle. According to

[21], the size of the wheels affects not only the performance of the vehicle, but also the noise level, the comfort level and the fuel economy of the motorized vehicles. Nevertheless, for the IVDS model the diameter of the tire is not only considered, but a dynamic diameter of the tire is also formulated as well. This dynamic diameter of the tire contemplates that a certain percentage of the tire is flattened constantly by having contact between the tread surface and the road surface.

The contact of the tire with the road surface is defined by means of two coefficients. The first coefficient is the rolling resistance coefficient that quantifies the opposition of the road to the movement of the tire. The dependance relation between the forces acting on the tire and the slip ratio is explained by Rajamani et al. [22]. The second coefficient is the adherence coefficient in the interface zone between the tire and the road surface, which is variable and dependent on various characteristics of the tire related to the construction and operation of the tire.

In the tires, there is a relation between the vertical loads that are carried out in the tire and their correspondent lateral forces generated. Many studies in the literature have noted and reported data related to the tire behavior [23], [24]. The relationship between vertical and lateral loads at the tires is explained and illustrated by Smith [23]. On the other hand, Deakin and Crolla [24] presented a comparative among the relation of vertical and lateral loads exerted on tires for both Formula SAE and Formula One.

2.1.4. Aerodynamic data module

The aerodynamics of a motorized vehicle are very relevant in the case of a racing car. The invested time on the development and study of the aerodynamics of racing cars can translate into a higher threshold of performance in the dynamic events of the competition. As reported by Wordley and Saunders [25], the use of an aerodynamic package in a Formula SAE car may bring some benefits such as increased speed while taking corners and a greater braking potential with the trade-off of a slightly reduced acceleration in straight-line and incremented fuel consumption. The aerodynamic package of a formula-style racing car consist of several components of bodywork, including the front and rear wing, undertray, sidepods, nosecone, and many others. Besides this, the aerodynamics of a Formula SAE car should lead to the best performance possible.

To evaluate the aerodynamics of the vehicle, a standard value for the air density is proposed, together with some other parameters such as the frontal surface or the vehicle and both the drag and lift coefficients respectively. The drag coefficient quantifies the resistance of the vehicle against the air flow in the direction of travel, while the lift coefficient quantifies the resistance of the vehicle to ascend or descend as a reaction due to the air flow. Although, in an early stage of the design process it is still complicated to estimate the aerodynamic data of the vehicle, the initial data used for this analysis is merely an approximation.

2.1.5. Engine and transmission group module

Since the dynamics of a motorized vehicle is analyzed using an internal combustion engine (ICE), some relevant data must be provided to the model. This data corresponds to the power, torque and angular frequency of the engine, as well as the gear ratios and the overall transmission ratio used to transfer the power from the engine and transmission to the elements of the powertrain. In the case of the Formula SAE cars, an assumption is made towards the powertrain configuration. This is because the vast majority of the cars for the competition use a rear wheel drive (RWD) powertrain.

In the dynamic model of the vehicle some specific data is introduced. This data includes the idle speed and the red line speed of the ICE. In order to evaluate the operation of the engine within the range defined by the idle speed and the red line speed, a set of torque data related to the engine revolutions per minute (rpm) is required by the model. Another important parameter to be defined is the engine angular acceleration, which is important to define the engine behavior and the interaction with the transmission. This information enables the possibility to graph the engine performance curves, mainly referring to the power and torque curves. In the case of the transmission and powertrain, the gear ratios for each gear shift of the transmission, the global efficiency and the final drive ratio are relevant parameters to be considered.

With the engine and transmission group data defined, it is possible to plot the engine performance curves. Some other important plots correspond to the vehicle performance curve and the engine speed versus the vehicle speed characteristic curves. For instance, the vehicle performance curve is a graphic representation of the relationship between the tractive effort and the ideal vehicle speed; meanwhile, the engine speed versus the vehicle speed characteristic curves describe how the engine's angular frequency and the ideal vehicle speed interact. Using this information, it is possible to simulate the effects that take place during gear shifts, such as the engine angular frequency drop during upshift transitions.

2.2. Preliminary calculations

In order to provide a point of departure and enhance the simulation, some assumptions and initial estimations are required. Among the preliminary calculations to develop the initial dynamic simulation, the static mass distribution considering the total mass of the driver and vehicle and the plots corresponding to performance curves are listed.

For the total static mass distribution (*tmf*), it must be considered the mass distribution of the vehicle for the front axle (md_f) and for the rear axle (md_r). The mass distribution refers to the total mass of the vehicle (vm), the location of the center of gravity of the vehicle (h_{cg}) and the wheelbase (wb). Later, the driver's mass (dm) is assumed to be acting in a specific location within the wheelbase using a percentage centered location (dl). With this previous data, the total static mass distribution for the front axle and the total static mass distribution for the rear axle can be determined as follows:

$$tmd_f = \frac{md_f + (dl)(dm)}{(vm + dm)} \tag{2.1}$$

$$tmd_r = \frac{md_r + (1 - dl)(dm)}{(vm + dm)} \tag{2.2}$$

To generate the engine performance curves, it is necessary to calculate the mechanical power developed by the engine (P_e) with the following equation:

$$P_e = T_e \omega_e \tag{2.3}$$

Where T_e is the crankshaft torque of the engine, ω_e is the angular speed of the crankshaft.

After the calculations of the mechanical power developed by the engine, it is possible to plot both the torque against the angular speed and the power against the angular speed curves.

Using the transmission ratio, the torque and the angular speed at the output shaft of the primary transmission of the engine are both calculated. The equation (2.4) provides the transmission ratio that relates to the angular speed (ω) to the teeth number of the gear (Z) of both the input and output shafts, which are referred for input (ω_i, Z_i) and for output (ω_o, Z_o).

$$\frac{\omega_o}{\omega_i} = \frac{Z_i}{Z_o} \tag{2.4}$$

However, it is also necessary to take into account the losses that are produced in the transmission elements. Considering the transmission efficiency parameter (η). The equation (2.5) establishes the relation between the angular speed (ω) and the torque (T), both referring to input and output respectively.

$$\frac{\omega_o}{\omega_i} = \eta \frac{T_i}{T_o} \tag{2.5}$$

The output torque and angular frequency of the driven wheels of the car are computed with the equation (2.5). Notwithstanding, in order to calculate the traction effort that is exerted on the driven wheels (F_t) and the linear velocity of the vehicle drive wheels (v_w), the equation (2.6) and the equation (2.7) are employed. In general, it is set that the torque at the driven wheels (T_w) is defined as the rotational force in relation to the distance from the axis of rotation, where in this case the force corresponds to the traction effort and the distance is established as the diameter of tire of the driven wheels (d_w). On the other hand, the mechanical power developed at the wheels (P_w) is in this case defined as the traction effort in relation to the linear velocity of the vehicle driven wheels.

$$T_w = (F_t)(d_w) \tag{2.6}$$

$$P_w = (F_t)(v_w) \tag{2.7}$$

From this data it is possible to generate the vehicle performance curve and the engine frequency versus the vehicle speed characteristic curves.

2.3. Linear acceleration of the racing car

The dynamic analysis of the vehicle is based on the use of the principles of classical mechanics because the dimensions are much greater than a nanometer and the speed that can develop is smaller than the speed of light. In this analysis, uniformly accelerated rectilinear motion (UARM) is used as a basis, in which the idea is to consider a constant acceleration. With the previous statements considered and in circumstances of constant acceleration, some of the following equations are directly related to the equations of motion, which are in fact vectorial equations, although only the magnitude of the vectors is necessary in this model.

The equation (2.8) states the relation between the initial angular velocity developed at the engine (ω_{e0}), the angular acceleration of the engine (α_e) and the time interval (t_i) to calculate the instantaneous angular velocity developed at the engine (ω_{ie}).

$$\omega_{ie} = \omega_{e0} + \alpha_e t_i \tag{2.8}$$

Considering the engine tabulated data for torque and angular velocity, the instantaneous angular velocity is used as input data in order to compute the instantaneous torque developed by the engine through interpolation. Additionally, the equation (2.5) is used to calculate the instantaneous torque at the driven wheels, which is used to determine the traction effort (F_t) with equation (2.7), where the distance is the dynamic diameter of the tires of the driven wheels (D_{dw}). The dynamic diameter of the tires is calculated with the equation (2.9) in relation to the average tire compression ratio (tcr) for the driven wheels' tread surface.

$$D_{dw} = (1 - tcr)d_w \tag{2.9}$$

By means of the special case of the second Newton's law in which the mass is constant, the acceleration in terms of g-force is calculated using the equation (2.10). The equation (2.10) involves the traction effort, the total mass of the car considering both the vehicle mass and the driver mass, as well as the gravity acceleration (g).

$$F_t = (vm + dm)g \tag{2.10}$$

According to Smith [23], the fact that it is possible to reach a specific acceleration in g-force depends on factors such as the vertical loads in the tires of the driven wheels, the resistance exerted between the tread surface of the tire and the road surface, or the slip angle of the tires in relation to the road surface. This series of factors, and even more, can modify the g-force that acts under acceleration. This is why the calculations made on these topics are considered as approximations.

2.3.1. Longitudinal load transfer

When the car is under acceleration or braking, the movement that the cars experience is known as pitch in reference to a fixed coordinate system. Hence, the load transfer that occurs during linear acceleration is produced in relation to a longitudinal plane; in order words, the vertical loads at the tires are distributed between the tires at the front axle and the rear axle of the car.

A relevant aspect of the analysis of the load transfer is the point where the forces are assumed to be applied. This point depends on the reference frame in which the analysis is based. The g-forces can be applied in the center of gravity, in accordance with Hamilton's principle, which states that the path of the forces acting on the car follows a trajectory that minimizes the action. In other reference frames, the point where the forces are assumed to be applied could be the roll center, which is related to the suspension geometry.

In accordance with conservation laws, when a g-force is applied on the center of gravity on the direction of travel, a reaction causes a longitudinal load transfer (LT_{long}). This load transfer can be estimated with the equation (2.11), which involves the longitudinal acceleration of the vehicle in terms of g-force (g_{long}), the total mass of the vehicle, the gravity acceleration, the height of the center of gravity and the wheelbase.

$$LT_{long} = g_{long} \frac{(vm + dm)(g)(h_{cg})}{wb} \tag{2.11}$$

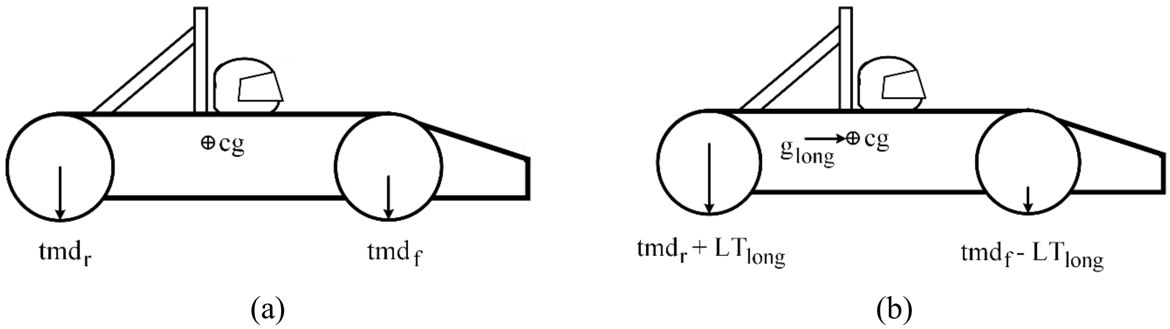

Figure 2.2. Longitudinal mass distribution for the vehicle (a) in static conditions and (b) under acceleration.

The longitudinal load transfer is then either added or subtracted to the vertical load exerted on the tires of both the front axle and the rear axle of the car. The application of the g-force acceleration in the direction of travel and the addition or subtraction of the load transfer is illustrated in Figure 2.2. Another consideration to be established is that the longitudinal load transfer addition or subtraction depends basically on the direction in which the g-force acceleration is acting.

2.3.2. Resistive forces of the vehicle's motion

In general, the resistive forces to the linear motion of the vehicle are the aerodynamic resistance force, the rolling resistance force and the grade resistance force.

The aerodynamic resistance force (F_{ar}) is the force reaction to the air flow around the vehicle as it travels. This has as a result a force in the opposite direction to the direction of travel. Nevertheless, the air flow develops two forces of interest to the dynamics of the vehicle, which are the aerodynamic drag and the aerodynamic lift.

The drag force is the aerodynamic resistance that the car experiences as it moves through the air and opposes the motion of the vehicle. On the other hand, the lift force is a vertical aerodynamic force acting on the car due to the airflow. The aim of a high-performance car is to provide a negative lift, usually known as downforce, which increase the normal force at the tires and translates into enhanced traction and handling. The drag force and lift force are computed using equations (2.12) and (2.13) respectively. The drag force (F_{ard}) is calculated towards the frontal area of the vehicle (A_f), air density (ρ), drag coefficient (C_d) and the linear velocity of the vehicle (v). Alternately, the lift force (F_{arl}) is calculated towards the planform area of the vehicle (A_p), air density (ρ), lift coefficient (C_l) and the linear velocity of the vehicle (v).

$$F_{ard} = \frac{1}{2}(\rho)(A_f)(C_d)(v^2) \tag{2.12}$$

$$F_{arl} = \frac{1}{2}(\rho)(A_p)(C_l)(v^2) \tag{2.13}$$

With regards to the rolling resistance force, this term refers to the resistive force that exists in the contact interface between the tread surface of the tire and the road surface. The rolling resistance force (F_{rr}) is calculated using the rolling resistance coefficient (C_{rr}) and the vertical force exerted on the wheels and tires (F_{wv}) with equation (2.14).

$$F_{rr} = (C_{rr})F_{wv} \tag{2.14}$$

It is worth noting that the rolling resistance coefficient is dependent on various factors such as the tire construction, the characteristics of the tread surface of the tires, the conditions in the interface between the tread surface of the tire and the road surface, the tire temperature, among others.

On the other hand, while climbing a slope the car experiences a component of force that acts in the direction of travel or against the direction of travel. This component of force can be named as a gradient resistance force (F_{gr}). The gradient resistance force can be calculated based on the resultant force that corresponds to the weight of the vehicle while driving through a road surface that has a slope angle (θ_g), as is presented in the equation (2.15).

$$F_{gr} = (vm + dm)(g)\sin(\theta_g) \tag{2.15}$$

The racing car is represented by climbing a slope in Figure 2.3. illustrating the relevant parameters to calculate the gradient resistance force for the car as a resistive force.

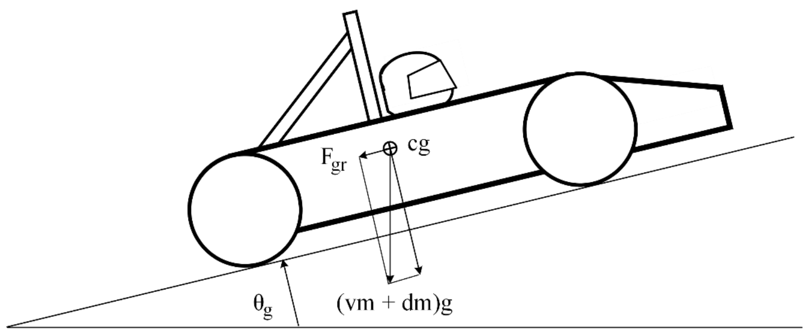

Figure 2.3. Lateral view of the vehicle in ascent of a slope.

By knowing the forces acting in the direction of travel and the resistive forces that act against the motion of the car, it is possible to determine the acceleration thrust. The acceleration thrust (F_{at}) corresponds to the force exerted on the car to overcome the resistive forces in the opposite direction of travel. Notwithstanding, when applying the D'Alembert principle, the system of the car must consider that the sum of the real forces and the inertial forces equals zero in a non-inertial reference frame. Under Newtonian mechanics, the equation (2.16) presents the sum of the traction forces (F_t) and the resistive forces that act in the opposite direction of motion (F_r) for the vehicle that led into the acceleration thrust of the car.

$$\sum F_{at} = \sum F_t - \sum F_r \tag{2.16}$$

By means of the special case of the second Newton's law in which the mass is constant, the equation (2.10) enables the possibility to calculate the instantaneous linear acceleration of the vehicle (a) when substituting the force for the acceleration thrust determined previously and the mass for the sum of the mass of the vehicle and the driver. Within UARM, the equation (2.17) states the relation between the initial linear velocity developed at the vehicle (v_0), the linear acceleration of the vehicle

(α) and the time interval (t_i) to calculate the instantaneous linear velocity of the car (v); while the equation (2.18) is used to calculate the displacement of the car (Δx).

$$v = v_0 + at_i \tag{2.17}$$

$$v^2 = v_0^2 + 2a(\Delta x) \tag{2.18}$$

2.4. Vehicle behavior in curved segments

When a motorized vehicle changes direction, the concept of center of curvature appears. The center of curvature is located at an imaginary distance from the center of gravity of the car that is called the radius of curvature (r_c). To have a clearer perspective of this, a top view of the car is illustrated in Figure 2.4., which represents a vehicle at the time of taking a corner and with the set of parameters defined for the analysis.

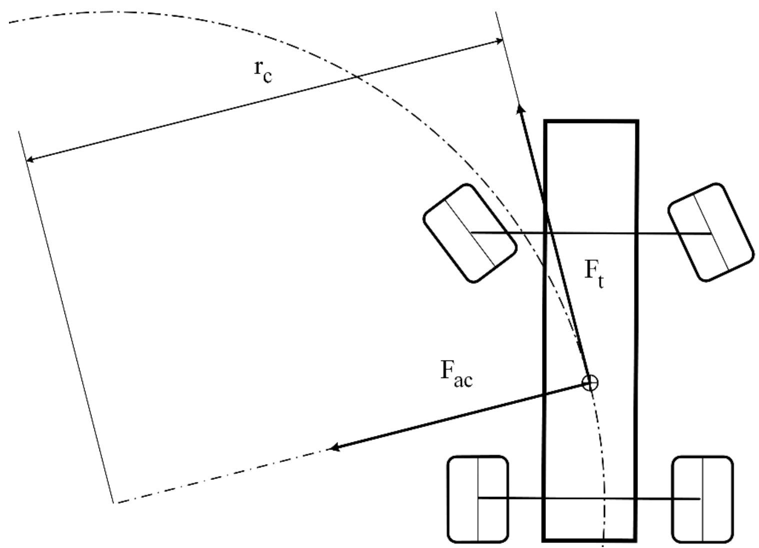

Figure 2.4. Top view of the vehicle while taking a corner.

Making a reference to Figure 2.4. and the parameters illustrated, the radius of curvature is a distance that may vary depending on the geometry and the variables regarding to the direction of the car. The traction force (F_t) is assumed as a tangential component in relation to the radius of curvature and the centripetal acceleration appears in the direction towards the center of the curvature while the car is moving in a circular path. The force due to the centripetal acceleration (F_{ac}) is calculated by means of the equation (2.19), in which the total mass of the vehicle, the linear velocity of the car and the radius of curvature are related.

$$F_{ac} = \frac{(vm + dm)(v^2)}{r_c} \tag{2.19}$$

As discussed in [26], one of the fundamental definitions towards the vehicle dynamics and stability is the critical speed. The critical speed of the vehicle while taking a corner is dependent on the dimensions and the characteristics of the car. The findings of Ni [27] state that once the driving force in the tires of the vehicle is greater than the maximum friction static force at the tire, then the car will skid. In other words, there is a grip limit condition in the tires while having a contact zone towards the road surface.

In the interface between the tread surface of the tire and the road surface of each of the tires of the car there exist forces that can be represented as force components on every axis used as reference. That said, the equation (2.20) is used to obtain the resultant force previously described named as grip limit resultant force (F_{gl}).

$$F_{gl} = \sqrt{F_{wt}^2 + F_{wa}^2} \tag{2.20}$$

As marked previously, the concept of grip limit appears in action towards a plane that is parallel to the road surface contact points of the tires. The grip limit of the tire can be determined with a conditional, which is set with a mathematical inequality equation just as shown in the equation (2.21). The equation (2.21) formulates a condition in which the resultant force that forms from the sum of the longitudinal or tangential wheel force (F_{wt}) and the lateral or axial wheel force (F_{wa}) of the tire must not overcome the vertical load that is exerted on the analyzed tire (F_{wv}) while considering the grip coefficient. It is important to note that the grip coefficient (C_g) is dependent on the track conditions and can be considered as variable.

$$\sqrt{F_{wt}^2 + F_{wa}^2} \leq C_g F_{wv} \tag{2.21}$$

Based on the equation (2.20) and (2.21), to avoid the vehicle entering an understeer or oversteer circumstance, the vertical load exerted on every tire must be greater than grip limit resultant force that act in the contact zone of the tire with the road surface.

2.4.1. Lateral load transfer

Derived from the change in direction and the corresponding centripetal acceleration in the car, the vehicle experiences a lateral load transfer (LT_{lat}). In a similar way to the longitudinal load transfer, the lateral load transfer occurs in relation to a parallel plane to the frontal plane of the car, concerning to the tires of both the front axle and the rear axle. The equation (2.22) relates the lateral load transfer with the lateral acceleration in g-force (g_{lat}) and the parameters of the vehicle, which are the total mass of the vehicle, the height of the center of gravity and the track width of the front and rear axle respectively.

$$LT_{lat} = g_{lat} \frac{(vm + dm)(g)(h_{cg})}{tw} \tag{2.22}$$

A graphic representation of the car while taking a corner is illustrated in Figure 2.5., where the application of the g-force from the centripetal acceleration and the lateral load transfer is shown before and after the effect on the vehicle.

In an analogous way to the longitudinal load transfer, with the lateral load transfer a vertical force in the tires is established among the tires of a single axle of the vehicle, either the front or rear axle. The vertical load directly influences the lateral force developed on the tires, as reported by [23],

[24]. Therefore, the lateral force on the tire (F_{wa}) is acquainted in relation to the vertical force at a given moment within the analysis timeframe.

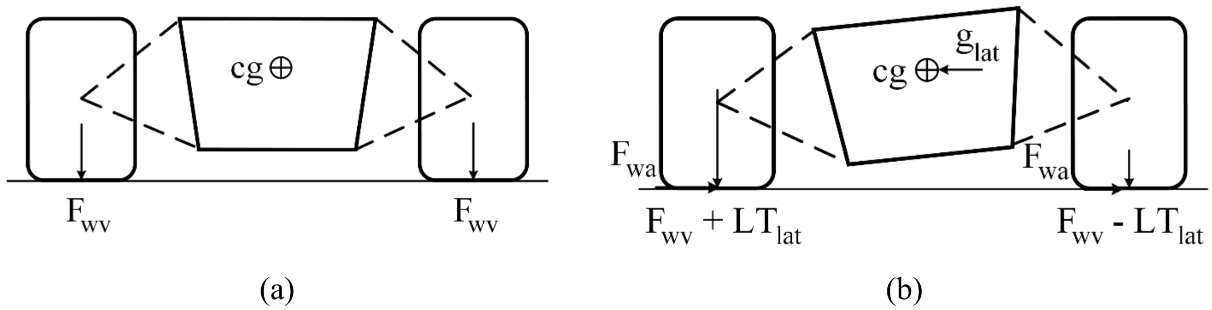

Figure 2.5. Rear view of the vehicle (a) in static conditions and (b) taking a corner.

2.5. Model and validation for the IVDS

With the aim of developing a practical tool for vehicle dynamics analysis, the simplified model is structured using a flowchart, as illustrated in Appendix A. This model is named as the initial vehicle dynamics simulation (IVDS) model. Once the model is developed, the results obtained are benchmarked against the reported event times set by a participating vehicle during the competition. The following development of the IVDS model and the validation performed is presented below. Additionally, it is noteworthy that the IVDS model is developed in a programming language in accordance with MATLAB. After setting this, the procedure and the plots presented further on in this section correspond to the usage of software with the mentioned programming language.

2.5.1. Modeled racing car used as reference

First step is to define the vehicle used as reference with the aim of setting the modeled vehicle data to be introduced in the IVDS model. The vehicle used as reference is selected by considering the availability of the data to establish a better modeled car. Nevertheless, a vast majority of the data concomitant to the car used as reference will not be presented in this thesis project for the sake of preservation of the confidentiality. For the purposes of simplicity, the racing car used as reference is going to be noted as RC in this section.

The data of the RC is analyzed and then implemented within the modules of the model for the IVDS. From this information, a group of plots are performed and utilized as graphical reference towards the modeled vehicle. The engine performance curves that belong to the behavior of the ICE mounted in the RC are shown at Figure 2.6.

The RC mounts a motorbike engine, which eventually connects to a primary transmission that consists of a six-gear transmission. With this into account, the related plots for the vehicle performance curve and the engine frequency versus the vehicle speed characteristic curves are presented eventually in Figure 2.7.

With the information of the modeled vehicle covered, now it is possible to carry out the dynamic simulation for the modeled vehicle. The model used to perform the IVDS is based on two sections: the first section corresponds to the acceleration event and the second section corresponds to the skidpad event of the Formula SAE competition or spin-offs. By working with two different sections in the IVDS, the results of the dynamic simulation are presented separately for the acceleration and skidpad events. The course utilized as a basis for both the acceleration and skidpad events is directly related to Figure 1.1 and Figure 1.2., considering that these two are standard events with no alteration in the competition from year to year. Additionally, the results of the dynamic simulation are presented graphically among a series of figures shown below.

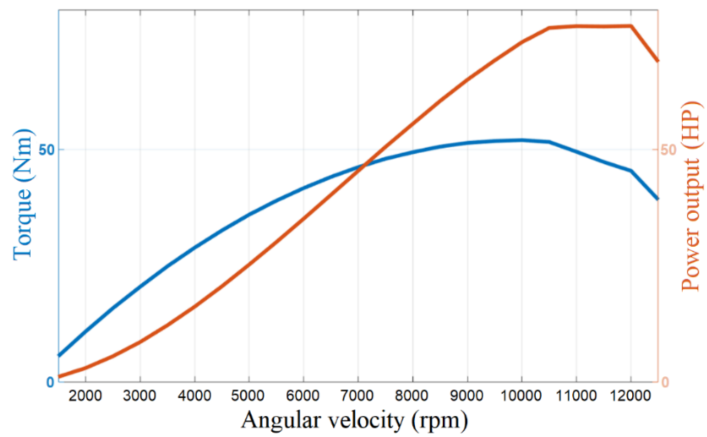

Figure 2.6. ICE performance curves for the engine associated with the RC.

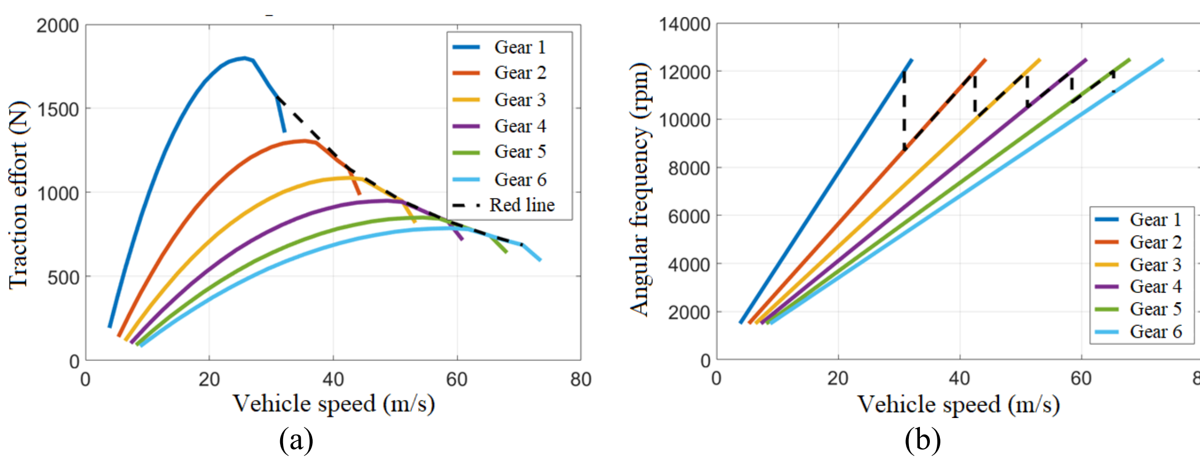

Figure 2.7. RC data plot for (a) vehicle performance curves and (b) engine frequency against vehicle speed.

The results for the RC modeled vehicle in the corresponding section for the acceleration event are graphically illustrated in Figure 2.8. These results imply the linear velocity of the vehicle, the gear shifted in the transmission, the displacement of the vehicle and the longitudinal acceleration in g-force, all of these in relation to the time elapsed during the simulation of the event.

On the other hand, the total time that the modeled vehicle obtained at the IVDS for the acceleration event is 5.06 seconds. It is important to note that this time calculated at the IVDS is considering a series of assumptions, such as that the gear shifts are made just in time, that there is no slip on the tires at the start of the event and the conditions for both the track and the vehicle are optimum. Therefore, the time calculated at the IVDS must be lower than the results obtained by the RC at the completion.

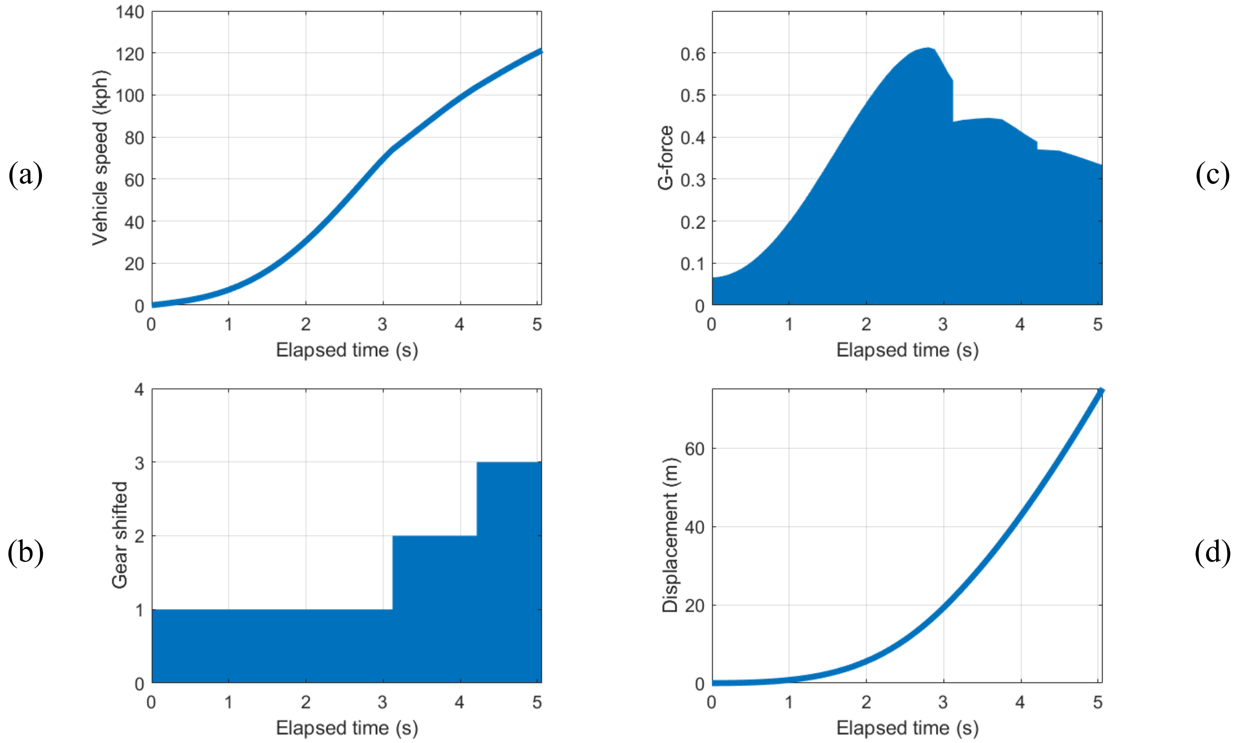

Figure 2.8. IVDS results of the acceleration event in relation to elapsed time for (a) speed, (b) longitudinal acceleration, (c) gear shifted and (d) displacement.

In a similar way, the results for the RC in the skidpad event are graphically illustrated in Figure 2.9. The correspondent results imply the linear velocity of the vehicle, the gear shifted in the transmission, the displacement of the vehicle and the lateral acceleration in g-force, all of these in relation to the time elapsed during the simulation of the event. On the other hand, the event time of the skidpad event is 5.73 seconds. This event time must consider that the whole skidpad event consists of the use of the course in accordance with the regulations of the competition, so this time just fits the part of the event to be clocked. It is important to note that this time calculated at the IVDS is considering a series of assumptions, such as that the gear shifts are made just in time, that there is no slip on the tires at the start of the event and the conditions for both the track and the vehicle are optimum. Therefore, the time calculated at the IVDS must be lower than the results obtained by the RC at the completion.

With the results of the IVDS for the modeled vehicle, the simulation results are contrasted with the results of the RC obtained at the acceleration and skidpad events at the competition. The information of the results for the RC and many other racing cars can be consulted at the website of the corresponding organization for the Formula SAE or other spin-offs [7], [9]. The results are benchmarked and presented in Table 2.1. for comparison, where the approximation error is calculated in relation to the difference between real results of the RC against the simulation results of the modeled vehicle.

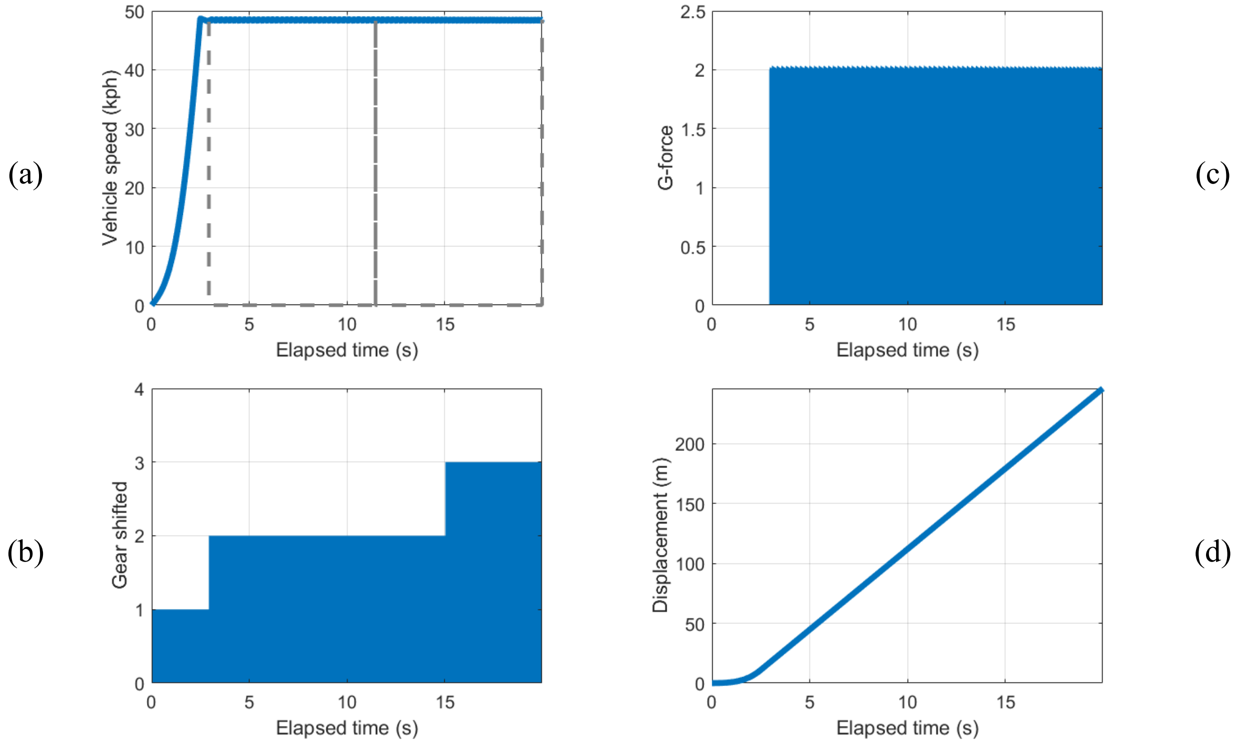

Figure 2.9. IVDS results of skidpad event in relation to elapsed time for (a) speed, (b) lateral acceleration, (c) gear shifted and (d) displacement.

Table 2.1. Results comparation and approximation error of the RC.

Dynamic event	**Simulation result**	**Approximation error**
Acceleration event	5.06 s	4.17%
Skidpad event	5.73 s	4.34%

In reference to Table 2.1., it is important to note that the results of the IVDS show lower times than the results reported for the RC during the participation of the car in the competition events. Additionally, the approximation error has a similar value for both the acceleration and skidpad events. The outcome of this analysis is that the IVDS can be carried out as a useful tool to determine a prediction or estimation of the performance of the vehicle in accordance with the dynamics of the vehicle. The effectiveness of the IVDS lies in the veracity of the modeled vehicle and the parameters used to conduct the simulation. In this thesis project, the data and results for the design process of the formula-style racing car are strongly related to the IVDS, as mentioned in further chapters.

Chapter 3: Conceptual development of the racing car

At the conceptual development stage of the formula-style racing car, the design specifications and the technical requirements presented in Chapter one are related with physical concepts and operating principles to perform the desired functions for the single seater. Later, a list of criteria is determined and that is used as basis to evaluate and select the concepts and components that are best suited to the requirements. Moreover, it is in the stage that the key component selection and the material selection for the formula-style racing car are developed.

The design process is used to perform the conceptual development stage. To ensure accurate results in the design process, a methodology is defined for the formula-style racing car design process. This methodology for this design process is based on approaches that are reported in the literature [6], [23]. Notwithstanding, the methodology used for the design of the formula-style racing car is adjusted and modified through the course of this thesis project. Furthermore, the detailed explanation of the methodology used is reported on future sections of this document.

The conceptual development stage for the Formula SAE consists of the functional requirements, the key component selection, the criteria for generation and evaluation of conceptual alternatives and finally the analysis and evaluation of conceptual alternatives. For the sake of simplicity, the sequence for the conceptual development stage is presented in a different order to which the design process was carried out.

3.1. Functional requirements

As mentioned previously, the evaluation of the performance of the participant racing cars at the Formula SAE and spin-offs competitions is defined by the accomplishment of the static and dynamic events. Hence, the effectiveness of a designed single seater is strictly related to the events of the competition and the functional requirements must be based on these events. With the aim of the definition of operational principles for the motorized vehicle, a group of activity analysis tools are utilized as a basis for the functional requirements.

The first activity analysis method to be presented is the usage-disposure method. The usage-disposure method enables the examination of the tasks for the use of the formula-style racing car until the retirement of the car. The usage-disposure method may serve as a basis for maintenance planning, operation manual and technical data allocation. These tasks are directly carried out by the team that works with the vehicle, which in accordance with the Formula SAE regulations must be integrated only by graduate or undergraduate students. The sequence on which the activities are presented into the usage-disposure method does not consider the effective time that it takes to perform the listed tasks. The usage-disposure method for the formula-style racing car is presented in Table 3.1, in which the activities are classified into usage or disposure and later subclassified into assembly, inspection, set up and usage, storage, repositioning and disposure for the motorized vehicle.

Table 3.1. Usage-disposure method for the formula-style racing car.

Classification	Stage	Activities
Usage	Manufacture	Standard parts acquisition Quality control check and metrology OEM parts manufacture
	Assembly	Engine assembly and tuning Racing car assembly Wiring set up
	Inspection	Detailed inspection Compliance with regulations Fluid and fuel check Performance testing
	Set up	Tire compound selection Powertrain configuration Vehicle systems calibration Vehicle settings customization
	Use	Pre-stint and safety inspection Engine ignition protocol Strategy execution Engine shutdown protocol
	Maintenance	Regular check Wear monitoring Fluid check and refill Powertrain maintenance plan
Disposure	Disposal	Car decommissions after competition life cycle Disposal of used tires and fluids
	Recycle	High-value components salvage Material recycling Part repurposing End-of life recycling

Later, the function-behavior and function-structure matrix (FBM) framework is developed for the vehicle. The objective of this framework is to map the functions for the racing car to the behavior of the car during operation and the components that integrate the car. The framework helps to better understand the system works and how the components work together and support each other to achieve the car's overall goal. Another important use for the matrix is to mark the operating threshold for the car and define possible opportunity areas for the vehicle in further analysis. The function-behavior and function-structure matrix (FBM) for the formula-style racing car is presented in Table 3.2. The function-behavior and function-structure matrix is integrated by a column for the functions, the operating or working principles, the behavior and the structure for the racing car. The structure is set for the clusters defined previously in Chapter one with the information in Table 1.4.

Table 3.2. FBM method for the formula-style racing car.

Function	Working principle	Behavior	Structure
Propulsion	Newton's laws of motion Energy conservation Torque and power transmission Friction and traction Bernoulli's principle	Vehicle acceleration and torque delivery	Power transmission cluster
Braking	Newton's laws of motion Energy conservation Friction and traction Pascal's principle Bernoulli's principle	Vehicle deceleration and motion response	Dynamic control cluster
Handling	Torque and power transmission Newton's laws of motion Continuum mechanics	Steering input response	Dynamic control cluster
Stability	Damped harmonic oscillator Continuum mechanics Bernoulli's principle	Vehicle balance, handling and stability	Dynamic control cluster; Enclosure cluster
Continuous operation	Continuum mechanics Thermodynamics Resonance Material fatigue Circuit theory Embedded electronics	Maintain the systems for the engine and the vehicle operating in range	ICE systems cluster; Electrical cluster
Safety	Continuum mechanics Resonance Material fatigue	Provide safety conditions for operating the vehicle	Dynamic control cluster; Enclosure cluster
Comfort and control	Continuum mechanics Driver feedback	Vehicle ease of control	Enclosure cluster
Aesthetics	Visual identity Surface texture Auditive threshold	Vehicle identification and operation	ICE systems cluster; Enclosure cluster

The information of the FBM for the formula-style racing car in Table 3.2. helps to directly recognize the clusters related to working principles for the racing car. Both methods presented above are used to define the initial aspects of conceptual development.

3.2. Selection of key components for IVDS

With the functional requirements defined by means of the methods presented above, the next step for the conceptual development stage corresponds to the key components' selection. This section implies considering the functional requirements and the objectives of the racing car for the intention to define the parameters to be used in an IVDS for the formula-style racing car.

Eventually in the selection process, the weighted rating evaluation matrix (WREM) is used as a method to evaluate alternatives within a list of criteria. For the sake of standardization, a unique rating scale is set for the selection process in this stage and further selection processes in this thesis. The rating scale for the selection process is presented in Table 3.3.

Table 3.3. Rating scale for the WREM for the selection process.

Rating	Label	Description
1	Extremely poor	Does not meet the requirements, it includes significant deficiencies.
2	Poor	Meets the requirements, but with significant deficiencies.
3	Average	Meets the requirements adequately, with room for improvement.
4	Good	Meets the requirements well, with minor issues.
5	Excellent	Exceeds the requirement, with no apparent issues.

3.2.1. Selection process of the ICE and transmission group

The ICE and transmission group are selected from among commercial options to be part of the vehicle to be designed. These options correspond, but are not limited, to motorbike engines and transmission. Even though there are many more options, the motorbike engines and transmission are considered as the best alternatives because of the performance threshold that could take advantage of. For instance, the selection of the ICE and transmission group is limited by the design specifications listed in Table 1.5. Therefore, the alternatives proposed for the selection of the ICE and transmission group must be compliant with the design requirements and, consequently, with the Formula SAE regulations.

The alternatives listed are included in view of characteristics such as the displacement of the engine, the number and arrangement of the engine cylinders and the peak power, as well as the compliance of the four-stroke cycle. Other characteristics that the listed alternatives share is the dual overhead camshaft, the liquid cooling system for the engine and the 6-gear primary transmission. The alternatives for the ICE and transmission group are detailed below in Table 3.4. The code for identification of the make and model of the ICE and transmission group indicates a make and a specific model.

It is important to note that many of the possible alternatives for this selection process are discarded because of several reasons. One of the main reasons is the availability of the engine and transmission group or the ability to find spare parts for some of the options. Later, more data for the selection process is used to determine the criteria of selection.

Table 3.4. Alternatives for the ICE and transmission group selection.

Code reference	Displacement	Cylinders	Peak power
ARS	659 cc	2 cylinders inline	98.56 HP (73.5 kW) at 10,500 rpm
HCB	599 cc	4 cylinders inline	118 HP (88 kW) at 13,500 rpm
KNZ	636 cc	4 cylinders inline	128 HP (95.4 kW) at 13,500 rpm
MVF	675 cc	3 cylinders inline	128 HP (94 kW) at 14,500 rpm
SGS	599 cc	4 cylinders inline	124 HP (92.5 kW) at 13,300 rpm
TDR	675 cc	3 cylinders inline	128 HP (94 kW) at 12,500 rpm
YZF	599 cc	4 cylinders inline	116 HP (86.5 kW) at 14,500 rpm

Within the alternatives listed in Table 3.4., most of the ICE and transmission group options exceed 75 kW of peak power. This is attributed to a design constraint proposed by the team, given that this thesis project covers the first formula-style racing car to be developed for the team and it is probable that the car is going to exceed the average weight of this type of car. Therefore, the torque capacity for the traction tires can be greater and a way to take advantage of this is to have the greater power possible available. The selection of the ICE and transmission group a set of parameters are considered and the impact on the engine and transmission is determined. With this data gathered, the parameters for the analysis of the selection process of the ICE and transmission group are listed in Table 3.5.

Table 3.5. Analysis parameters for the ICE and transmission group selection.

Code reference	Bore-to-stroke ratio	Weight-power ratio	Fuel economy	Relative cost
ARS	1.26 mm/mm	1.86 kg/HP	20.18 km/L	0.99
HCB	1.57 mm/mm	1.64 kg/HP	11.33 km/L	0.77
KNZ	1.48 mm/mm	1.54 kg/HP	17.70 km/L	0.77
MVF	1.72 mm/mm	1.35 kg/HP	11.68 km/L	0.83
SGS	1.57 mm/mm	1.51 kg/HP	14.86 km/L	0.75
TDR	1.41 mm/mm	1.43 kg/HP	13.09 km/L	0.75
YZF	1.57 mm/mm	1.64 kg/HP	15.22 km/L	0.91

One of the most difficult parameters to be acknowledged is the weight-power ratio of the ICE and transmission group. This parameter can be approximated with the weight of the motorbike to which the engine and transmission are normally associated and the peak power that is presented in Table 3.4. Another relevant parameter is the stroke-to-bore ratio of the engine. Aspects such as the internal friction and durability of the engine are dependent on an optimal stroke-to-bore ratio for the engine, as mentioned in the findings of Filipi and Assanis [28]. However, the stroke-to-bore ratio may help to define an engine's behavior towards efficiency, thermal loads and heat transfer capacity. On the other hand, the fuel economy is defined as a measurement of the relation between the distance traveled by the vehicle and the fuel consumption of the engine. There exist a compilation of data towards the analysis of fuel economy for the motorbikes listed [29]. The reported data is presented in this thesis project in the units of km traveled for every liter consumed. In a similar way, the relative cost parameter is obtained in a ratio of the cost of the motorbike and the most expensive motorbike from the alternatives consulted.

Finally, the criteria for the selection of the ICE and transmission group is defined using the information of Table 3.5. The criteria consist of NHV, efficiency, heat transfer capacity, reliability, relative cost, fuel economy, weight-power ratio and availability of the engine and transmission group. It is critical to take into account that these criteria are strongly related to the analysis parameters previously defined and that most of the criteria are highly associated with the engine rather than the transmission. The corresponding criteria for the selection of ICE and transmission group are listed in Table 3.6. The data is presented in the weighted raiting evaluation matrix (WREM) apart from the weights assigned to the criteria for the sake of confidentiality. Although, the weight assigned to the criteria may vary from vehicle design to others. The WREM is worked out using the standard rating scale in Table 3.3.

Table 3.6. WREM for the ICE and transmission group selection.

Criteria	**Alternatives for selection**						
	ARS	**HCB**	**KNZ**	**MVF**	**SGS**	**TDR**	**YZF**
NHV	0.2	0.4	0.4	0.3	0.4	0.4	0.4
Efficiency	0.12	0.48	0.36	0.6	0.48	0.24	0.48
Heat transfer	0.4	0.16	0.24	0.08	0.16	0.32	0.16
Reliability	0.4	0.5	0.4	0.5	0.5	0.5	0.5
Relative cost	0.3	0.6	0.6	0.45	0.6	0.6	0.3
Fuel economy	0.75	0.3	0.6	0.3	0.45	0.45	0.45
Weight-power ratio	0.4	0.6	0.8	1	0.8	1	0.6
Availability	0.3	0.5	0.5	0.2	0.4	0.2	0.4
Total score	2.87	3.54	3.9	3.43	3.79	3.71	3.29

Based on the WREM in Table 3.6., the selected ICE and transmission group corresponds to the group labeled with KNZ. As a reference to further analysis, a list of technical specification data for the KNZ ICE and transmission group is presented in Table 3.7.

Table 3.7. Technical specification data for the ICE and transmission group for the formula-style racing car.

Item	**Specification**	**Item**	**Specification**
Engine type	Four-strokes	Cooling system	Liquid cooled
Cylinder configuration	4 cylinders inline	Lubrication system	Wet sump
Displacement	636 cc	Clutch type	Wet multi-disc
Compression ratio	12.9:1	Transmission	6-speed

3.2.2. Selection process of the wheels and tires

The assembly of the wheels and tires must integrate parts such as the knuckle, the wheel hub or the elements for the brake system, as mentioned by Wheatley and Zaeimi [30]. Therefore, the wheel assembly contemplates the union of elements to provide interaction with the suspension system, the brake system, the steering system or the powertrain. Although, at this stage the wheel assembly is not properly defined, neither are the elements of the other systems. However, the wheels and tires selection process aboard the wheel assembly among two specific elements: the rim and the tire.

The first element to be selected is the tire. The tires for the formula-style racing car are involved directly in the performance of the car because of their relation to the traction capacity and other behavior characteristics that may vary during the action on track. For this design, the formula-style racing car mounts an ICE and transmission group. The previous selection of an ICE and transmission group serves as a basis for the selection of the tires for the racing car.

The mechanical power developed by the ICE is later transmitted to the primary transmission with the coupling of the clutch. Then, the secondary transmission receives the mechanical power and guides it to the traction axle of the car. While the power transmission takes part from element to element, the torque and angular frequency vary in relation to the drive ratio. Consequently, the torque transmitted to the wheels is one of the main factors to be considered for the selection of the tires. Among the variables that define the behavior of the tires, parameters such as the friction coefficient, the slip ratio, the camber stiffness, the normal load sensitivity and the load transfer sensitivity affect the vehicle's capacities and handling, as described in the findings of Smith [31]. Nevertheless, other relevant parameters that might be used as a criterion are the weight of the tire, the tire compound, the tire construction and the size of the tire.

With the aim of clearance, the size of the tires is presented as commonly reported by most of the manufacturers. The tire size consists of the height of the tire, the width of the tire and the diameter of the wheel, reporting these dimensions in inches.

The tire compound has a direct impact on the durability of the tire. A harder compound allows better damping for the loads applied on the tire, the load capacity is greater, and the wear of the tire tends to be lower. On the other hand, a softer compound has a greater friction coefficient, which translates into a better grip than the grip for harder compounds.

A reduced weight of the wheels implies a lower unsprung mass and facilitates the action of the vehicle's suspension [21]. Additionally, the weight of the wheels and the tires is involved in the dynamics of the vehicle, being part of the weight of the vehicle and affecting the acceleration and deceleration times of the car. Another aspect is the tire spring rate, which is a measurement of the stiffness that the tire construction has towards the application of a certain load. The tire spring rate plays a significant role in this analysis because of the relation with the overall handling, ride comfort, and performance of the car. A higher tire spring rate may provide less compression while being loaded and more precise handling, but it may affect ride comfort.

A set of manufacturers for FSAE tires are listed in the literature [32]. The tires for the Formula SAE competition must be compliant with the guidelines emitted by the organizers of the competition but also must be available with a tread surface for dry and wet conditions on the track. However, not many of the manufacturers provide the data of the tires adequately out of specialized databases. The tire selection alternatives and the available data for the tires are listed in Table 3.8.

Table 3.8. Alternatives for tire selection of the formula-style racing car.

Model	**Tire size**	**Mass**	**Compound**	**Tire spring rate**	**Relative cost**
H070	$16.0 \times 6.0 - 10$	3.17 kg	LCO, R20	126.44 kN/m	0.88
H075	$16.0 \times 7.5 - 10$	3.63 kg	LCO, R20	150.43 kN/m	0.98
H100	$18.0 \times 6.0 - 10$	4.08 kg	R20	141.52 kN/m	0.88
H105	$18.0 \times 7.5 - 10$	4.53 kg	R25B	156.38 kN/m	0.98
A616	$16.0 \times 6.0 - 10$	3.4 kg	A92	DNA	DNA
A716	$16.0 \times 7.0 - 10$	3.5 kg	A92	DNA	DNA

In relation to the data in Table 3.8., the LCO compound is the softer compound available among the alternatives presented, while the R20 and R25B are both harder and relatively similar in characteristics. The A92 compound is a soft compound and there is no hard compound equivalent for this tire model. In addition, the tire spring rate presented for the alternatives listed are reported from the data provided by the manufacturer at a tire pressure of 14 psi and a reported load of 1780 N as a reference.

The tire selection is continued with the criteria explained above and the WREM for the tire selection process is presented in Table 3.9. Although only four of the alternatives are taken into account for the evaluation as the characteristics are similar in some of the alternatives. The data is presented in the WREM apart from the weights assigned to the criteria for the sake of confidentiality and simplicity. The WREM is worked out using the standard rating scale in Table 3.3.

Table 3.9. WREM for the tire selection.

Criteria	**Alternatives for selection**			
	H070	**H100**	**H105**	**A616**
Mass and inertia	0.4	0.4	0.3	0.4
Tread surface	0.3	0.3	0.4	0.3
Durability	0.6	0.75	0.75	0.6
Grip	0.6	0.45	0.45	0.6
Load capacity	0.3	0.4	0.4	0.3
Handling	0.45	0.6	0.6	0.3
Comfort	0.2	0.15	0.15	0.1
Relative cost	0.8	0.8	0.6	0.6
Total score	3.65	3.85	3.65	3.2

Based on the WREM in Table 3.9., the selected tire corresponds to the model labeled with H100. This tire is available is R20 compound and the tire size is reported in Table 3.8. Once the tire is selected, the alternatives for a rim are searched based on the dimensions of the tire.

Table 3.10. Alternatives for wheel rim selection of the formula-style racing car.

Model	**Rim size**	**Material**	**Process**	**Mass**	**Fastening**	**Relative cost**
KLA	6 × 10	Aluminum	Forging	DNA	4 Lug nuts	0.34
KCA	6 × 10	Aluminum	Forging	DNA	Central nut	0.34
OZC	7 × 10	Magnesium	Casting	1.66 kg	Central nut	0.48
BLA	6 × 10	Aluminum	Forging	2.26 kg	4 Lug nuts	0.80
BCA	6 × 10	Aluminum	Forging	3.17 kg	Central nut	1.00
GTM	7 × 10	Aluminum	Forging	DNA	4 Lug nuts	0.14

The wheel rim can be designed and manufactured with different structures, materials and processes. Within the commercial options available, rims can be found made by casting or forging, as well as with materials such as aluminum or magnesium alloys. Additionally, another characteristic to mark is the fastening method used to secure the rim to the wheel hub. Lug nuts are one of the main fastening methods, while another method is using centerlock wheel rims. Taking this into account, the wheel rim selection alternatives and the available data for the rims are listed in Table 3.10.

It can be noticed in Table 3.10 that some manufacturers omit some data in relation to the parameters listed in the information. This complicates the definition of the criteria to select the wheel rims for the vehicle. Enabling only four of the alternatives for the wheel rims, the data is presented in the WREM apart from the weights assigned to the criteria for the sake of confidentiality and simplicity in Table 3.11. The WREM is worked out using the standard rating scale in Table 3.3.

Table 3.11. WREM for the wheel rim selection.

Criteria	Alternatives for selection			
	KLA	**OZC**	**BLA**	**GTM**
Weight	0.6	1.0	0.8	0.6
Practicality	0.4	0.3	0.4	0.4
Strength	0.6	0.45	0.6	0.6
Availability	0.3	0.2	0.3	0.4
Durability	0.45	0.6	0.6	0.6
Size	0.3	0.4	0.3	0.3
Relative cost	0.8	0.6	0.4	1.0
Total score	3.45	3.55	3.4	3.9

According to WREM in Table 3.11., the selected wheel rim corresponds to the model labeled with GTM. The GTM wheel rims are manufactured with a negative offset, which means that the wheel's mounting surface is located forward the back of the centerline of the rim. This feature is commonly encountered in performance cars, although the selected wheel rims are not intended for this car style. For the sake of being able to reference the dimensions of the wheel rim, the wheel rim dimensional parameters are illustrated in Figure 3.1.

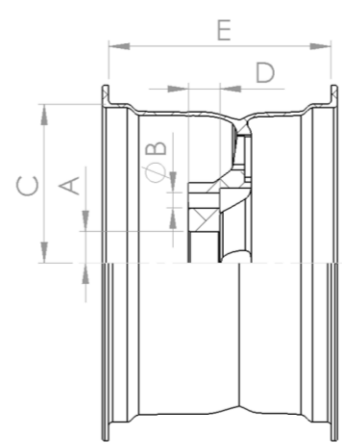

Figure 3.1. Wheel rim geometry and dimensional parameters.

In reference to the measurements, as shown in Figure 3.1., the dimensional parameters are defined as follows:

- Parameter A: Nominal radius of the center bore of the wheel rim (A_{wr}).
- Parameter B: Nominal diameter of the lug holes of the wheel rim (B_{wr}).
- Parameter C: Nominal radius of the barrel of the wheel rim (C_{wr}).
- Parameter D: Width of the hub mount plate of the wheel rim (D_{wr}).
- Parameter E: Wheel rim width (E_{wr}).

Later, with the ICE and transmission group, the tires and the wheel rims already selected, the first approach for the performance of the formula-style racing car can be carried out with the IVDS.

3.3. Criteria for the generation and evaluation of conceptual alternatives

The conceptual alternatives for the formula-style racing car are provided in relation to the clusters presented in Table 1.4. Below, the conceptual alternatives are listed in relation to the systems and components that integrate the clusters of the formula-style racing car.

3.3.1. Conceptual alternatives for the power transmission cluster

The powertrain connects the ICE and transmission group with the wheels and tires of the car through different elements with the aim of transmitting the mechanical power developed by the ICE and enable the traction force at the tread surface of the tires of the drive wheels in the configuration of the car. Therefore, the powertrain must incorporate a series of components that provide a link from the primary transmission to the wheels of the car in the rear axle. Among the elements that participate in the transmission of mechanical power are the secondary transmission, the differential and the axles.

Taking this into account, one of the main decisions to consider in the powertrain is the connection between the secondary transmission and the axles. The formula-style racing car must include a differential to define the turning efficiency, prevent tire wear, distribute the power to the drive wheels and enable traction in different conditions. There are several types of differentials for the use in all kinds of vehicles. Open differentials, limited slip differentials and locking differentials are examples of the types of differentials available, as mentioned by Marciano et al. [33].

Although, the secondary transmission for the vehicle must consider the possibility to incorporate either chain, belt or gear drive. The priority option is the one similar to the secondary transmission of a motorbike, which is a chain drive. In addition, the axle joints can be worked out depending on the differential alternatives and the design of the wheel assembly. CV joints, U-joints and slip yokes are among the alternatives that can represent an option to connect axles, differentials and wheels.

On the other hand, the wheel assembly consists of several elements. This is because the wheel is an interface of the functions of many vehicle systems. The wheel assembly is integrated in general of the tire, the wheel rim, the wheel hub, the knuckle and the bearings. However, the connection and interaction between these elements may vary depending on the components selected.

For instance, the selection of the wheel rims and the tires has already been done at this point and the selection of the bearings must consider the geometry of the parts that the bearings is going to connect. Therefore, the conceptual alternatives for the wheel assembly are separated into alternatives for the wheel hub and the knuckle. The conceptual alternatives must consider aspects such as how the bearings are going to be mounted in relation to wheel hub and knuckle, how the power transmission is done from the axles to the wheel assembly and the way both the wheel hub and the knuckle connect with other elements of the steering, suspension and braking systems are carried out. The conceptual alternatives for the power transmission cluster are listed below and presented into three different concepts in Table 3.12.

Table 3.12. Conceptual alternatives for the power transmission cluster.

Functions	**Conceptual alternatives**		
	Concept A	**Concept B**	**Concept C**
Transmission	Chain drive	Belt drive	Gear drive
Power split	Open differential	Limited slip differential	Locking differential
Axle joints	U-joints	CV joints	Slip yoke
Bearing mounting	Outer ring to wheel hub with press fits	Inner ring to wheel hub using withdrawal sleeves	Inner ring to wheel hub with set screws
Power transmission to wheel assembly	Spindle	CV joint and spline shafts	Direct shaft connection
Wheel hub links to brake elements	Integrated hub and disc	Bolted joint	Floating brake disc
Mounting of the wheel hub	Welded joint	Studded joint	Tapered joint
Knuckle link to steering and suspension parts	Integrated joints	Bolted mount brackets	Machined mount surface

3.3.2. Conceptual alternatives for the ICE systems cluster

The ICE and transmission group requires assistance from various systems to provide adequately the air flow and fuel injections for the combustion reaction and the escape of the combustion products out of the combustion chambers, as well as to maintain correct lubrication and the operating range of temperature inside the ICE and transmission group. Consequently, the ICE systems cluster is integrated by intake system, injection system, exhaust system, cooling system and lubrication system. The conceptual alternatives for these systems are outlined below for your reference.

The ICE systems cluster design is directly related to the ICE and transmission group selected. Therefore, the parameters of the ICE and transmission group selected as well as the systems for the motorbike must be acknowledged to be considered further on in the generation of alternatives to serve as a basis. The relevant technical data concerning the ICE systems of the motorbike KNZ are presented in Table 3.13.

In relation to the intake system, the sequence of the elements of the intake system for the formula-style racing car must satisfy the Formula SAE regulations. In fact, forced induction is not considered in this analysis because of the power threshold delivered by the ICE as an atmospheric engine. Without considering forced induction for the ICE, the sequence defined by the Formula SAE regulations must be throttle body, restriction and engine [8]. This sequence is slightly different to the one used in the motorbike KNZ. Consequently, it is difficult to maintain some of the elements in the intake system that were used in the KNZ. Besides the sequence of the intake system, the conceptual alternatives must consider the air cleaner element, the plenum geometry and the attachment of the system.

Table 3.13. Technical data of the ICE systems from the KNZ.

Item	Specification	Item	Specification
Air cleaner element	Viscous paper	Exhaust emission control	Three-way catalytic converter
Throttle body assembly	Dual throttle valve	Lubrication system	Wet sump
Throttle body bore	38 mm	Oil viscosity	SAE 10W-40
Carburetion system	Fuel injection	Oil capacity	3.6 L
Fuel injector type	EAT289	Cooling system	Liquid cooled
Fuel minimum octane rating	95 RON	Thermostat opening temperature	58 – 62°C
Fuel pump discharge	1 L/min	Coolant mix ratio	1:1 (water, coolant)
Fuel tank capacity	17 L	Coolant capacity	2.5 L

For the injection system, the Formula SAE regulations state the use of fuels provided by the organizers of the events and the guidelines regarding the fuel tank and fuel lines for the system [8]. The KNZ injection system consists of the fuel tank, the fuel pump, the fuel lines, the fuel rail, the injectors and the throttle body. Notwithstanding, the injection system for the formula-style racing car must consider the sequence for the elements of the intake system and the possibility to use only some elements from the KNZ fuel injection as a basis for the car. A non-modified fuel rail is permitted for the car in compliance with the Formula SAE rules, so the injectors and the fuel rail must remain in the system. Therefore, the conceptual alternatives for the injection system involve geometry, ventilation and attachment of the fuel tank. However, other parts such as the fuel lines must be considered further in the analysis.

The KNZ exhaust system integrates a three-way catalytic converter and an exhaust valve. Although these are important components for the motorbike, for the formula-style racing cars are not considered as there is no significant use for those components. Hence, the exhaust system for the vehicle consists of the exhaust manifold, the exhaust pipes and the muffler. As the exhaust manifold can be used from the KNZ exhaust system, the conceptual alternatives for the exhaust system consider the muffler geometry and the attachment of the system.

On the other hand, the cooling system for formula-style racing car is constrained by the Formula SAE regulations in terms of the coolant, which must be soft water with no other additives [8]. This assumption is considered in the analysis of the cooling system and the components for the racing car are selected for the operation with soft water and the ideal coolant. In relation to the cooling system of the KNZ, the coolant pump is integrated in the ICE and transmission group and no other parts can be used rather than connections and pipes. Consequently, the alternatives for the cooling system are towards the geometry of the radiator and the radiator fan.

In the case of the lubrication system, there are barely any aspects directly regarding the lubrication of the engine and transmission in the regulations of the competition. As a result, the alternatives for the lubrication system of the formula-style racing car are just towards the use of a modified lubrication system for the ICE and transmission group.

Table 3.14. Conceptual alternatives for the ICE systems cluster.

Functions	Conceptual alternatives		
	Concept A	**Concept B**	**Concept C**
Air cleaning	Foam air filter	Cotton gauze air filter	Carbon fiber air filter
Plenum flow	Single-plane long-runner plenum	Single-plane short-runner plenum	Dual-plane short runner plenum
Intake system attachment	Mounting clamps	Quick-release mounts	Hanging mounts
Fuel storage	Split tank	Bladder tank	Vertical tank
Fuel tank ventilation	Open ventilation	Check valve ventilation	Carbon canister
Fuel tank attachment	Floor mounting	Direct bolt-on mounting	Cradle mounting
Noise reduction	Chambered muffler	Straight-through muffler	Multi-pass muffler
Exhaust system attachment	Rubber hanger mounts	Spring-loaded brackets	Rigid bracket mounts
Heat transfer	Crossflow radiator	Downflow radiator	Dual-pass radiator
Radiator air flow	Mechanical fan	Electric fan	Variable-speed fan
Lubrication	Wet sump lubrication	Semi-dry sump lubrication	Dry sump lubrication

3.3.3. Conceptual alternatives for the electrical cluster

The electrical cluster includes components that enable the ignition, charging and control of the ICE and transmission group parameters and operation. To provide a reference for the components and systems of the electrical cluster, the KZN electric and electronics technical data specifications are listed in Table 3.15.

Table 3.15. Technical data of the electrical system from the KNZ.

Item	Specification	Item	Specification
Battery capacity	12 V 8 Ah	Electric starter system	Starter motor
Charging system	Three-phase AC	Ignition system	Transistor ignition
Charging voltage	14.3 – 14.7 V	Spark plug type	NGK CR9E

Even though the components and systems for the electrical cluster are almost related to the KNZ motorbike, there are still some regulations to be evaluated with the aim of being compliant with the Formula SAE rules. As mentioned in the Formula SAE rules [8], the battery must be securely mounted to the chassis, the engine must be started every time using a starting system on board and the electrical wiring must consider the inclusion of a set of switches in a circuit for different purposes in the car.

The KNZ electrical installation includes a battery, an alternator, a starter motor, a set of ignition coils and spark plugs, an ECU, an arrangement of sensors and switches, a fuse box and a relay box. These elements integrate the ignition system, the electric starter system, the charging system and the engine control system for the KNZ motorbike. Even though most of these elements could remain for the formula-style racing car, some elements are mandatory for the electrical installation of the car and others must be removed. One of the main elements to analyze are the sensors available for the KNZ electrical system. After carrying out the scrutiny, the sensors that must remain for the formula-style racing car are listed in Table 3.16.

Table 3.16. Sensor scrutiny for the electrical cluster of the formula-style racing car.

Sensor	Function	Use in the electrical cluster
IAT	Measure air temperature at the intake system.	ECU adjustment of the fuel mixture.
IMP	Measure air pressure at the intake manifold.	ECU adjustment of air and fuel ratio.
CKP	Monitor the crankshaft position and speed.	Ignition timing and fuel delivery.
TPS	Detect the position of the throttle valve.	Throttle response and fuel management.
ECT	Measure engine coolant temperature.	ECU adjustment of ignition timing, fuel mixture and cooling system parameters.

Similar scrutiny is carried out for the switches in the electrical system. Although most of the switches in the KNZ electrical system are also useful for the operation of the ICE and transmission group in the racing car, still some switches such as the sidestand switch do not meet any function in the car and must be removed from the electrical installation for the vehicle. As mentioned further in the design process for the racing car, some other switches must be incorporated to be compliant with the Formula SAE regulations.

Taking this information into account, the conceptual alternatives for the electrical cluster must consider the display of the information at the cockpit, the starting procedure for the engine, the scale of the telemetry used in the car, the battery type and the ECU tuning. The conceptual alternatives for the electrical cluster for the formula-style racing car are presented in Table 3.17.

Table 3.17. Conceptual alternatives for the electrical cluster.

Functions	Conceptual alternatives		
	Concept A	Concept B	Concept C
Information display	Dashboard	Steering wheel display	Gauge
Starting mechanism	Key ignition	Push-button start	Switch start
Telemetry	Basic telemetry	Intermediate telemetry	Advanced telemetry
Battery use	AGM battery	VRLA battery	Flooded battery
ECU tuning	OEM ECU	OEM ECU tuning	ECU programming

3.3.4. Conceptual alternatives for the dynamic control cluster

The suspension, the steering and the braking system play a significant role in the safety and the driving experience of the driver. For instance, the suspension system must provide stability, the steering system allows precise control of the car, and the braking system ensures the ability to decelerate or stop when it is necessary during the operation of the formula-style racing car. Another important aspect to consider is that these three systems converge in a common point: the wheel assembly. Because of this reason, dynamic control cluster design depends on the wheels, as well as other relevant parts such as the chassis.

Starting with the suspension system, the suspension system can be classified based on several factors. However, most of the racing cars for the Formula SAE competition still use a particular type of suspension system. As noted by Bhatt [34], the double wishbone independent suspension is the common for performance cars because it is lighter than other suspension elements and offers easy packaging with a high degree of freedom in the design of suspension geometry. In addition, the double wishbone suspension is widely studied in the literature regarding synthesis and kinematics [35], [36].

Additionally, the double wishbone suspension can be defined by a pushrod or pullrod geometry. The racing car behavior is affected using either pushrod or pullrod suspension geometry in terms of aerodynamics or the location of the center of gravity. As stated in the findings of Saurabh et al. [37], many formula student cars use either pushrod and pullrod suspension in both front and rear wheels and a common arrangement is pushrod in the front with pullrod in the rear. Besides the common use of the suspension in other cars, the suspension geometry must be adapted to the racing car systems and stick to the design objectives defined previously. This decision is one of the most important towards the suspension system design for the racing car.

Considering the double wishbone suspension geometry and the possibility to incorporate either pushrod or pullrod suspension, the conceptual alternatives for the suspension system are generated regarding the acting of the suspension components, the spring type and the shock absorber type for the formula-style racing car.

Later, the steering system is established with the mechanism defined by the Ackermann geometry. In fact, the Ackermann geometry must adjust to the parameters of the car, mainly to the tires selected. Notwithstanding, the behavior of the tires is dependent on several factors. Among the factors that have a relation to steering geometry and the behavior of the tires, one to highlight is the slip angle and how it is affected by the lateral forced exerted on the contact zone of the tire's tread surface and the road surface.

Swamy et al. [38] reported several findings regarding the behavior of tires for a Formula Student racing car. Within these findings, one to emphasize is the strong correlation between lateral force, cornering stiffness and lateral grip of a tire and a faster reaction to steering output, as well as a lower energy loss. Hence, the use of Anti-Ackermann geometry can be proposed to improve grip, stability and response in steering during high-speed cornering.

The anti-Ackermann geometry or reverse Ackermann geometry is obtained when the intersections of the two rockers of the mechanism of the steering geometry are positioned in front of the front axle, as mentioned by Veneri and Massaro [39]. In other words, the steer exerted in the inner wheel while taking a corner is smaller than the steer in the outer wheel using an anti-Ackermann geometry. Therefore, a better option for the formula-style racing car is to use anti-Ackermann geometry because of several factors such as lateral load transfer, tire characteristics, high-speed cornering and stability.

In view of the anti-Ackermann geometry for the racing car and the need to translate a rotation input at the steering wheel of the car to the linear movement to control the mechanism of the steering system, the conceptual alternatives for the steering system must include the joints for the connection between the steering wheel and the mechanism, the steering column support, the mechanism to translate rotation into linear movement, and tie rod adjustment geometry.

Finally, the braking system for the formula-style racing car is mainly based on similar braking systems and components reported in the literature [13], [40], [41]. It is commonly found that the braking system incorporates a brake pedal within a pedal box, a pair of master cylinders to separate the front and rear wheels braking, brake fluid lines, calipers and brake discs. Therefore, the use of calipers and brake discs is widely encountered in Formula SAE cars, in detriment to use of drum brakes. The reduced ventilation, the complexity of the arrangement, the mounting and packaging, as well as not having the need for a parking brake are the reasons why the drum brakes are not considered for this type of car. Due to this, the alternatives for the braking system also consider the use of a caliper and a brake disc.

As a result, the conceptual alternatives for the braking system involve the use of the master cylinders in the circuit, the caliper type and the geometry of the disc brakes to be used in the formula-style racing car. The conceptual alternatives for the dynamic control cluster are all presented below in Table 3.18.

Table 3.18. Conceptual alternatives for the dynamic control cluster.

Functions	**Conceptual alternatives**		
	Concept A	**Concept B**	**Concept C**
Suspension action	Pushrod suspension	Direct-acting suspension	Pullrod suspension
Spring use	Rubber springs	Progressive coil springs	Linear coil springs
Damping	Gas-charged shock	Electromagnetic shock	Air shock
Steering joints	Single U-joint	Double U-joint	Right-angle steering
Steering column support	Hanging bearings	Mounted bearings	Rigid mounts
Steering mechanism	Rack and pinion	Recirculating ball	Cable steering
Tie rod adjustment	Threaded tie rods	Sliding sleeve tie rods	Turnbuckle tie rods
Master cylinder use	Single master cylinder	Tandem master cylinders and balance bar	Tandem master cylinders
Caliper use	Single-piston caliper	Double-piston caliper	Four-piston calipers
Disc brake use	Drilled disc	Ventilated disc	Slotted disc

3.3.5. Conceptual alternatives for the enclosure cluster

The enclosure cluster is integrated by the chassis, the cockpit, the driver controls and the bodywork for the formula-style racing car. These components may acquire different functions for the racing car, but still these elements have some common points. Although all these parts are relevant for the car, one of the most crucial for the design of the formula-style racing car is the chassis.

The chassis design must be compliant with the Formula SAE regulations and a great amount of guidelines and constraints are mentioned in the rules for the competition [8]. First, the chassis for a Formula SAE car must be either a tubular spaceframe or a monocoque. For the sake of simplicity and with the aim to develop the first racing car design, the selected option for the chassis of the vehicle is a tubular spaceframe. Thus, the chassis consists of two roll hoops, which are the front hoop and the main hoop, and a front bulkhead; these sections of the chassis are connected by means of frame members to form a side impact structure, supports and braces. The chassis sections and structures for the tubular spaceframe are mandatory and, in most cases, must be considered a proper triangulation, which means that the frames must form a structure composed entirely of triangles in a side view. Finally, the chassis is completed when an anti-intrusion plate and an impact attenuator are assembled at the front of the tubular spaceframe in accordance with the guidelines marked by the competition.

Some other guidelines of the competition, such as the structural equivalency spreadsheet (SES), provide more information in relation to a correct triangulation of the structures for the chassis and the adequate tubing dimensions and materials for certain sections of the tubular spaceframe. Before a correct triangulation is planned for the chassis, an important step is to define the front bulkhead and the roll hoops. These sections may serve as a basis to define the rest of the tubular spaceframe.

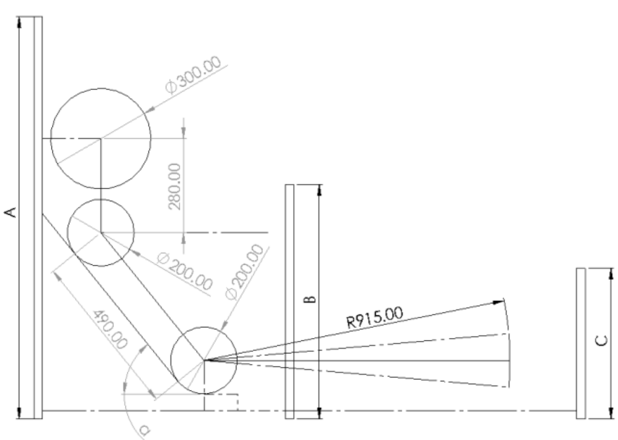

Figure 3.2. Driver template positioned in relation to front bulkhead and roll hoops.

The chassis must consider the cockpit geometry and the dimensions of this cockpit to be capable of providing accommodation for a vast range of drivers. As mentioned in the Formula SAE rules [8], the vehicle must be able to accommodate drives with sizes in range between 5th percentile female and 95th percentile male. In order to be compliant with this, the rules of the competition provide anthropometric data and three templates that can serve as a guideline for cockpit design. Those templates include the cockpit opening, internal cross section and driver template. A graphical representation of the location for the driver template and the roll hoops and front bulkhead of the chassis is shown in Figure 3.2. This illustrates the relation between the cockpit and the chassis, and it is used for the first approach for the chassis and cockpit geometry.

The parameters A, B and C represent the height of the main hoop, front hoop and front bulkhead, the α is the angle of the seat in relation to a horizontal line and all dimensions are in millimeters. In the case of the posture of the driver at the cockpit, the anthropometric data plays a significant role in the position, dimensions and angles of the cockpit. A comfortable position for the seat at the cockpit of a single seater must be considered [42]. In the findings of Sanchez-Alejo et al. [42] it is important to note that a comfortable position for the seat at the cockpit is defined by a set of angles to prevent injuries. For the specific case of the first iteration of the chassis and cockpit design, the angle for the driver's seat is established considering a 95^{th} percentile male.

Thus, the conceptual alternatives for the chassis consider three specific triangulations for the tubular spaceframe, which are presented with illustrations in Table 3.19. It is relevant to mention that the alternatives shown are directly taken from the SES and those take into account the front bulkhead supports, the side impact structure and the main hoop bracing supports. The shaded area in the alternatives of the main hoop bracing supports do not have to meet the requirement of proper triangulation.

In relation to the cockpit, not only the geometry and the dimensions for this zone are relevant, but the driver controls set for the driver. The driver controls consist of a steering wheel, a pedal box, a gear shifter and devices to operate towards the electrical installation and the ICE. Another relevant aspect is the seat and the harness to maintain the driver in the driving position during the operation of the formula-style racing car. In a similar way to the anthropological data in relation to the cockpit, the operation of some driver controls may vary from driver to driver. For example, a variation in the maximum force applied to the pedals at the pedal box exists in relation to males and females, as noted in the findings of Mačužić et al. [43]. For instance, the pedals and the pedal box must be able to adjust to different forces applied, mainly considering the activation of the braking system. Therefore, the conceptual alternatives for the driver controls and the cockpit contemplate the driver accommodation, the gear shifter activation, the pedal activation, the pedal box support and the interaction with the steering wheel.

On the other hand, bodywork for vehicles is one of the key features of design. The bodywork for the formula-style racing car not only determines the aesthetics and identification of the vehicle but also determines the aerodynamic response of the car. The aerodynamics is often more important than structural analysis for some designers as aerodynamics emerge to be the deciding factor between winner and loser [44]. Nevertheless, bodywork is integrated by different elements that may provide different functions for the car rather than aerodynamics. Therefore, the conceptual alternatives for bodywork take into account the bodywork joints, the aerodynamic devices included in the car, the floor design for the car and the aesthetics for vehicle identification.

Table 3.19. Conceptual alternatives for the enclosure cluster.

Functions	Conceptual alternatives Concept A	Concept B	Concept C
Front bulkhead support	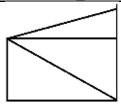	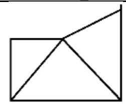	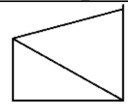
Side impact structure configuration	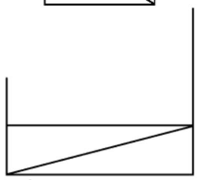	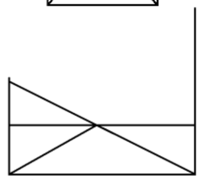	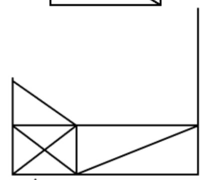
Main hoop bracing support	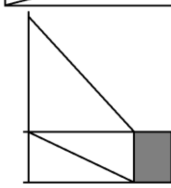	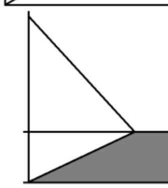	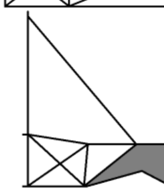
Driver accommodation	Custom seat	Adjustable seat	Standard seat
Gear shifter activation	Paddle shifter and fly-by-wire	Stick shifter and linkage mechanism	Stick shifter and cable
Pedal activation	Fly-by-wire pedal box	Mechanical pedal box	Custom pedal box
Pedal box support	Suspended pedal box	Floor-mounted pedal box	Integrated pedal box
Steering wheel interaction	Standard steering wheel	Steering wheel with integrated display	Multi-function steering wheel
Bodywork joints	Permanent joint	Non-permanent joint	Quick-release joints
Aerodynamic control	No devices	Complete aerodynamic devices	Basic devices
Floor air flow	Flat floor	Ventilated floor	Diffuser
Aesthetics	Vinyl wrap	Paint	Stickers

3.3.6. Criteria for the evaluation of the conceptual alternatives

For a proper evaluation, the criteria to evaluate the alternative concepts for the clusters must consider a vast range of factors. The criteria for the evaluation of the conceptual alternatives are divided into functional criteria, non-functional criteria, user-centric criteria and strategy criteria. The list and classification of the criteria for evaluation of the conceptual alternatives of the formula-style racing car is provided in Table 3.20.

Once the conceptual alternatives for the systems and components presented in the clusters above are listed, the concepts are evaluated using the criteria of evaluation in Table 3.20. With the aim of selecting properly the conceptual alternatives, the alternatives are combined to complete a combination matrix. The combination matrix consists of all the possible combinations of the alternatives for each of the concepts presented for the clusters, yet these combinations must consider physical principles and the practicality of the combination to be considered in the selection process. For the sake of brevity, the combination matrix is not provided here. However, the analysis of selected conceptual alternatives and key aspects are outlined below.

Table 3.20. Criteria for evaluation for conceptual alternatives of the formula-style racing car.

Classification	Criteria	Characteristics
Functional	Weight	Approximated mass of the alternatives
	Crashworthiness	Ability to protect the driver during collision
	Adjustable settings	Ability to modify performance and driving experience
	Number of joints	Connecting points, complexity and rigidity
	Efficiency	Relative performance of the car
	NHV	Cockpit comfort regarding noise, vibration and harshness during operation
	Aerodynamic response	Ability to manage air flow and stability
	Heat transfer capacity	Ability to dissipate heat
Non-functional	Cost	Overall financial feasibility
	Sustainability	Environmental impact and recyclability
	Reliability	Ability to perform consistently over time
	Availability	Accessibility of parts and technology required
	Practicality	Usability and everyday functionality
	Durability	Ability to withstand wear and stress
	Manufacturing complexity	Difficulty of producing the concept in relation to technologies and precision required
	Ease of assembly	Compatibility, time and labor for assembly
User-centric	Comfort	Ability to provide a pleasant driving experience
	Driving feedback	Ability to provide clear and responsive sensations from the car to the driver
	User interface	Functionality of the driver controls and systems
	Aesthetics	Visual appeal of the design of the car
Strategy	Competitive advantage	Unique features or capabilities

3.4. Analysis of conceptual alternatives

Furthermore, the selected alternatives are analyzed to determine the feasibility of the concepts proposed. Below, the analysis of the selected alternatives for some of the clusters is presented.

3.4.1. Power transmission cluster conceptual alternatives selection and analysis

As established in Table 3.12., the conceptual alternatives for the power transmission cluster consider transmission, power split, axle joints, bearing mounting for the wheels and aspects related to wheel hub and knuckle conceptual design.

First, the selected concept for the transmission function is the chain drive. This is not only because the KNZ motorbike secondary transmission uses chain drive, but also because it is the most practical way to link the output shaft of the ICE and transmission group to the differential. Chain drive power transmission allows constant transmission without critical slip between elements.

Using the information available in the literature for roller chain design [45] and the data from the ICE and transmission group selected, the chain drive is analyzed. The equation (3.1) defines the horsepower to be transmitted (H_d) taking into account the nominal horsepower (H_{nom}), a service factor (K_s) and a design factor (n_d). The horsepower to be transmitted is going to be contrasted with the allowable horsepower (H_a) defined by a correction factor (K_c) in case of a different number of strands or the use of other number of teeth rather than 17 and the tabulated horsepower (H_{tab}) in equation (3.2).

$$H_d = K_s n_d H_{nom} \tag{3.1}$$

$$H_a = K_c H_{tab} \tag{3.2}$$

Using the equation (3.1) and (3.2) as well as the nominal horsepower of the ICE and transmission group, the tabulated horsepower for the roller chain is determined. It can be used either chain number 428 or chain number 520. However, the most common type for motorbikes is chain number 520. Therefore, the chain drive is adequate for the formula-style racing car and the chain number is defined.

Hence, the selected concept for the power split function is a limited slip differential (LSD). A limited slip differential is a passive device used to improve traction capabilities, handling, and ultimately performance of racing cars, as noted by Gadola et al. [46]. The use of an LSD for the formula-style racing car may be considered at some point as a competitive advantage in terms of traction capabilities towards some scenarios such as limited grip track conditions. Later, after selecting an LSD for the racing car, the axle joints must be selected to best form the assembly.

In relation to wheel hub and knuckle conceptual alternatives, the selected concept consists of mounting the bearings for the assembly of wheel hub and knuckle so that the inner ring of the bearings is mounted towards the wheel hub and set in position using withdrawal sleeves for a practical assembly and disassembly. Meanwhile hub concept receives the power transmission through cv joints and splines in the geometry of the hub, uses bolted joints to link the disc brakes to the wheel hub geometry and studded joints to allow the connection with the rim of the wheels; meanwhile, the knuckle concept uses a fixed geometry to which a bolted mounted brackets link to be able to adjust the performance parameters with a higher level of adjustability.

3.4.2. ICE systems cluster conceptual alternatives selection and analysis

In reference to the information in Table 3.14., the conceptual alternatives for the ICE systems cluster are listed in relation to the intake, injection, exhaust, cooling and lubrication systems. Air cleaning, plenum flow and attachment are the functions for the intake system; fuel storage, fuel tank ventilation and attachment for the injection system; noise reduction and attachment for the exhaust system; heat transfer and radiator air flow for cooling system and finally lubrication for lubrication system.

The air cleaning elements may vary for the intake system, but still the cotton gauze air filter is the most practical option and the selected alternative for the racing car. For the plenum flow, the selected alternative corresponds to the single-plane short-runner plenum. Having short runners allows an improved throttle response and optimal torque at higher angular frequency of the engine, while a single-plane plenum reduces the volume required for the installation and simplifies the manufacture of the plenum. To attach these elements in compliance with the guidelines of the competition, the selected alternative is to secure the elements with mounting clamps.

For the injection system, the selected fuel storage concept is a bladder tank. An important characteristic of a fuel tank is the crashworthiness, defined as the ability of the fuel tank structure to protect the fuel inside and retard any possible fire after a crash [47]. Therefore, the best alternative for crashworthiness is a bladder tank, although it may be expensive, and the availability may vary. For the fuel tank ventilation, a single-way ventilation using a check-valve is the selected option because of factors such as fuel vapor release, safety and environmental impact. To attach the fuel tank, the selected concept is to mount the tank case to the floor of the racing car as it is a practical way to secure the tank in position.

The exhaust system considers the noise reduction, and the best concept regarding this function is a straight-through muffler. The straight-through muffler allows the flow in a straight path, which translates into a minimal restriction and increased power output. For the attachment of the exhaust system, rubber hanger mounts are the alternative selected because of simplicity and vibration insulation.

In relation to the heat transfer of the cooling system, the preferred alternative is a dual-pass radiator. However, it is possible that, at least in terms of availability, the best concept is a crossflow radiator. A crossflow radiator improves cooling efficiency at higher speeds, making this option a practical alternative for the racing car. For the radiator air flow, the selected concept is an electrical fan with the adequate flow to perform correctly with the radiator for the cooling system.

Finally, the lubrication system concept selected is a wet sump lubrication system. It implies setting the lubrication system of the ICE and transmission group without any major modification. The lubrication system of the KNZ motorbike includes a heat exchanger for the oil, which may help maintain the oil properties stable during operation. Also, the lubrication system was designed for a motorbike, where the oil pan may vary in angle due to the operation of the vehicle. Alternatively, a modification for the oil pan of the ICE and transmission group can be proposed for the system; mainly when considering that a Formula SAE racing car is designed to participate in events such as the skidpad event, subjecting the car and the ICE to significant lateral acceleration. These modifications include baffles and a windage tray for the design of an oil pan for the ICE, as proposed in the literature [48].

3.4.3. Electrical cluster conceptual alternatives selection and analysis

As presented in Table 3.17., the conceptual alternatives for the electrical cluster are listed in relation to the information display, starting mechanism, telemetry, battery use and ECU tuning functions. First, the most practical and cost-effective concept for information display is to provide a gauge at the cockpit to display the data for the driver. Some gauges may adapt directly to the ECU, leading to an easier connection and compatibility between the data display and the ECU in the formula-style racing car. Therefore, the selected alternative for the ECU tuning is to connect a new ECU and develop a configuration specifically for the use of the unit in the racing car.

For the telemetry function, it is important to highlight the use of a data acquisition system. A data acquisition system is an electronic memory unit that stores user-defined parameters as a function of time while the car is on track [49]. Hence, for the formula-style racing car the selected concept regarding telemetry is a basic telemetry package, involving a data acquisition system with just a limited set of parameters to be monitored in the car.

In terms of the starting mechanism, the selected option is to use a push-to-start button. This button is set to be located at the cockpit, for easier access for the driver and allowing the driver to start the engine always in a driving position inside the car. Meanwhile, the selected alternative for the battery use for the electrical installation is a VRLA battery, which is a sealed and maintenance-free lead-acid battery with a valve-regulated system to manage internal pressure.

3.4.4. Dynamic control cluster conceptual alternatives selection and analysis

The suspension system contemplates the suspension action, spring use and damping functions for the conceptual alternatives. To begin with, the selected alternatives for the suspension action are both pushrod and pullrod suspension. In accordance with the performance objectives, aerodynamic response and practicality, the front suspension of the formula-style racing car is formed by a pullrod suspension geometry, and the rear of the car includes pushrod suspension geometry.

To define properly the spring use and damping of the suspension system, the parameters and the operation of the suspension are analyzed. As noted by Milliken and Milliken [50], a simplified spring-mass-damper (SMD) system is used to avoid suspension system kinematics complexities. This is used not only because of simplicity, but also because many systems are very closely approximated by a spring-mass-damper system. Using some assumptions, a quarter car spring-mass-damper system is defined for the analysis of the suspension, as shown in Figure 3.3. The use of the quarter car SMD system allows a static and dynamic analysis of the suspension system of the racing car. The dynamic analysis for the SMD system of the car implies the use of the equation of motion defined by the equation (3.3), which involves parameters such as the applied force to the system (F), inertial reaction in terms of the mass (m), the spring force in terms of the spring constant (K), the damping force in relation to the damper constant (C) and the variable of reference (y) that defines the displacement, velocity and acceleration in the system.

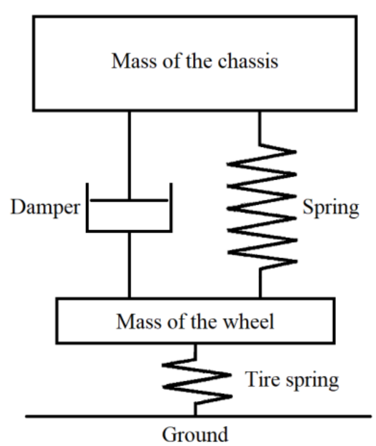

Figure 3.3. Quarter car SMD system model.

$$m\frac{d^2y}{dt^2} + C\frac{dy}{dt} + Ky = F \tag{3.3}$$

Further on, the equation (3.3) that models the quarter car SMD system for the racing car is used as a basis for the configuration of the geometry for the suspension system and the selection of the spring and shock absorber. In terms of practicality, the selected alternatives for the spring and the damping for the suspension system are both the linear coil springs and the gas-charged shock absorber.

Following, the steering system is conducted in relation to the use of anti-Ackermann geometry for the subsequent selection of the alternatives and the configuration of the parts regarding this system. In fact, the Ackermann geometry is studied in the literature through various approaches [39], [51], [52]. Nevertheless, for the development of the anti-Ackermann geometry it is important to define the parameters of the mechanism to be able to define the kinematics and the selection of the steering system for the racing car. Particularly, the mathematical model for the anti-Ackermann geometry of the car is defined by the set of equations listed in the findings of Drakulić et al. [52].

The steering system demands a reliable and responsive use of the elements that are involved in the mechanism. In view of this, the selected concepts for the system are double U-joints that connect the steering column to the steering wheel, supported by a mounted bearing, and the rack and pinion mechanism; these are followed by turnbuckle tie rods to be able to adjust the steering parameters. The double U-joints allow a more flexible assembly angle for both the steering column and the mechanism, while the mounted bearing facilitates the support of the joints to connect the steering column to the steering wheel of the system. As a matter of fact, the rack and pinion mechanism are common elements in steering systems for many cars, and it mainly is because it offers direct and responsive steering output and great feedback for the driver. Finally, the use of turnbuckle tie rods enables the steering adjustment to reduce effects such as bump steering or to define the steering capabilities to serve as tools for the driver.

For the braking system of the racing car, it is important to note that the guidelines of the Formula SAE competition state there must be only one input for the driver in relation to the force applied to the system [8]. As usually employed, a single brake pedal must be able to control both the front and rear brake elements of the vehicle. Therefore, the use of a brake balance or brake bias is required to ensure correct application of the forces at the brake elements arranged in the car. The brake balance or brake bias is generally defined as the distribution of the total brake effort for each axle of the car. The ratio of braking forces is calculated to determine the ideal braking force distribution of the car, which requires individual braking forces for the front and the rear axle [19].

To determine the brake balance of the racing car, an illustration of the racing car during braking is presented in Figure 3.4. It defines the forces held in the interface between the tread surface and the road surface, as well as the relevant parameters to define the behavior of the car. It is also assumed that the car decelerates on a flat surface and the resistance effects due to aerodynamics are neglected. Considering both the forces due to braking (F_b) and due to rolling resistance (F_{rr}), the equation (3.4) defines the equilibrium of forces in the longitudinal direction of the car towards the longitudinal acceleration in g-force for the racing car (g_{long}).

$$\sum(F_b + F_{rr}) = (m_v g)(g_{long}) \tag{3.4}$$

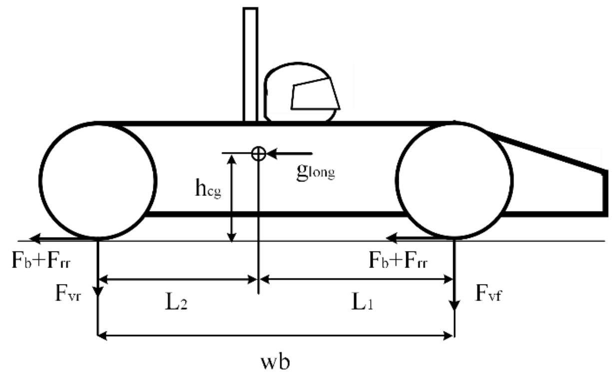

Figure 3.4. Braking forces and parameters of the racing car.

Hence, the vertical force exerted on the wheels and tires (F_{wv}) can be expressed into vertical loads for the front axle (F_{vf}) and the rear axle (F_{vr}). Using as basis the design dimensions for the racing car and the forces in the longitudinal direction, the vertical loads for the front and the rear axle can be calculated with the equation (3.5) and equation (3.6) respectively.

$$F_{vf} = \frac{(m_v g)(L_2)}{wb} + \frac{(F_b + F_{rr})(h_{cg})}{wb} \tag{3.5}$$

$$F_{vr} = \frac{(m_v g)(L_1)}{wb} - \frac{(F_b + F_{rr})(h_{cg})}{wb} \tag{3.6}$$

Therefore, the brake force distribution ratio (BFD) is defined as the relation between the vertical loads for the front and rear axle and it can be determined for the front axle with the equation (3.7) and for the rear axle with the equation (3.8).

$$BFD_f = \frac{L_2 + (g_{long})(h_{cg})}{L_1 - (g_{long})(h_{cg})} \tag{3.7}$$

$$BFD_r = (1 - BFD_f) \tag{3.8}$$

The brake bias or brake force distribution is variable in terms of the acceleration exerted in the vehicle. This variability requires a compromise between the brake forces in order to prevent the rear axle wheels from locking during acceleration. If the rear axle wheels lock during braking, the vehicle experiences loss of stability, reduced braking efficiency and incremented tire wear. Setting this trade-off for the brake balance is important and is going to be covered further with the configuration of the braking system.

Bearing in mind the brake balance analysis above, the selected alternatives for the braking system are a tandem master cylinder with a balance bar. The tandem master cylinder enables the use of a natural brake bias, but still the balance bar allows the team to adjust the brake balance for the racing car at any moment to adapt to the driver inputs. A double-piston caliper is preferred for the car as it enables a more uniform force applied to the brake pads and a drilled disc brake to include a lightweight option for the brakes, although it may be prone to cracking under extreme heat cycles, reducing the lifespan of these elements.

3.4.5. Enclosure cluster conceptual alternatives selection and analysis

As defined in Table 3.19., the conceptual alternative for the chassis consists of triangulation compliant front bulkhead supports, side impact structure and main hoop bracing supports. Even though all the options can be used because of the possibility of being integrated into the design of the chassis, to select the best concept for the chassis a series of factors are considered. Factors such as practicality, crashworthiness and ease of assembly are taken into account to determine the concept to be proposed for the chassis. Still, the selected concept for the chassis is considering the defined alternatives for other components and systems for the racing car, mainly towards the suspension system, the wheels and tires or even the bodywork. The selected chassis geometry concept is shown in Figure 3.5.

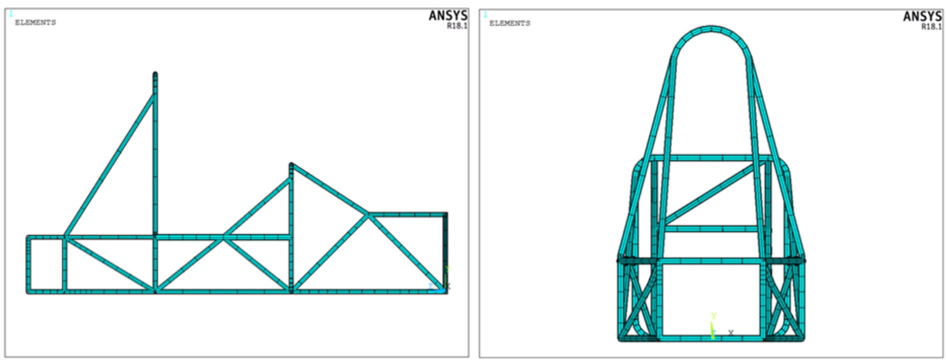

Figure 3.5. Conceptual chassis geometry for the racing car.

In relation to the cockpit and driver controls, the selected concepts are a standard seat with the capability to be placed in the cockpit, a stick shifter with a linkage mechanism to gear shift, a floor-mounted standard mechanical pedal box and a standard steering wheel. These concepts are chosen considering simplicity, ease of assembly, adjustable settings, comfort and driving feedback. Even though most of these components are selected and placed in the car, it is important to determine the conditions and the practicality of the use of these elements in the formula-style racing car.

Finally, the selected concepts for the bodywork of the racing car implements quick-release joints to assemble the bodywork and floor components, using only a set of basic aerodynamic packages for the car including a diffuser, and vinyl wrap to enable the identification of the car.

One of the most studied topics regarding Formula SAE racing cars is the aerodynamics of multiple elements for vehicles. A complete aerodynamic package includes the design of front aerodynamics [53], [54], the design of rear aerodynamics [55], [56] and the design of the underbody aerodynamics [57]. Although the performance of the car needs to examine the aerodynamics of the front, rear and underbody, not every racing car must include aerodynamic devices. The main goal for aerodynamic devices is to provide an aerodynamic force that pushes down the car, defined as a ground effect and causing a force that sums to the vertical loads exerted in the wheels of the racing car.

In fact, a basic aerodynamic package for the design of the formula-style racing car in this thesis project contemplates the overall bodywork geometry regarding the aerodynamic response, especially in relation to the nose cone, sidepods and the diffuser. A diffuser is a device which converts a flow's kinetic energy into a pressure rise, as mentioned by Zhang et al. [58]. These elements are considered the basic aerodynamic package mentioned as a selected concept.

With the selected concepts defined above, the conceptual development stage of the design process is completed, and it continues to the system-level design stage.

Chapter 4: System-level design of the racing car

The system-level design stage is crucial for the performance of the car during the competition. This stage defines the structure and the architecture of the racing car through the functions of the systems and components that integrate the vehicle. At the system-level design stage, the special purpose parts and standard parts are determined for every cluster that were mentioned previously in the conceptual development stage. Even though the selected concepts take into account the engineering design specifications, the system-level design examines the design specifications once more. Also, the configuration of parts and systems for the racing car must be compliant with the regulations of the Formula SAE competition and relevant guidelines are going to be mentioned during the system-level design stage.

4.1. Architecture of the racing car

The architecture of the formula-style racing car is modular, statement that is supported clearly by the clusters listed in Table 1.4. As a matter of fact, the architecture of the racing car needs to be established adequately for the purpose of the vehicle, as the performance of the car is highly dependent on the trade-offs and decisions taken at this stage in relation to the components and systems that integrate the vehicle. To define properly the modular architecture of the racing car, a group of tools are used to present in a graphical manner the relation between the modules that integrate the vehicle and the functions that must be accomplished by each component or system.

First, the modular architecture of the racing car is going to be presented in a block diagram, usually reported as a module breakdown structure (MBS) or functional decomposition diagram. The purpose of this block diagram is to group elements into logical chunks that represent functional modules for the vehicle, including in this case the systems and components that were proposed in Table 1.4. The module breakdown structure diagram for the formula-style racing car is presented in Figure 4.1. In fact, the MBS diagram includes not only the modules, but also the functions and the connections between the modules with the legend set at the diagram to define the link from one function performed to another. The legend at the bottom of the MBS diagram in Figure 4.1. corresponds to three different interactions between the logical chunks and functions of the racing car. The data flow interaction defines the use of sensors and actuators for the systems in relation to the electrical installation, the energy flow interaction defines the path for mechanical and electrical energy for the components and systems, and finally the physical connections are provided to set the attachment of different sections of the racing car.

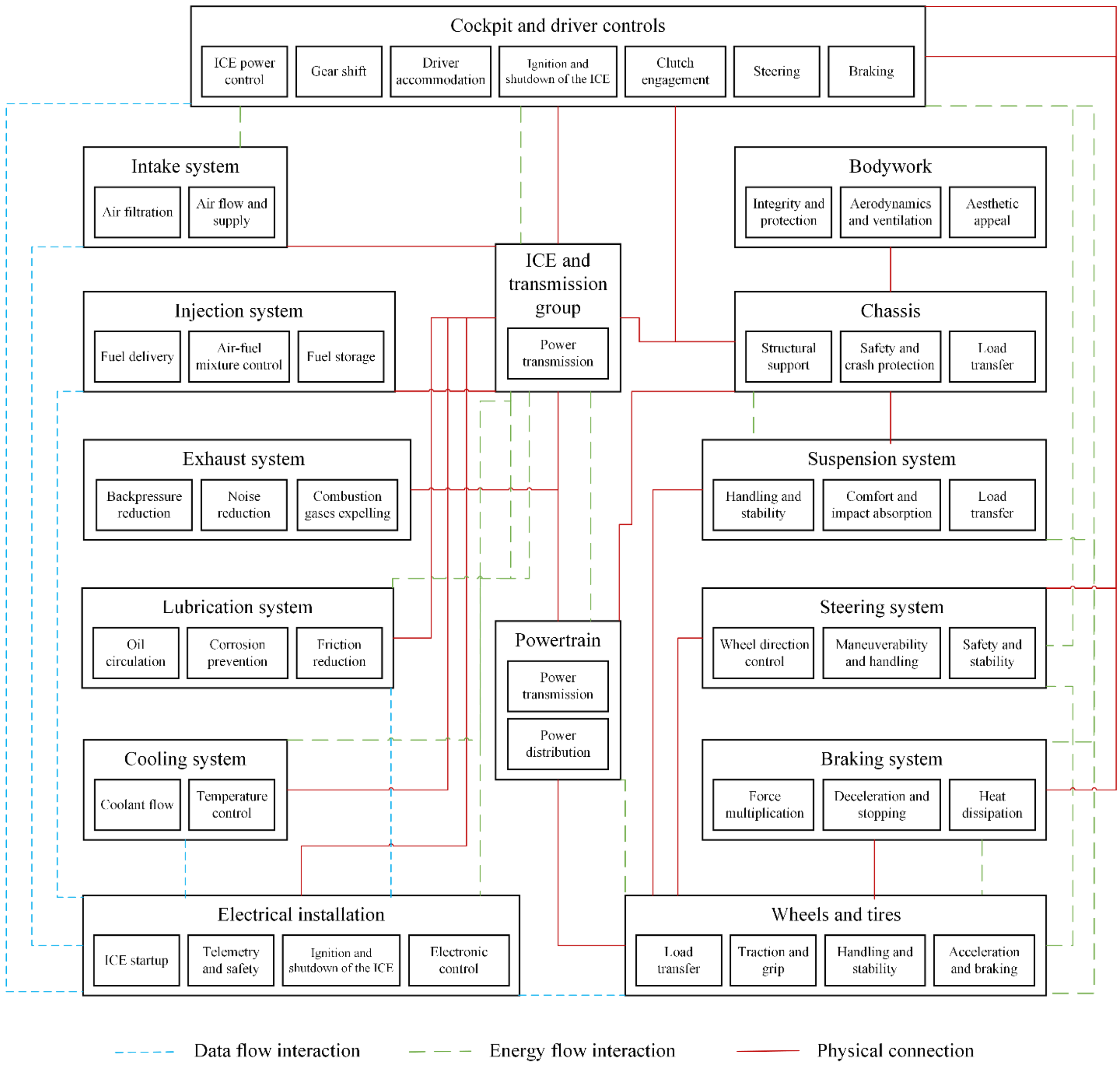

Figure 4.1. Module breakdown structure diagram for the formula-style racing car.

Another common diagram for the architecture presentation is the sketch interaction diagram. In this diagram, the interaction between the different modules of the architecture of the racing car are defined based on the functions that are required to be performed for the operation of the vehicle. The sketch interaction diagram shows the flow of information, processes, and functions for various elements in the architecture, and the corresponding diagram for the racing car is presented in Figure 4.2. As a complement for this diagram, each block for the modules of the architecture is labeled to indicate if it either consists of special-purpose parts (spp), standard parts (stp) or a combination of both special purpose and standard parts (cpp). The arrows in the sketch interaction diagram establish the orientation of the interactions among the blocks shown in Figure 4.2.

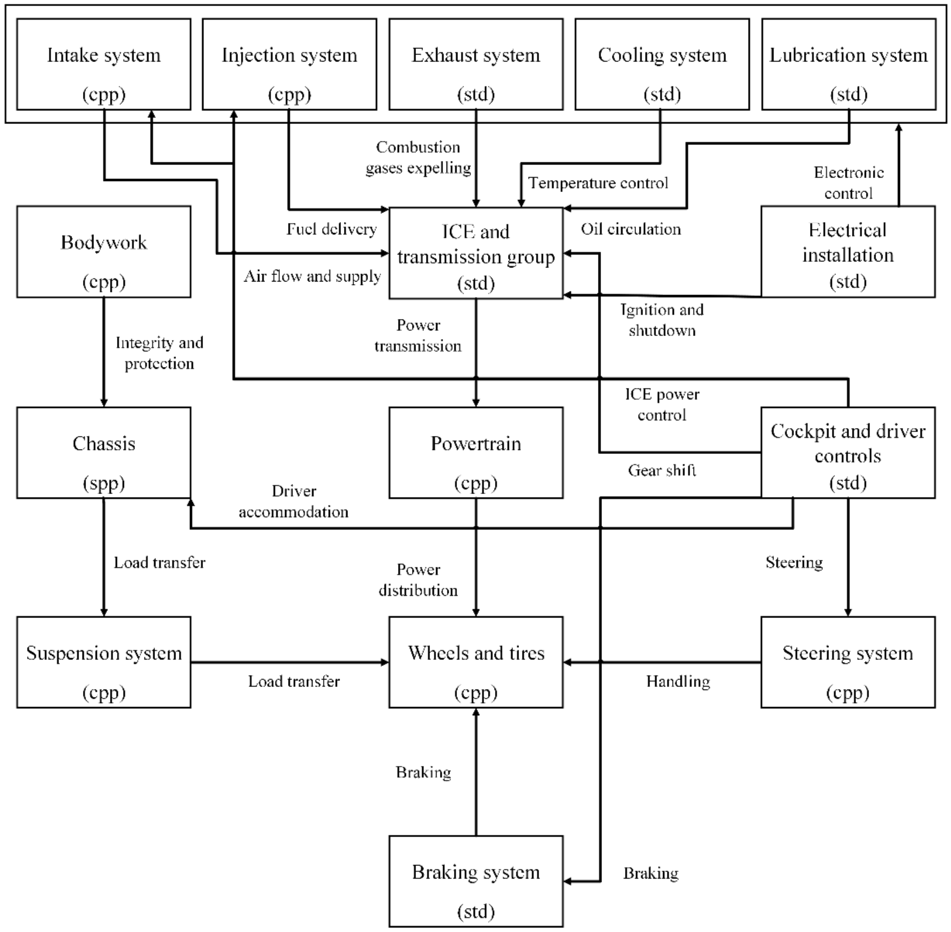

Figure 4.2. Sketch interaction diagram for the formula-style racing car.

4.2. Material selection

The material selection is related to the manufacturing processes to fabricate the components of the racing car. Material selection is not only centered in manufacturing these parts, but also in the design process of those components. Considering these statements, the material selection process is developed for the special-purpose parts of the formula-style racing car.

4.2.1. Key considerations for material selection

Material selection is a multifaceted process that must consider a series of key factors and criteria. These factors and the proposed criteria for selection ensure that the selected materials for the special-purpose parts may withstand the operational conditions to fulfill their functional requirements in the high-performance vehicle. Among the operational conditions to which the components are going to be summited, the list consists of static and dynamic loads, heat transfer, vibrations, impact loads, etc. Hence, this must be considered as the main factors that affect the behavior of the materials as the specific parts in the car.

Given this, the criteria for material selection are classified into four categories: performance requirements, operational requirements, manufacturing compatibility and sustainability. These four categories are established within the global concept of the racing car and the guidelines emitted by the Formula SAE competition. Particularly, the manufacturing compatibility criteria are set considering the fact that only graduate and undergraduate students must manufacture the vehicle and the parts that form the vehicle. For the sake of confidentiality, the weighting of the listed criteria is omitted. The criteria for material selection is classified and listed in Table 4.1.

Table 4.1. Criteria for evaluation for material selection of the special-purpose parts for the racing car.

Classification	Criteria	Characteristics
Performance requirements	Density	Mass of the material per unit of volume
	Strength	Ability to withstand applied forces
	Hardness	Ability to withstand scratching or indentation
Operational requirements	Fatigue strength	Ability to withstand applied cyclic loads
	Corrosion resistance	Ability to withstand degradation caused by environmental factors
	Thermal conductivity	Ability to conduct heat
	Thermal expansion	Tendency to change in volume in response to changes in temperature
Manufacturing compatibility	Machinability	Ability and ease to be shaped, cut or finished
	Weldability	Ability to be welded without forming defects
	Availability	Accessibility of the material to be sourced
	Relative cost	Financial feasibility
Sustainability	Recyclability	Ability to be processed and reused
	Embodied carbon	Total amount of carbon dioxide emissions associated with production and processing of the material
	Embodied water	Total amount of water used in the production and processing of the material

Material selection for the formula-style racing car is conducted by these requirements and the use of charts and software databases of available materials. As mentioned in the findings of Fentahun and Savaş [59], a better result for material selection can be obtained if software is used instead of charts. In fact, the list of materials and properties that made part of the material selection process are listed in the Appendix section of this thesis document. The materials presented are analyzed and selected using WREM and the criteria listed above in an equivalent manner to the method presented in Table 3.6., using the rating scale in Table 3.3.

4.2.2. Special-purpose parts material selection

The special-purpose parts are related to intake and injection systems, bodywork, chassis, powertrain, steering and suspension systems, as well as wheel assembly, in reference to the information in Figure 4.2. Based on the conceptual development stage and the architecture for the racing car, the corresponding list of special-purpose parts consists of wheel hub, knuckle, wishbone arms, rocker, tie rods, steering column, powertrain protection, manifold intake, fuel tank, chassis and bodywork. These parts are determined as a special purpose for the racing car considering that other parts that integrate the vehicle assembly may be used as standard parts that should be selected in the design process as well. In a general perspective, the material selection for this parts is conducted with the four-step methodology of translation, screening, ranking and supporting reported in the literature [59].

The wheel hub may be defined as a solid revolution, which means it is a solid figure that can be obtained by rotating a plane figure around an axis of revolution. Considering this, the selected material is a 7000-series aluminum alloy bar stock; particularly, the selected aluminum alloy can be named as a lightweight, strong and relatively easy to machine material. Meanwhile, the knuckle for the wheel assembly is usually formed of a complex geometry, so it is important to define the manufacturing process for this part. There exist several knuckle in relation to the manufacturing process used, such as welded, machined, cast, 3D printed or even composite knuckles [60]. Nevertheless, every manufacturing process presents both advantages and disadvantages; moreover, some processes may suppose a challenge for the team. Hence, for the knuckles of the racing car it is only considered the welded, machined and cast knuckles as options, having ASTM A36 steel, 6000-series aluminum alloy and 43300 cast aluminum alloy as alternatives. The selected material for the knuckles is 43300 cast aluminum alloy, i.e., a lightweight, castable, corrosion resistive high-strength aluminum alloy.

For the suspension system, wishbone arms and bellcrank linkage are listed as special-purpose parts due to the geometry that is required for these elements in the racing car. In relation to the wishbone arms, materials such as carbon steel, chromoly steel alloy and aluminum alloy are proposed as alternatives. Notwithstanding, the selected material is an AISI 1018 HR low-carbon steel, mainly because of moderate strength, weldability and relatively low cost. In addition, the bellcrank part consider materials like 2000-series, 6000-series and 7000-series aluminum alloys. Similar conditions can be found in these alternatives, but still the chosen material is a 6000-series aluminum alloy bar stock.

On the other hand, the steering system implies tie rods and steering column as special-purpose parts. To begin with, the tie rods propose materials such as carbon steel, chromoly steel alloy and aluminum alloy as options, similar to the wishbone arms. Hence, the chosen material is again AISI 1018 HR low-carbon steel, a low-cost option. Conversely, the selected material for the steering column is a SAE AISI 4140 chromoly steel alloy. This selection is even more critical, considering the function that this element is going to perform at the racing car.

Among 3000-series, 6000-series and 7000-series aluminum alloys, the designated material for the powertrain protection is a 6000-series aluminum alloy sheet to form the case that is intended to enclose the transmission elements in the powertrain, as compliant with the Formula SAE regulations.

The intake manifold must be designed to be compliant with the regulations of the Formula SAE competition; thus, material selection of the intake manifold consider different alternatives like wrought aluminum alloy, cast aluminum alloy or even polyetheretherketone. A lot of materials and manufacturing processes can be used to form the intake manifold. Nevertheless, the chosen material for the intake manifold is a cast aluminum alloy, as it may help form a complex geometry and low-cost part. In contrast, the injection system requires a fuel tank or a fuel tank case to protect a fuel tank made from a flexible material. High-density polyethylene, stainless steel of 5000-series aluminum alloy are among the materials that can be proposed as options for the fuel tank or fuel tank protection. The material designated for the fuel tank is 5000-series aluminum alloy sheet. Even though this material may not provide a high level of impact resistance, the 5000-series aluminum alloy has a great corrosion resistance, enough strength and weldability.

One of the most important material selection processes to perform is the chassis material selection. To begin with, the chassis must be compliant with the listed material for different sections of the tubular spaceframe, as noted in the Formula SAE regulations [8]. Materials including stainless steel, non-alloy steel, and low-alloy steel are considered for the tubes to form the tubular spaceframe. The selected material for the sections required in steel is A513 low-alloy steel. The A513 is known for its high strength, versatility, weldability, and good impact resistance at low temperatures, which place it as a great option for the tubular spaceframe. In spite of this steel selection, other possible materials to form the tubular spaceframe in some zones of the rear are 3.7035 grade 2 titanium and 6000-series aluminum alloy, as alternative materials for the chassis.

There exist a wide range of materials that may be used to manufacture bodywork panels and aerodynamic devices. In fact, three common materials used to form bodywork for a formula-style racing car are aluminum alloys, fiberglass and carbon-fiber [44]. Nevertheless, each of these materials suppose a different challenge for the team to manufacture the bodywork. Fiberglass and carbon-fiber are both composite materials that are made by fibers embedded with a resin matrix to form a strong and durable material. To perform adequately this manufacturing process is crucial to have some experience, making these processes difficult to use in the first racing car to design. Because of this and other factors like weight, manufacturability or costs, the selected material for the formula-style racing car bodywork is a 3000-series aluminum alloy sheet.

All of the materials selected above are presented in the Appendix section, particularly in section A1, including the mechanical and thermal properties. This information is used in the design process from now on for these special-purpose parts. Some specific materials may be presented further in the design process; those materials being selected in a concurrent engineering process while developing the configuration of the parts and systems of the racing car. Hence, the configuration design of the parts and systems of the formula-style racing car is presented below.

4.3. Configuration of parts and systems for the racing car

At the system-level design stage it is important to define the arrangement and the interconnection between components and subsystems within the larger system of the racing car in order to achieve the desired functions and the high performance expected for the vehicle. Thus, the configuration of parts and systems involves selecting the appropriate parts, the design of special-purpose parts, defining how these parts interact with each other, and determining how those parts must be placed in the racing car.

The configuration of parts and systems for the racing car is influenced by several factors, namely mechanical constraints, thermal considerations, material properties, electrical conductivity, among others. As the formula-style racing car is considered a complex system, effective configuration is essential for a successful development of the systems of the car. Below, the configuration of parts is divided into the different subsystems that integrate the racing car. For the sake of simplicity, the configuration of parts is presented with no particular order, as this stage was conducted during a concurrent engineering process.

4.3.1. Powertrain configuration

As a first step, the ICE and transmission group is placed in the rear of the chassis, behind the main hoop of the tubular spaceframe. To mount the ICE and transmission group, the mounting points of the KNZ engine are located and alternative mounts are located to place the engine fixed to the tubular spaceframe. In fact, welded plates can be used in the tubular spaceframe to allocate the mounting points for the ICE and transmission group. The mounts for the engine consist of two elements: engine mount bracket and engine mount insulator.

In this particular case, the engine mount bracket are defined as triangular structural components to connect the engine to the frame. These engine mount brackets can be found as standard parts; however, custom-designed engine mount brackets can be proposed to better adjust to the distance that may be required between the engine and the frame at some mounting points. The engine mount brackets design is dependent on several dimensions, namely the engine mounting holes, the distance between the mounting holes and the weld plates on the tubular spaceframe, etc. The design of these engine mount brackets is neglected in this configuration analysis, but still the selected material for these parts is 6000-series aluminum alloy. The bolts and nuts used for the KNZ engine may be reused for this assembly. On the other hand, the engine mount insulators are selected as rubber bushings to be adapted to the assembly of the engine and the chassis. The rubber bushings needed for the assembly are six because the engine counts with three mounting points and a bushing may be placed at each side of the mounting assembly.

Further, the ICE and transmission group connects to the powertrain elements. To begin with, the output shaft of the ICE and transmission group has a sprocket mounted and must connect to the secondary transmission using the chain drive that was selected in the conceptual development stage. As calculated in the conceptual development stage, the chain drive transmission must use a standard 520 roller chain to connect both drive and driven sprockets. A standard 520 roller chain dimensions include roller chain pitch, bearing pin diameter and width, roller diameter and width, plate height and thickness, etc. The relevant dimensions and geometry of the standard 520 roller chain are shown in Figure 4.3. The dimensions are presented in millimeters.

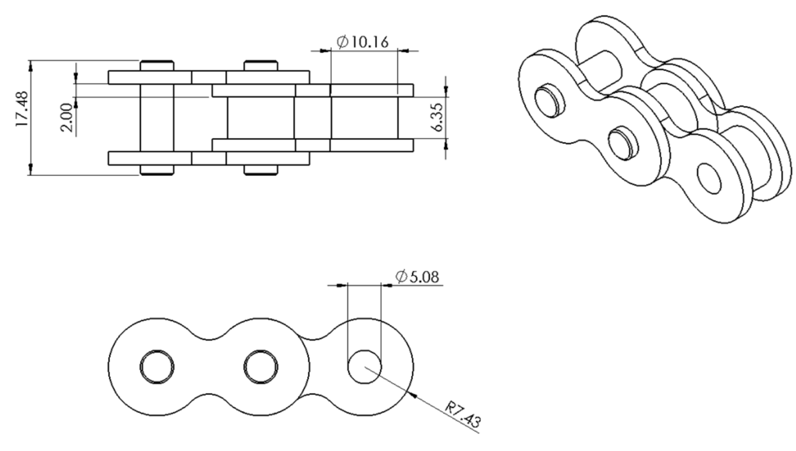

Figure 4.3. Standard roller chain for the powertrain of the racing car.

In the secondary transmission of the KNZ powertrain, sprockets made from chromoly steel can be found. These sprockets can be reused in the racing car powertrain. One of these sprockets is mounted on the output shaft of the ICE and transmission group, has an internal splining and has a total of 16 teeth. Meanwhile, the driven sprocket to be used in the racing car must be able to connect to the differential of the powertrain. A particular geometry for the driven sprocket is a floating sprocket that has a flange to be able to adjust the sprocket to another element, such as a sprocket carrier or mounting plate. The corresponding number of teeth for the sprocket of the input shaft (Z_i) and the floating sprocket (Z_o) determine the transmission ratio.

With the aim to be compliant with the Formula SAE regulations, the chain drive scatter shield must follow the guidelines emitted by the organizers. Therefore, the chain drive scatter shield is made of a minimum thickness steel and have at least a width three times the width of the chain. The drivetrain shield geometry is defined after determining the length of the chain and the assembly of the chain drive in relation to the center-to-center distance for the sprockets. The equations (4.1) and (4.2) are both used to define the geometry of the assembly for the roller chain and involve the length of the roller chain (L), the pitch of the roller chain (p), the variable A, the number of teeth of the sprockets, and the center-to-center distance (C).

$$A = \frac{Z_i + Z_o}{2} - \frac{L}{p} \tag{4.1}$$

$$C = \frac{p}{4}\left[-A + \sqrt{A^2 - 8\left(\frac{Z_o - Z_i}{2\pi}\right)^2}\right] \tag{4.2}$$

Previously at the conceptual development stage, a limited slip differential (LDS) was defined as the selected transmission split concept for the racing car. In view of this selection, alternatives of LSD compatible with the racing car are searched in the aftermarket. Despite the fact that there are not many LSD options available that are compatible with the dimensions and the scope of the vehicle, a specific aftermarket LSD is proposed for the racing car. The proposed aftermarket LSD is a clutch-type limited slip differential that can be manufactured with three different lengths. However, the LSD version to be analyzed is the version that has an intermediate length, which also is related to an equivalent length from the center of the differential unit to each side of the LSD. The corresponding geometry and dimensions of the aftermarket LSD are shown in Figure 4.4.

Based on the geometry of the LSD in Figure 4.4., it is important to note that the driven sprocket and mounting plate must be assembled in the left side of the LSD and that the proposed mounting points for the corresponding bearings are presented marked by the letter *B* and *C* respectively. The analysis criteria needs to establish the critical loads under the operation of the differential. Using the information of the IVDS for the formula-style racing car, the maximum torque applied to the driven sprocket is obtained with the first gear and calculated with the transmission ratio defined by the number of teeth for the sprockets.

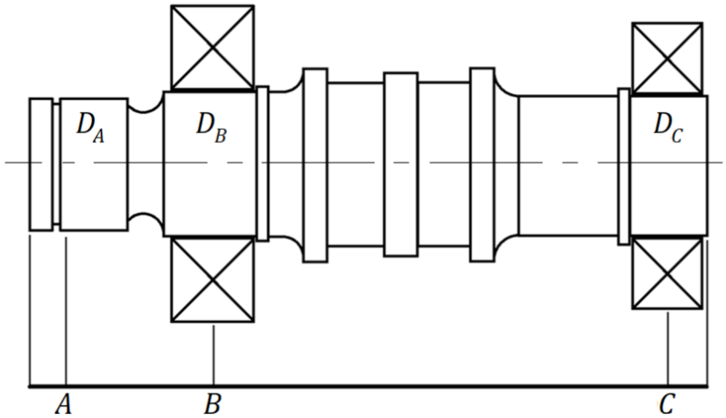

Figure 4.4. Geometry of the aftermarket LSD.

The maximum torque applied to the driven sprocket is the torque applied at the section marked with letter A (T_A) in Figure 4.4. To calculate the tangential force acting at section A in the differential, the equation (4.3) implies the definition of torque, with a tangential force applied to the cross-section ($F_{t,A}$) multiplied by its distance from the lever's fulcrum of the cross-section.

$$T_A = F_{t,A}\left(\frac{D_A}{2}\right) \tag{4.3}$$

After this, the corresponding reaction forces at section B (R_B) and C (R_C) are determined using the equilibrium equations for a static analysis of the LSD in a rectangular coordinate system. Once the reaction forces are calculated and assuming that the tangential force at section A is a concentrated force, the analysis for bending moment and shear force is conducted. The reaction force at section B is the critical point for the analysis. For that reason, the stress combination is carried out for normal and shear stress at section B, considering that the relevant point of analysis is located at the external diameter at point B cross-section. Normal stress due to bending moments is calculated using the equation (4.4); meanwhile, the shear stress due to torque is computed using the equation (4.5).

$$\sigma_B = \frac{32M(d_B)}{\pi(D_B^4 - d_B^4)} \tag{4.4}$$

$$\tau_B = \frac{16T(d_B)}{\pi(D_B^4 - d_B^4)} \tag{4.5}$$

Hence, the plane stress state is determined by the normal and shear stress calculated at section B in a specific point located in the external diameter of the cross-section. The next step is to perform the combination of stress at this specific point, directly involving these normal and shear stresses at the equation (4.6) used to compute the principal stresses ($\sigma_{1,2}$). Following the calculation of the principal stresses, the maximum distortion energy criterion is applied to the principal plane stress with the equation (4.7) and the von Mises stress (σ_v) is computed.

$$\sigma_{1,2} = \frac{\sigma_x + \sigma_y}{2} \pm \sqrt{\left(\frac{\sigma_x - \sigma_y}{2}\right)^2 + \tau_{xy}^2} \tag{4.6}$$

$$\sigma_v = \sqrt{(\sigma_1^2 - \sigma_1\sigma_2 + \sigma_2^2)} \tag{4.7}$$

Although the aftermarket LSD material is not given, the computed von Mises stress for the differential is about 70 MPa. Thus, stress analysis of the aftermarket LSD may be concluded, determining that stress may be much lower than the yield stress of most of the possible materials used to manufacture the differential case.

Before the selection of the bearings to be mounted at points *B* and *C* in the LSD, the slope and deflection at those points is determined to ensure that the bearings operation is not carried out with critical misalignment. Therefore, the slope and deflection analysis for the differential as a beam is performed, and the beam bending theory establish the use of the Euler-Bernoulli equation presented in equation (4.8).

$$EI\frac{d^2y}{dx^2} = M(x) \tag{4.8}$$

The bending moment equations are directly related to the beam geometry. These equations are determined as a function of position x through the length of the differential. The corresponding bending moment equations for the beam in span *AB* (*a*) and span *BC* (*b*) are expressed in equation (4.9) and equation (4.10) respectively. The equations are presented considering the force acting at point *A* (*F*) and the reaction force at point *B* (R_B).

$$M(x) = -Fx \tag{4.9}$$

$$M(x) = -Fx + R_B(x - a) \tag{4.10}$$

With the bending moment equations defined and applying the integration method to solve the Euler-Bernoulli equation for the different spans of the beam, the slope and deflection equations are obtained in terms of four constants of integration. The concomitant equations of slope and deflection for span *AB* and span *BC* are listed below as equations (4.11), (4.12), (4.13), and (4.14) sequentially.

$$\frac{dy}{dx} = -\frac{Fx^2}{2EI} + C_1 \tag{4.11}$$

$$y(x) = -\frac{Fx^3}{6EI} + C_1x + C_2 \tag{4.12}$$

$$\frac{dy}{dx} = -\frac{Fx^2}{2EI} + \frac{R_B(x-a)^2}{2EI} + C_3 \tag{4.13}$$

$$y(x) = -\frac{Fx^3}{6EI} + \frac{R_B(x-a)^3}{6EI} + C_3x + C_4 \tag{4.14}$$

Considering that flexural rigidity (*EI*) may vary through the length of the LSD and using both boundary and continuity conditions, the slope and deflections equations for the differential as a beam are finally obtained. The boundary and continuity conditions for this analysis are listed in Table 4.2.

Table 4.2. Boundary and continuity conditions for LSD slope and deflection analysis.

Position x	Boundary condition	Position x	Continuity condition
$x = a$	$y(x) = 0$	$x = a$	$\left.\frac{dy}{dx}\right\|_{a} = \left.\frac{dy}{dx}\right\|_{b}$
$x = a + b$	$y(x) = 0$	$x = a$	$y(x)\|_{a} = y(x)\|_{b}$

The slope at points B and C, as well as the deflection at point A, are computed, and afterward, these values are going to be compared to the maximum ranges for slope and deflection reported in the literature [45]. Moving forward with the analysis of the LSD, the selection of roller contact bearings is carried out. Considering that the operation of the LSD does not involve axial loads of concern, the proposed bearings for the LSD assembly are either ball or cylindrical roller bearings.

With regard to the critical condition for the analysis, the IVDS data is consulted in relation to the maximum power transmitted to the LSD with a matching torque and angular frequency. Considering this data, the reaction forces at point B and point C of the LSD are recalculated with the equation (4.2) and the equilibrium equations. Using the information available for the selection of ball and cylindrical roller bearings [45], the multiple of rating life (x_D) dimensionless is determined with the equation (4.15) that involves the desired life ($\mathcal{L}_D$), the desired speed (n_D), and the rating life (L_{10}).

$$x_D = \frac{60\mathcal{L}_D n_D}{L_{10}} \tag{4.15}$$

Based on the multiple of rating life, the catalog load rating (C_{10}) can be determined to select the adequate bearings for each point. The equation (4.16) relates the catalog load rating with several factors, which include the application factor (a_f), the desired radial load (F_D), the multiple of rating life, the three parameters for Weibull distribution, the reliability parameter (a) for different roller bearings, and the desired reliability (R_D). The three-parameter Weibull distribution consist of a guaranteed parameter (x_0), a characteristic parameter (θ), and a shape parameter (b) that are used exclusively to define the reliability of roller bearings. Here, the application factor is determined for a low or medium impact machine and the related parameters for the roller bearings are defined.

$$C_{10} = a_f F_D \left[\frac{x_D}{x_0 + (\theta - x_0)(1 - R_D)^{1/b}}\right]^{1/a} \tag{4.16}$$

Once the catalog load rating is calculated for point B and C in the LSD geometry, this computed value is used to select the corresponding roller bearings for each point. The selected roller bearings are defined using the catalog load rating, the inner diameters of point B () and point C (), and the guidelines of specialized manufacturers and distributors of roller bearings. Fo point B, with the most critical catalog load rating, the chosen roller bearing is a single row cylindrical roller bearing;

meanwhile, the selected roller bearing for point C is a single row deep-groove ball bearing. As mentioned before, these roller bearings must contemplate that the operation at the LSD must be within the range of the maximum slope. The maximum range of slope for deep-groove ball roller bearings is between 0.001 and 0.003 rad, while the range of slope for cylindrical roller bearings is about 0.0008 and 0.0012 rad. After the analysis of slope and deflection for the aftermarket LSD, the slopes at section B and C are both in range for the corresponding roller bearings designated for those points. Thus, the selected aftermarket LSD for the formula-style racing car is feasible and suitable for the powertrain.

To establish a link from the LSD to the wheel assembly, the LSD is designed with internal splines at both sides to be able to connect the differential to joints, so that these joints can transmit power to the half shafts and then to the wheels. Hence, the next step is to determine the joints to be used in the powertrain. Using the IVDS data corresponding to the maximum power transmitted to the LSD, the analysis of the splines for the joints to be connected to the differential is conducted.

In this context, the input data for the analysis is the geometry and dimensions of the LSD, particularly at the inside of the differential. The selected joints must match the geometry and dimensions of the LSD, even though the number of splines is not specified. Therefore, the analysis is set to determine the approximated number of splines in the joints and the viability of the interaction for power transmission. To determine this, the analysis contemplates the equation (4.17), (4.18), and (4.19) to establish the relation between the height of the spline (h), the pitch (p), the external diameter (D_e), the pitch diameter (D_p), and the number of splines (N).

$$D_e = D_p + 2h \tag{4.17}$$

$$h = \frac{D_p}{2N} \tag{4.18}$$

$$p = \frac{\pi D_p}{N} \tag{4.19}$$

After the determination of the geometry for the splines, the normal and shear stress at the spline section are calculated. The equation (4.20) involves an application factor for the splines (k_a), a distribution factor (k_f), a fatigue-life factor (k_f), the torque applied (T), and geometric parameters of the spline and shaft, such as the pitch diameter, the number of splines, the effective length (L_e), and the thickness of the spline (t) to compute the shear stress at the spline (τ). In addition, the equation (4.21) calculate the normal stress at the contact surface for the spline (σ) with the relation of similar parameters including an application factor for the splines, a distribution factor, a fatigue-life factor, the torque applied, the pitch diameter, the number of splines, the effective length and the height of the spline. After these stresses are obtained, the computed values are then compared to allowable shear and normal stress respectively for the material of the splines, specifically in reference to the hardness of those materials, to determine the safety factors (n) to each condition with the equation (4.22).

$$\tau = \frac{4k_a k_m T}{k_f D_p N L_e t} \tag{4.20}$$

$$\sigma = \frac{2k_a k_m T}{9k_f D_p N L_e h} \tag{4.21}$$

$$n = \left(\frac{\sigma_{fail}}{\sigma_{allowable}}, \frac{\tau_{fail}}{\tau_{allowable}}\right) \tag{4.22}$$

This procedure is used to determine the safety factors for normal and shear stress at the splines for each spline interaction in the powertrain. Those interactions allow the power transmission from the differential to the wheel hub using the CV joints and the half shaft. Even though the half shafts can be either acquired in the aftermarket or manufactured, the minimum diameters for the half shaft must be determined.

On that account, the maximum torque condition is now used to calculate the critical geometry for the half shaft with the IVDS data. Employing the maximum distortion energy criterion for an isotropic material subjected to pure shear, the equation (4.23) is obtained. This equation compares the von Mises stress to the scalar value of stress obtained from the Cauchy stress tensor. When the von Mises stress reaches the value of yield stress, the yield shear stress can be determined.

$$\sigma_v = \sqrt{3}|\sigma_{12}| \tag{4.23}$$

Following the calculation of the critical geometry and dimensions for the half shaft, the next step is to use the torsion shear stress presented in the equation (4.24). At this point, the input data for the equation are the yield shear stress (τ_y) for the material of the half shaft, the maximum torque applied, and the external diameter of the half shaft, which is directly related to the dimensions of the tripod element used to link the half shaft to the CV joints at each side.

$$\tau_y = \frac{16T(D)}{\pi(D^4 - d^4)} \tag{4.24}$$

The half shafts are considered as standard parts for the formula-style racing car because of the accessibility of shafts with a wide range of lengths to be easily assembled to the standard CV joints and tripod elements at each side.

4.3.2. Wheel assembly configuration

Once the CV joints are selected, the wheel assembly can take part into the configuration stage. Although the configuration of the parts for the wheel assembly is a concurrent engineering process, the wheel assembly is directly related to the powertrain elements.

To determine the torque available at the wheel and tire assembly for the formula-style racing car, the analysis of torque threshold for the tires of the car for both conditions: acceleration and braking. The analysis is based on the equation (4.25), in which the friction coefficient (μ), the radius of the tire (r), and the vertical force exerted on the tire (F_v) are used to determine the torque available at the tire (T_a).

$$T_a = \mu(F_v)(r) \tag{4.25}$$

As stated in the Formula SAE regulations, the tires for the competition are classified into two main groups: dry tires and wet tires. Dry tires are the selected tires for dry conditions on track and, in the case of the formula-style racing car, are slick tires and are made from a specific compound. In contrast, the wet tires are tires that must be used for wet conditions or a limited grip on track and the selected tires for this condition are treaded and have similar but slightly different dimensions when compared to the dry tires selected.

The torque threshold analysis is conducted with two distinct conditions, which are maximum traction torque and maximum braking torque. These conditions are established using the IVDS data, specifically for the acceleration in terms of g-force in the car and the vertical force exerted on specific tires, in addition to the equivalent calculation for both acceleration and braking torque. Hence, the dry tires and wet tires data, as well as the acceleration and braking torque conditions, are employed to compute the torque available at the tires. The results of this analysis are presented in Table 4.3. In this context, the available torque ratio (R_T) is the relation of the computed torque available (T_a) with the torque determined in the maximum conditions of the analysis (T_c), as shown in equation (4.26). If the available torque ratio results lower to one, the implemented torque does not overpass the torque threshold. Alternatively, if the available torque ratio results higher than one, the implemented torque overpasses the torque threshold, and the tire might experience a loss of traction, instability, or even potential damage.

$$R_T = \frac{T_a}{T_c} \tag{4.26}$$

Table 4.3. Results of the analysis of available torque at the tires of the racing car.

Dry track conditions		**Wet track conditions**	
Racing car analysis condition	**Available torque ratio**	**Racing car analysis condition**	**Available torque ratio**
Traction torque	0.8894	Traction torque	1.2903
Braking torque	1.0336	Braking torque	1.4993

Even though the torque threshold is surpassed in two parts of the analysis, those parts correspond to the wet or limited grip conditions, and the proposed acceleration and braking torque conditions might be difficult to reach in a real scenario. Thus, the torque threshold analysis finds the selected tires and the acceleration and braking conditions as feasible for the racing car, as well as optimized for dry track conditions.

The next step for the configuration of the wheel assembly for the racing car is to determine the operating critical conditions for the design and selection of the parts corresponding to the wheel assembly. These conditions are, once again, two critical requirements for the operation of the wheel assembly to enable power transmission. First, the loads acting of the wheel assembly are classified into axial, tangential and radial loads based on the direction of those loads and what consequences may exert in terms of stress.

The radial loads in the wheel assembly are defined as loads that act in the vertical direction mainly and that can be found during several circumstances in the racing car due to the weight of the car and both lateral and longitudinal load transfer on front and rear axle. To define the maximum radial loads at the wheels of the car, the IVDS data is used to determine the lateral and longitudinal load transfer for each wheel considering the static mass distribution for the car and the maximum acceleration that the racing car may experience.

In contrast, the tangential loads in the wheel assembly are due to the torque transmitted during acceleration or braking. These tangential loads enable power transmission to the tires of the racing car and the maximum torque for this analysis occurs during acceleration.

Finally, the axial loads are due to the reaction forces in the tire contact surface against the road surface under specific circumstances, in particular while taking a corner. In corner handling, the racing car experiences a lateral load transfer and a reaction in the tire is exerted in that lateral direction, which is parallel to the axis of the wheel assembly. Therefore, again the IVDS data is used to determine the maximum axial loads in the wheel assembly.

Once the different loads in the wheel assembly are defined and the corresponding circumstances to find the maximum loads using the IVDS data, the parameters to be used in the configuration of the wheel assembly are listed and classified in Table 4.4. The two conditions to which the maximum loads can be obtained are the maximum acceleration condition and maximum load transfer condition.

Table 4.4.Wheel assembly loads under critical conditions.

Maximum acceleration condition		**Maximum load transfer condition**	
Item	**Specification**	**Item**	**Specification**
Torque	$T_{w,max}$	Torque	T_w
Radial load	F_{rw}	Radial load	$F_{rw,max}$
		Axial load	$F_{aw,max}$

Following the configuration of parts for the wheel assembly, the rim attachment is determined. At this point, the geometry and dimensions of the rim for the wheels are known. Consequently, the next step is to search for available options for studs that enable the attachment and to be analysis for feasibility in relation to this function. The required parameters to be defined for this analysis and to provide alternatives for attachment are mainly the lug holes diameter and the hub mount plate width and diameter, as shown in Figure 3.1. With the studs defined as options, the analysis is conducted as shown below.

One of the premises of the analysis is that each wheel stud is submitted to shear forces due to power transmission. To determine the shear force applied to the wheel studs, the maximum acceleration condition data of Table 4.4. is used. Contemplating this shear force (V) and the effects of centripetal force, the equation (4.27) involves these forces within the corresponding cross-sections (A) of the wheel studs to compute the shear stress (τ). The rim has a hub mounting plate for a total of four studs; as a result, the equation (4.27) contemplates four as the number of times those cross-sections (n) oppose to the shear force. In addition, equation (4.28) is used to calculate normal stress due to bearing (σ) in the wheel studs by relating the minimum proof strength (S_p) to the design factor (n_d). To determine this design factor, the equation (4.29) is solely based on the maximum distortion energy criterion for an isotropic material subjected to pure shear of equation (4.23).

$$\tau = \frac{V}{nA} \tag{4.27}$$

$$\sigma = \frac{S_p}{n_d} \tag{4.28}$$

$$\tau = \frac{1}{\sqrt{3}} \frac{S_p}{n_d} \tag{4.29}$$

At this point, the preload is defined to determine the tightening torque for the wheel studs. To specify the torque and preload, the first step is to analyze the fastener stiffness. The procedure to analyze the fastener stiffness is the Rotscher's pressure-cone method, as suggested in the literature [45]. Hence, the analysis of the clamping of the wheel hub and wheel rim consist of three cone geometries or frustums, which differ from each other. Still, the frustum geometries for the analysis of fastener stiffness are defined by the dimensions of the clamping and the wheel studs. To begin with, the equation (4.30) is employed to calculate the stiffness of the frustum (k) with the relation of the modulus of elasticity (E), the nominal diameter of the fastener (d), the head diameter of the fastener (D), and the length of the frustum of the analysis (t).

$$k = \frac{0.5774\pi E d}{ln\left(\frac{(1.155t + D - d)(D + d)}{(1.155t + D + d)(D - d)}\right)} \tag{4.30}$$

Using the equation (4.30), the stiffness of the three frustums for the clamping of the wheel hub and wheel studs are calculated. After this, the spring rate of the members (k_m) and the estimated effective stiffness of the fastener (k_b) must be calculated. The spring rate of the members is computed with the equation (4.31), which is the sum of the stiffness of the frustums in series. In contrast, the estimated effective stiffness of the fasteners is determined by the equation (4.32), which relates the modulus of elasticity to the geometric parameters of the clamping, including the area of unthreaded portion (A_d), the area of threaded portion (A_t), the length of the unthreaded portion in grip (l_d), and the length of the threaded portion in grip (l_t). Therefore, the length of the unthreaded portion in grip and the length of the threaded portion in grip are determined by the geometry and dimensions of the clamping, as shown in Figure 4.5., as well as the equations (4.33) and (3.4).

$$\frac{1}{k_m} = \sum_{i=1}^{n} \frac{1}{k_i} \tag{4.31}$$

$$k_b = \frac{A_d A_t E}{A_d l_t + A_t l_d} \tag{4.32}$$

$$l_d = L - L_t \tag{4.33}$$

$$l_t = l - l_d \tag{4.34}$$

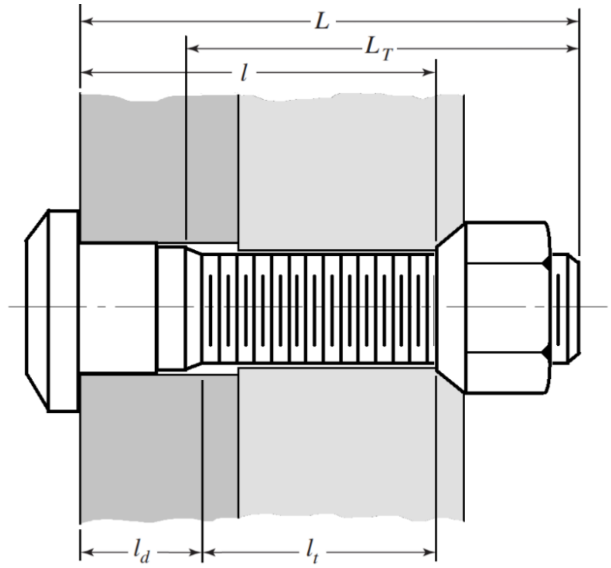

Figure 4.5. Wheel stud and lug nut clamping wheel hub and wheel rim.

Subsequently, the stiffness constant of the joint (*C*) is determined with the equation (4.35). This constant is a relation of the spring rates for the members and the fasteners. It is one of the parameters to be established to define the feasibility of the preload and tightening torque. The equation (4.36) establishes the association between the preload (F_i), the tightening torque (T_i), the torque coefficient (*K*), and the thread diameter (*d*).

$$C = \frac{k_b}{k_b + k_m} \tag{4.35}$$

$$T_i = KF_i d \tag{4.36}$$

Thereafter, the axial load in the wheel is introduced to the analysis. This axial load is defined as the external load applied to the fasteners (P_{total}) and the individual load applied to the fastener (*P*) is obtained with the equation (4.37), taking into account the number of fasteners (*n*). To compute the resultant fastener load (F_b), the equation (4.38) involves the stiffness constant of the joint, the load at the fastener and the preload. Finally, the normal stress in the fastener can be calculated and the factors of safety are obtained for yielding against the static stress exceeding the proof strength (n_p), the load factor (n_L), and the factor of safety against joint separation (n_0) with the equations (4.39), (4.40), and (4.41) respectively.

$$P = \frac{P_{total}}{n} \tag{4.37}$$

$$F_b = CP + F_i \tag{4.38}$$

$$n_p = \frac{S_p A_t}{CP + F_i} \tag{4.39}$$

$$n_L = \frac{S_p A_t - F_i}{CP} \tag{4.40}$$

$$n_0 = \frac{F_i}{(1 - C)P} \tag{4.41}$$

Notwithstanding, the wheel studs are submitted to fatigue loads. For that reason, the previous analysis is complemented with the fatigue analysis of the fasteners. Initially, the alternating stress (σ_a) and the midrange stress (σ_m) experienced by the fasteners are determined by means of the equation (4.42) and (4.43) for the maximum and minimum individual load at the fastener. In the particular case of the wheel studs, the individual load fluctuates between a maximum value and a minimum value of zero applied load. In this context, the fatigue factor of safety (n_f) is given by the equation (4.44) using the Goodman failure line and defining previously the normal stress due to the preload (σ_i), the endurance limit (S_e) and the ultimate tensile strength (S_{ut}).

$$\sigma_a = \frac{C(P_{max} - P_{min})}{2A_t} \tag{4.42}$$

$$\sigma_m = \frac{C(P_{max} - P_{min})}{2A_t} + \frac{F_i}{A_t} \tag{4.43}$$

$$n_f = \frac{S_e(S_{ut} - \sigma_i)}{\sigma_a(S_{ut} + S_e)} \tag{4.44}$$

In an equivalent way, the corresponding fasteners to clamp the disc brake to the wheel hub are analyzed using the same procedure until the factors of safety of the equations (4.39), (4.40), (4.41), and (4.44) are determined for that joint.

Subsequently, the design of the wheel hub is carried out. The wheel hub design must be complemented by the information on the previous fastener analysis, as well as with the design requirements. Nevertheless, the wheel hub critical scenarios can be separated into the analysis of the two conditions established in Table 4.4.

In a static analysis, the wheel hub geometry and dimensions are determined with several information. To begin with, the wheel hub geometry must allow the connection to the wheel rim through the wheels studs previously analyzed, must enable the connection to the disc brake with the fasteners selected, must interact with the CV joint to allow power transmission, and mount the bearings to support the wheel assembly in relation to the knuckle. The initial wheel hub dimensions are defined with similar equations to the ones presented in equations (4.4) and (4.5). These equations are now used to calculate the internal nominal diameter of the wheel hub in relation to the normal and shear allowable stress, considering both a safety factor and the material for the wheel hub. In a general perspective, those equations are now rearranged into the equations (4.45) and (4.46).

$$\sigma_{allowable} = \frac{32M(D)}{\pi(D^4 - d^4)} \tag{4.45}$$

$$\tau_{allowable} = \frac{16T(D)}{\pi(D^4 - d^4)} \tag{4.46}$$

The geometry and the dimensional parameters for the design of the wheel hub are shown in Figure 4.6. As illustrated, the wheel hub geometry consists of the flange to connect to the wheel rim, a flange to connect to the disc brake and section to allow the roller bearings to be mounted. The analysis will consider that the axis parallel to the length of the wheel hub is designated for the x-coordinate. Therefore, three different cross-sections of the wheel hub are designated as the critical sections for the analysis, which are located as lengths A, B and C in Figure 4.6.

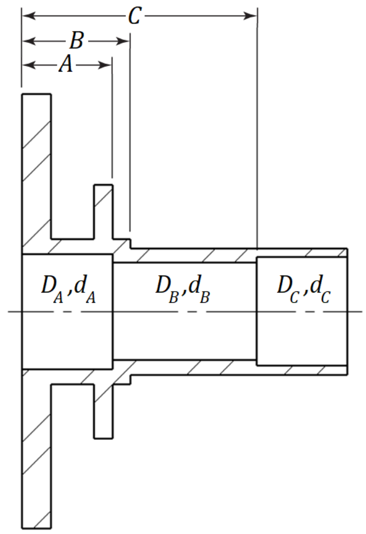

Figure 4.6. Geometry of the wheel hub.

The wheel hub geometry is first analyzed using the maximum load transfer condition established in Table 4.4. Therefore, the loads applied with this condition to the wheel hub led to normal stress due to bending and axial loads, as well as shear stress due to torsion. With this defined and the critical cross-sections established, the bending, axial and torsion stress is calculated in function of the geometry and sections in a static analysis. It is important to mention that the mounting points for the roller bearings at the wheel hub were approximated to determine the bending moment equations. The wheel hub can be simplified as an overhanging simply supported beam with a distributed load due to the interaction with the knuckle. Once the bending moment equations for the wheel hub are determined, the Euler-Bernoulli form at equation (4.8) is applied with the integration method to compute the slope and deflection at the mounting points for the roller bearings.

Therefore, the critical cross-sections are now contemplated to develop the fatigue analysis of the wheel hub geometry. Notwithstanding, to determine the plane stress state for the analysis, some specific points are considered in each internal section. Those points in the critical sections develop different stress conditions for plane stress state. For the points at the critical cross-sections coincided with the vertical axis, the normal stress and shear stress can be calculated with the equations (4.47) and (4.48). In a similar way, the normal stress and shear stress for points coincided with the horizontal axis can be determined with the equations (4.49) and (4.50).

$$\sigma = -\frac{MD}{2I} - \frac{F}{A} \tag{4.47}$$

$$\tau = \frac{TD}{2J} \tag{4.48}$$

$$\sigma = -\frac{F}{A} \tag{4.49}$$

$$\tau = \frac{TD}{2J} + \frac{4V}{3A} \tag{4.50}$$

Hence, the normal and shear stress for both points in the critical cross-sections are calculated with the corresponding equations (4.47), (4.48), (4.49), and (4.50) in order to define the plane stress state for each point of analysis. At this point, it is clear that points at cross-sections located in *A* and *B* must be only analyzed with the maximum load transfer condition, but the points at the cross-section located at *C* may require to be analyzed with both the maximum torque and maximum load transfer conditions.

Following the fatigue analysis of the geometry of the wheel hub, the endurance limit (S_e) is determined for the material and configuration of the wheel hub. The endurance limit must be defined through the endurance limit of reference (S_e'), which is the rotating-beam specimen endurance limit, and with the corresponding endurance limit modifying factors or Marin factors. Those Marin factors include the surface condition modification factor (k_a), size modification factor (k_b), load modification factor (k_c), temperature modification factor (k_d), reliability factor (k_e), and miscellaneous-effects modification factor (k_f). Therefore, the Marin equation for the endurance limit approximation is presented in equation (4.51).

$$S_e = k_a k_b k_c k_d k_e k_f S_e' \tag{4.51}$$

In fact, the stress determined at points from critical cross-sections *A* and *B* are not fluctuating. Therefore, the equation (4.52) is used to define the number of cycles-to-failure (*N*) in relation to a completely reversed stress (σ_{rev}). For this reason, the constant *a* is obtained with the equation (4.53) and the constant *b* with the equation (4.54) with regard to the ultimate tensile strength of the material.

$$a = \frac{(f S_{ut})^2}{S_e} \tag{4.52}$$

$$b = -\frac{1}{3} log\left(\frac{f S_{ut}}{S_e}\right) \tag{4.53}$$

$$N = \left(\frac{\sigma_{rev}}{a}\right)^{\frac{1}{b}} \tag{4.54}$$

Using the information in the literature [45] and the critical cross-section *C* of the geometry for the wheel hub, the stress-concentration factor (K_t) is approximated in order to establish the fatigue stress-concentration factor. The equation (4.55) is associated with the fatigue stress-concentration factor for normal stress (K_f), while the equation (4.56) calculates the fatigue stress-concentration factor for shear stress (K_{fs}). In both cases, the notch sensitivity (q, q_s) must be approximated as well. Therefore, the equation (4.57) is used to compute the notch sensitivity in relation to the Neuber constant for the material depending on the loads applied.

$$K_f = 1 + q(K_t - 1) \tag{4.55}$$

$$K_{fs} = 1 + q_s(K_{ts} - 1) \tag{4.56}$$

$$q = \frac{1}{1 + \frac{\sqrt{a}}{\sqrt{r}}} \tag{4.57}$$

In the case of the wheel hub, the maximum normal stress is achieved when the bending and axial normal stresses are summed and the minimum normal stress when those bending and axial normal stresses are subtracted. For the maximum shear stress, the maximum shear stress corresponds to the maximum torque condition in Table 4.4. Taking into account this information, the alternating stress (σ_a, τ_a) and the midrange stress (σ_m, τ_m) are all determined with the equations (4.58), (4.59), (4.60), (4.61), (4.62), and (4.63) respectively.

$$\sigma_{max} = K_f \sigma \tag{4.58}$$

$$\tau_{max} = K_{fs} \tau \tag{4.59}$$

$$\sigma_a = \left| \frac{\sigma_{max} - \sigma_{min}}{2} \right| \tag{4.60}$$

$$\sigma_m = \frac{\sigma_{max} + \sigma_{min}}{2} \tag{4.61}$$

$$\tau_a = \left| \frac{\tau_{max} - \tau_{min}}{2} \right| \tag{4.62}$$

$$\tau_m = \frac{\tau_{max} + \tau_{min}}{2} \tag{4.63}$$

Based on the combination of stress at the specific points at cross-section *C* and the maximum distortion energy criterion, the equation (4.6) used to compute the principal stresses ($\sigma_{1,2}$) and the equation (4.7) for the von Mises stress (σ_v) of both the alternating and midrange normal and shear stresses. Finally, applying the design equation for modified Goodman line at equation (4.64) and the Langer first cycle yielding at equation (4.65), the fatigue factor of safety (n_f) and the yield factor of safety (n_y) for this analysis are determined. The factors of safety for both maximum conditions at critical cross-section *C* are presented in Table 4.5.

$$\frac{\sigma_{v,a}}{S_e} + \frac{\sigma_{v,m}}{S_{ut}} = \frac{1}{n_f} \tag{4.64}$$

$$\sigma_{v,a} + \sigma_{v,m} = \frac{S_y}{n_y} \tag{4.65}$$

Table 4.5. Results of the fatigue analysis of the geometry of the wheel hub.

Factor of safety	Maximum load transfer condition at section *C*	Maximum torque condition at section *C*
Fatigue (mod-Goodman)	4.18	2.86
Yield (Langer)	7.59	5.34

Once the geometry is defined for the wheel hub, the roller bearings to be mounted on the wheel hub are then selected. Due to the loads applied to the wheel hub, this part is going to be submitted to significant thrust and radial loads. Therefore, tapered roller bearings are options to be mounted in the wheel hub.

In the previous analysis of the geometry for the wheel hub, the mounting points for the bearings are determined to conduct the bending calculations. With the condition of maximum load transfer at the wheels, the loads perpendicular to the longitudinal axis of the wheel hub consist of both tangential and radial loads. These loads are considered for the roller bearing selection as a resultant perpendicular reaction (R_r) at the mounting points' cross-sections. Using the direct mounting configuration for the tapered roller bearings at the wheel hub, the loads are analyzed for the roller bearing selection procedure.

Actually, any radial load exerted on the tapered roller bearing is going to induce a thrust reaction [45]. The equation (4.66) is set for the induced thrust load (F_i) due to a radial load in the load zone and in relation to the K factor as a geometry-specific ratio. At this equation, the corresponding radial load is the resultant perpendicular reaction for both mounting points.

$$F_i = \frac{0.47(R_r)}{K} \tag{4.66}$$

Since these roller bearings are going to experience both radial and thrust loads, it is necessary to determine an equivalent radial load. Also, the mounting of the roller bearings in the wheel hub defines which of the roller bearings carries the net axial load. In this particular case, the tapered roller bearings are then named as A and B, being the A roller bearing the one that is mounted first in the wheel hub. Considering this, the inequality equation presented in equation (4.67) establishes the net axial load carried by the roller bearings in this instance, being defined the induced thrust loads and the external axial load (F_{ae}) at this point. Thus, the corresponding equivalent radial loads for the roller bearings A and B are calculated using the equations (4.68) and (4.69).

$$F_{iA} > (F_{iB} + F_{ae}) \tag{4.67}$$

$$F_{eB} = 0.4(F_{rB}) + K_B(F_{iA} - F_{ae}) \tag{4.68}$$

$$F_{eA} = F_{rA} \tag{4.69}$$

With the equivalent loads calculated, the next step is to apply both equations (4.15) and (4.16) to ascertain the multiple of rating life (x_D) and the catalog load rating (C_{10}) for the tapered roller bearings to be mounted in the wheel hub. After the iterative procedure, the tapered roller bearings for the wheel hub are selected. It is important to mention that the design of the wheel hub and the selected roller bearings are established for every wheel assembly for the race car.

Finally, the design of the knuckle completes the configuration of parts for the wheel assembly, The knuckle must be designed to enable the interaction with different elements, in dependance of the location of the knuckle in the racing car, being different at the front axle than the knuckles at the rear axle. Jawad and Polega [61] mentioned in their findings that the uprights or knuckles main function is to connect the upper and lower ball joints, and note the importance of weight reduction of the upright to achieve a lower unsprung mass.

In fact, the geometry of the knuckle is dependent on the geometry of the wheel rim, the selected roller bearings, as well as the location of the brake, steering and suspension elements. One of the most relevant analyses for the knuckles is to define the mounting points for the suspension joints. The usual configuration for the tunning of the geometry for the wheel assembly is mentioned in the literature. Sun et al. [62] present wheel car alignment parameters in their project, considering from kingpin inclination to caster, camber and toe angles. These are relevant parameters that must be able to tune in order to adjust the racing car's behavior in track.

For instance, the caster is defined by Bhatt [34] as the angle that the steering axis deviates from vertical in the side view of the car, considering that a positive caster generates negative camber on the outside tire and positive camber on the inside tire when both wheels are steered. To be able to achieve adequate behavior of the racing car, parameters such as the caster and mechanical trail are defined for the front and the rear axle knuckles.

As the caster, mechanical trail and kingpin inclination vary in the geometry of the racing car from the front to the rear axle, the geometry of the knuckle is designed as a modular part. This means that a general geometry for the knuckle is developed for the wheel assembly, and the different mounting points for the interaction with the braking, steering and suspension systems are carried out with additional brackets to be designed specifically for the front and rear axle. The general geometry of the knuckle is based on several designs reported in the literature [30], [60], [62].

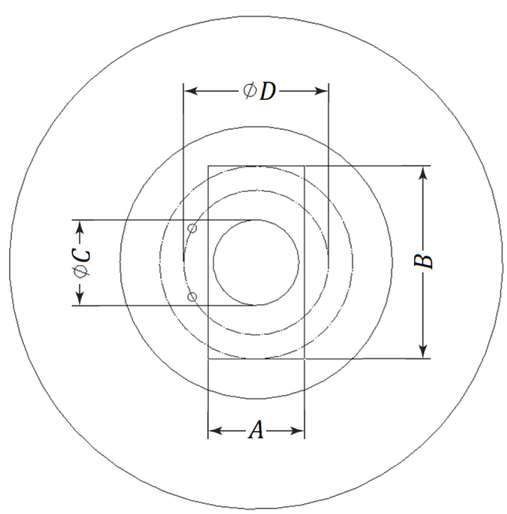

Figure 4.7. Side view of the wheel assembly and knuckle dimensions.

Using the data of the wheel assembly parts and other systems of the racing car, the corresponding dimensions for the knuckle are determined by means of scale and space available at the wheel assembly as shown in Figure 4.7. The parameters A, B, C and D at Figure 4.7. represent the dimensions for the knuckle with regard to the wheel rim and tire dimensions, as well as the brake elements to be mounted and presented further in the configuration section of this thesis project.

4.3.3. Intake system configuration

To begin with, the intake system for the racing car must adapt to both the ICE and transmission group selected and the Formula SAE regulations. As stated in the regulations of the competition [8], the intake system must be compliant with a sequence of throttle body, restriction and engine for naturally aspirated engines. With the aim of being compliant with this sequence, some intake systems reported in the literature use a single-point injection system [63]. Even though the single-point injection may be a simple alternative, it also introduces some disadvantages such as uneven fuel distribution or higher emissions. For this reason, the proposed air intake system corresponds to a multi-point fuel injection system, which is intended to improve fuel distribution, fuel efficiency and engine performance. Therefore, the complete suggested sequence for the air intake system, without taking into account the fuel injection, is shown in Figure 4.8. The sequence consists of an air filter, a throttle body, a restriction with a plenum and ends with the runners finding the way into the engine.

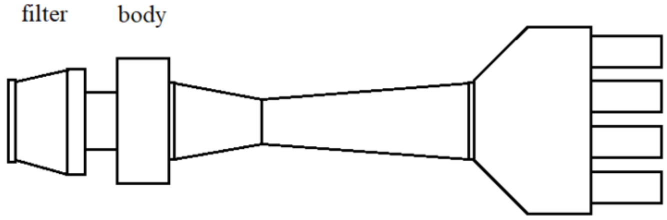

Figure 4.8. Air intake sequence for naturally aspirated ICE for the racing car.

Following the configuration of the air intake system, the air flow required to be supplied to the ICE is calculated. The equation (4.70) below is used to determine the theoretical air flow for the engine (Q_f), considering the mechanical power of the engine (P), the air factor (f_a) and the ideal thermal efficiency of the engine (η). As the fuel to be used in the competition is gasoline, the air factor is estimated towards the stoichiometric ratio of this fuel. To define the ideal thermal efficiency of the engine, the equation (4.71) defines this parameter in terms of the engine compression ratio (cr) and the adiabatic coefficient (k) of the mixture.

$$Q_f = \frac{P(f_a)}{\eta} \tag{4.70}$$

$$\eta = 1 - \frac{1}{cr^{k-1}} \tag{4.71}$$

With an approximate average velocity of the intake air (v) and the conservation equation of flow, the equation (4.72) is employed to determine the inner diameter of the required air flow calculated previously.

$$Q_f = \frac{\pi d^2}{4} \cdot v \tag{4.72}$$

After these parameters are defined, the air filter and throttle body may be selected. In the case of the throttle body, the function of fuel distribution is not considered to occur in the throttle body. For this reason, a simplified single-valve throttle body is selected for the racing car. The selected throttle body is determined by the inner diameter calculated with the equation (4.72) and with options to be able to operate the valve with a cable, with idle speed adjustments and the possibility to incorporate a throttle position sensor (TPS) to link this information to the engine control unit (ECU). Once the throttle body is selected, an air filter with similar diameter and adequate for the desired air flow is searched.

On the other hand, the restriction for the air intake system is formed by a geometry that must consider several aspects. Actually, the restriction may help the air intake system to provide a controlled pressure and velocity into the plenum and then into the runners, improving fuel efficiency in some cases. Besides this, if the geometry of the designed restriction provides to much restriction to the air flow, the consequences may vary to negative effects such as lower fuel efficiency or reduced power output. Since this geometry is that critical, the restriction for the racing car is based on the findings in the literature [12], [63]. Having the diameter of the throttle body defined, as well as the suggested convergence and divergence angles for the restriction [63], the geometry and dimensions for the restriction are ascertainable.

Another crucial geometry to be established is the plenum. As mentioned in the findings of Sharma et al. [63], the volume of the plenum must be defined in relation to the engine displacement in order to achieve an improved performance of the engine. However, due to the limited space at the racing car, the plenum geometry and inner volume is limited in relation to the ICE displacement. After the volume and geometry are established, the complete dimensions for the plenum are calculated. Therefore, both the restriction and plenum have characteristic and complex geometries. To manufacture these parts and avoid operational or assembly issues, both parts are made out of cast aluminum alloy.

In the case of the runners, the inner diameter is directly based on the ICE inlet ports at the head. The length of the runners is dependent on the location of the other elements in the air intake assembly. Still, short runners are preferred to achieve higher performance at high angular frequencies of the ICE, improved throttle response and to reduce air flow resistance. The fuel injection system is going to interact with the intake system at the geometry of the runners, placing the fuel rail near the runners and the injectors to provide fuel to the inside of the runners to form the mixture.

4.3.4. Injection system configuration

Associated with the selected ICE and transmission group, the required fuel supply is estimated in relation to the parameters and operation of the ICE. The equation (4.73) is incorporated into the analysis of the fuel supply of the engine (Q_f) in order to reach the peak mechanical power (P_{max}) as a function of the net calorific value of the fuel (*NCV*) and the ideal thermal efficiency of the engine.

$$Q_f = \frac{P_{max}}{\eta(NCV)} \tag{4.73}$$

Taking the fuel supply calculated with the equation (4.73) as a critical demand of fuel for the engine, the fuel tank capacity can be approximated considering the racing car participation in the dynamic events at the competition. To be precise, the fuel tank capacity must consider a minimum capacity to be able to complete the stints for the dynamic events of the competition and a safety margin to store additional fuel for any other desired action on track. Thus, considering the dynamic events standard information and the average speed of the car in those events, the fuel tank capacity (V_{ft}) for the racing car is established using equation (4.74) with regard to the fuel supply of the engine, the required time at the stints for the events (t) and a safety margin factor (f_m) for any maneuver on track.

$$V_{ft} = f_m Q_f t \tag{4.74}$$

In addition, a fuel pump for the racing car must be determined to have the capacity to provide the adequate fuel supply demanded by the ICE at any time. Actually, the simple way to determine this for the selected ICE and transmission group is to use the same or at least a similar fuel pump equipped in the system of the KNZ motorbike. The manufacturer of the fuel pump does provide information related to the fuel pump, including the operational pressure range, the fuel flow rate at certain pressure, voltage for the pump and some dimensions.

In a similar case, the fuel rail for the injection system of the racing car is established with the OEM fuel rail of the KNZ motorbike. This decision is mainly based on the dimensions, materials and adaptability of the OEM to not only the injection system of the car, but also to the air intake system. The injectors for the system are the OEM injectors as well, as those are related to the fuel rail and the demands of the engine. However, the fuel lines to connect the fuel pump to the fuel rail for this system must be chosen diligently, as these lines are subjected to pressure and other factors during the operation of the engine. With the dimensions reported by the manufacturer of the fuel pump and the Formula SAE regulations [8], the fuel lines for the racing car are determined between options that are considered as plastic fuel lines. In all cases, the length of the fuel lines (L) is checked for viability in terms of pressure drop (Δp) with the equation (4.75). At the equation (4.75) of the general form of Darcy-Weisbach equation, the friction factor (f), the density of the fluid (ρ), the fluid velocity (v), and the diameter of the fuel lines (d) are involved as well.

$$\Delta p = \frac{f L \rho v^2}{2d} \tag{4.75}$$

Another relevant topic to be compliant with the regulations of the competition is the fuel tank. One of the most important characteristics of a fuel tank is the crashworthiness, defined as the ability of the fuel tank to protect the fuel inside and to retard any chance of a post-impact fire [47]. As permitted by the organizers of the competition, the possibility to incorporate a bladder-type fuel tank into the racing car is considered as a safety measure.

Therefore, alternatives to bladder-type fuel tank are searched to be placed in the racing car injection system in order to be within the fuel tank capacity previously calculated. After finding options to select a fuel tank, the technical specifications of the fuel tank are considered to enclosure the tank inside a container to protect the tank and attach it to the racing car.

The fuel tank container must consider several factors, regulations and elements to be placed inside or at external portions of the container. First, the bladder-type fuel tank selected is provided with three ports and connections, one intended for fuel tank filling, another one for fuel line supply and the last one for fuel tank ventilation. The fuel tank filling is carried out with a hose and standard fuel tank cap that are compliant with the fuel filler neck and sight tube specifications at the Formula SAE regulations [8]. For the fuel line supply, barb fittings are used to connect an internal duck foot fuel trap with a filter with the fuel pump for suction. Once the fuel passes through the fuel pump, the fuel lines connect the system to the fuel rail, securely attached to the engine block with fasteners. Finally, the ventilation of the fuel tank is carried out with a check-valve connection and a hose that extends to the floor of the racing car.

4.3.5. Exhaust system configuration

Moving forward, the configuration of the parts for the exhaust system is performed. At the exhaust system, the exhaust manifold of the KNZ motorbike is partially used for the exhaust system of the racing car. This is because of the required geometry of both the runners and the collector to provide acceptable exhaust scavenging and a reduced backpressure. Notwithstanding, if any element blocks the way out of the exhaust gases after the collector, that element is eliminated from the geometry of the exhaust manifold in order to optimize exhaust gases removal.

In addition, the geometry for the exhaust system tubing is determined by analyzing the critical amount of exhaust gases to be removed from the engine. The volume of exhaust gases is approximated with the displacement of the engine. Hence, the exhaust tubing diameter is calculated using equation (4.72) and with the equation (4.76) that relates the exhaust flow rate (Q_f) to the engine displacement (V_e), the angular frequency of the engine (ω), and volumetric efficiency of the engine (η_v). The volumetric efficiency is determined by the ratio of the actual air intake volume and the theoretical air intake volume.

$$Q_f = \frac{\eta_v V_e \omega}{2} \tag{4.76}$$

As established in the Formula SAE regulations [8], the maximum permitted sound level for the racing car is directly measured towards the engine operation at the inspection for the competition. To be compliant with this regulation, the exhaust system must be designed to prevent the sound pressure level to surpass the permitted sound level at any speed. To determine the critical condition for the ICE selected, the sound pressure (p) is determined with the equation (4.77) that associates the mechanical power of the engine (P), the effective cross-section for the exhaust (A) and the reference speed of sound (c) for the exhaust gases. Additionally, the sound pressure level (spl) is calculated with the equation (4.78) in relation to the reference sound pressure (p_0). The sound pressure of reference employed for the calculation is directly associated with the threshold of hearing.

$$p = \sqrt{\frac{P}{(A)(c)}} \tag{4.77}$$

$$spl = (20)log_{10}\left(\frac{p}{p_0}\right) \tag{4.78}$$

Hence, the device that allows the reduction of the sound pressure level for the exhaust system is the resonator. For that reason, available options for a standard resonator are searched within the calculated tubing diameter for the exhaust system. To select one of the alternatives of resonator for the exhaust system, the equation (4.79) is used to compute the change in the sound pressure level (*Δspl*). This equation is similar to equation (4.78), but still the parameters to calculate the change in sound pressure level involve the resonator volume (*V*), the cross-section (*A*) of the input for the resonator, and the resonant frequency (*f*). Thus, to be able to determine the resonant frequency, the equation (4.80) is employed.

$$\Delta spl = (10)log_{10}\left(\frac{V}{Af^2}\right) \tag{4.79}$$

$$f = \frac{c}{2\pi}\sqrt{\frac{A}{V}} \tag{4.80}$$

The desired resonator for the exhaust system is the one that better presents a difference in acceptable range between the sound pressure level calculated for the exhaust and the change of sound pressure level for the resonator.

4.3.6. Cooling system configuration

The configuration for the cooling system is carried out in view of the heat to be dissipated from the ICE as the point of departure. The energy lost in the form of heat (*Q*) is estimated with the equation (4.81), which considers the thermal efficiency of the engine (η) and the mechanical power of the engine (*P*).

$$Q = (P)\frac{(1-\eta)}{\eta} \tag{4.81}$$

Considering the fact that the ICE selected does have a defined temperature range to open the thermostat in the design, this temperature range is then established as a constraint for the cooling system for the racing car. Another aspect to be considered is that the guidelines of the competition state that the only coolant for the engine has to be plain water with no additives. Even though this may suppose some issues such as corrosion, lack of lubrication for parts such as the water pump or affected heat transfer, the use of plain water is defined as well as a design constraint for the calculation of parameters and the decision-making process for the selection of the parts for the cooling system. Notwithstanding, the properties of both plain water and the suggested coolant by the engine manufacturer are used in the formulation below.

With the equation (4.82), the heat to be dissipated from the engine is related to the specific heat capacity (C_p) and the temperature change in the coolant (ΔT) to compute the volumetric flow rate of the coolant (Q_f). This calculation involves the density of the coolant (ρ) and is used to approximate the water pump flow rate for the system. After this, the inner diameter for the hoses of the water pump can be estimated as well with the equation (4.72).

$$Q = \frac{Q_f C_p \Delta T}{\rho} \tag{4.82}$$

In fact, OEM radiators do not provide sufficient cooling for the engine when restricted to the regulations of the Formula SAE competition, as stated in the finding of Padmaraman et al. [64]. Following the configuration, the radiator for the cooling system is determined based on the cooling capacity. Hence, the equation (4.83) is presented. At this equation, the amount of heat transferred (Q) is the cooling capacity of the radiator, while the change in temperature is the temperature difference between the air and the coolant, the surface area though which the heat is transferred (A) corresponds to the effective surface of the radiator and the overall heat transfer coefficient (U) is defined in relation to the construction characteristics of the radiator, including the number of rows (n).

$$Q = nAU(\Delta \mathrm{T}) \tag{4.83}$$

As a matter of fact, the radiator alternatives that may be considered for the analysis and selection process are a few given that the dimensions, materials and construction are limited for the application. For instance, a vast majority of the viable radiators for racing cars use aluminum as the main material for heat transfer. Actually, aluminum offers great thermal conductivity and corrosion resistance, together with the affinity with weight reduction. Those are characteristics desired for the racing car. On the other hand, there can be found different configurations of the radiator, including downflow and crossflow radiators. Concerning this configuration, a crossflow radiator allows a side-to-side coolant flow and are generally more efficient, more compact and easier to maintain than downflow radiators.

Presented as an example of the selection process, three different radiator alternatives technical specifications are presented in Table 4.6. The radiator alternatives include a downflow, crossflow and dual-core radiators from several manufacturers. It is important to note that these options consider that the inlet and outlet diameter from the radiator are similar to the inner diameter calculated previously with the volumetric flow rate of the coolant.

Table 4.6. Alternatives for radiator selection for the cooling system.

Parameter	**Downflow radiator**	**Crossflow radiator**	**Dual-core radiator**
Effective surface	1445.16 cc	1822.91 cc	1252.65 cc
Number of rows	2	4	2
Material	Aluminum	Aluminum	Aluminum
Relative cost	0.7187	1	0.6166

With the equation (4.83), the radiator cooling capacity is approximated with a defined overall heat transfer coefficient for the radiator alternatives. Once all this information is gathered, the radiator is selected within the selection criteria that entails the cooling capacity, the relative cost and the availability of the radiator. Once the radiator is selected, a viable radiator fan is determined to be mounted in the effective surface of the radiator. Using the equation (4.82), the volumetric flow rate is calculated with the cooling capacity computed previously for the selected radiator. With this data, a radiator fan is searched to be able to be mounted in the surface of the radiator and to be compliant with the volumetric flow rate.

The cooling system must integrate a coolant reservoir to allow the coolant to expand and contract in communication with the radiator cap. To determine the volume change in the coolant reservoir (ΔV), the equation (4.84) relates this volume change to the initial volume (V_0), the thermal expansion coefficient (β) and the temperature change. The initial volume for this formulation is referred to as the coolant volume reported by the manufacturer of the ICE.

$$\Delta V = V_0 \beta \Delta T \tag{4.84}$$

Therefore, the corresponding pressure reached by the coolant is calculated with the ideal gas law at the equation (4.85), approximating the behavior of the fluid. At this equation, the pressure (P), the temperature (T) and the volume (V) are established for the rough estimation of the coolant behavior as an ideal gas without considering the radiator cap pressure limitations and many other factors.

$$P = \frac{nRT}{V} \tag{4.85}$$

Hence, the coolant reservoir is selected considering both the change in volume and the maximum pressure that can be exerted inside the reservoir with a factor of safety. With all the elements for the cooling system configurated, the hoses and fittings to connect these elements are selected in order to prevent leaks and to be able to withstand pressure and to minimize coolant flow resistance.

4.3.7. Electrical cluster configuration

The electrical cluster for the formula-style racing car must consider several elements and subsystems to provide functional characteristics to the engine, the auxiliary systems of the engine and the car in general. Therefore, the aim is to concrete all the elements that integrate the electrical cluster and select the standard parts that are going to be implemented in the subsystems.

To begin with, the Formula SAE regulations state as mandatory the inclusion of a shutdown circuit, which integrates the master switch, the cockpit main switch and the brake overtravel switch (BOTS). The master switch is a direct-acting switch from which all battery current flows to any another electrical device in the installation. The cockpit main switch is an adjacent switch to the steering wheel in the cockpit for easy access of the driver that acts through a relay. Meanwhile, the brake overtravel switch is an analogic implemented switch that prevents brake pedal travel exceeding the normal range. These three switches must be placed in the vehicle and have different characteristics. With regard to these switches, detailed information about the switches is presented in Table 4.7.

Table 4.7. Technical specification of the shutdown circuit switches.

Specification	Master switch	Cockpit main switch	BOTS
Location	Accessible rear left side of the car	Dashboard of the cockpit	Near the brake pedal assembly
Rated current	300 A	10 A	10 A
Rated voltage	12 V	12 V	12 V
Number of poles and throws	SPST	SPST	SPST

Following the configuration of parts for the electrical cluster, the analysis of the required elements for the electrical installation in the vehicle is carried out. First, the corresponding elements to be connected to the electrical installation are grouped into different categories. For this reason, the electrical installation can be separated into charging system, ignition system, injection system, electric starter system, and engine control and data acquisition system. These systems do not consider the corresponding fuses and relays for the functional requirements.

The electrical starter system integrates the starter motor in conjunction with the starter solenoid to the electrical cluster. The OEM starter motor and starter solenoid used by the KNZ engine is proposed as the starter motor for the racing car as well. Therefore, the rated current and voltage for the starter motor are set as design constraints for other components for the electrical cluster.

To provide electrical energy supply constantly to the electrical cluster devices, the charging system incorporates the battery, the alternator and the voltage regulator to installation. In a similar way to the starter motor, the OEM alternator is implemented to the charging system of the racing car, as well as the voltage regulator. Notwithstanding, the battery is calculated for feasibility in the charging system considering the equation (4.86), which calculates the cold cranking amps of the battery (CCA) in relation to the peak current of the starter motor (I_s) and a scale factor (f). In order to estimate the peak current of the starter motor, the equation (4.87) considers the power of the starter (P), the voltage from the battery (V_b) and the efficiency of the starter motor (η) in regard to the losses due to friction and contact.

$$CCA = fI_s \tag{4.86}$$

$$I_s = \frac{P}{\eta(V_b)} \tag{4.87}$$

The selected battery type for the charging system is a VRLA battery with a minimum cold cranking amps calculated previously. After this, the ignition system components are defined. Once again, the OEM ignition system of the KNZ remains almost with no modification, using the same ignition coils, spark plugs and position sensors for the racing car. However, the ECU may be changed to be tuned for the racing car, making it necessary to provide an ECU that can provide the timing and sequence parameters for the spark events.

As the injection system incorporates the fuel pump and the injectors for an electronic injection system, both pump and injectors can be considered as actuators and must be placed in the electrical cluster as well. The fuel pump and the injectors are the OEM parts designated by the manufacturer of the engine.

Finally, the engine control and data acquisition system integrates the ECU, the sensors, the actuators, the communication protocol, the gauge at the dashboard of the cockpit and the telemetry elements if required. At this point, the sensors and actuators for the electrical cluster are defined. Nevertheless, the ECU is now selected considering feasible alternatives for the racing car, as well as similar elements required for the engine control and data acquisition system, such as the gauge for the cockpit, the wiring harness, etc.

In fact, the wiring harness is determined by several factors. Those factors include the wire gauge, the wire length, the voltage drop and the power loss. To be able to analyze the feasibility of the wiring harness for the electrical cluster, the Ohm's law at equation (4.88), the Joule's first law at equation (4.89) and the equation (4.90) for electrical resistivity are implemented to determine the voltage drop and the power loss of the wiring harness with the wire cross-section (A) and the length of the wire (L) for the harness.

$$V = IR \tag{4.88}$$

$$P = I^2R \tag{4.89}$$

$$R = \rho\frac{L}{A} \tag{4.90}$$

Once the elements for the electrical cluster are defined, a block diagram is developed for the electrical cluster to organize and clarify the integration of different elements in the systems and the interaction between those parts. The block diagram for the electrical cluster of the racing car is presented in Figure 4.9. This diagram may be used as the foundation for future works towards the electrical cluster, such as the wiring harness layout and cable routing.

Some relevant aspects to consider of the information presented in Figure 4.9. are clarified below. To begin with, the main fuse is intended as a safety measure to protect against short circuits between battery and master switch. The master switch, cockpit main switch and BOTS integrate the shutdown circuit, in compliance with the Formula SAE regulations. The ignition switch must be a multi-position switch to enable three different positions: off for no connection, run to enable power to the rest of the elements and start for a momentary position to crank the engine. Finally, the engine control and data acquisition is commanded by the ECU and the interaction with the sensors and the actuators, as shown in Figure 4.9.

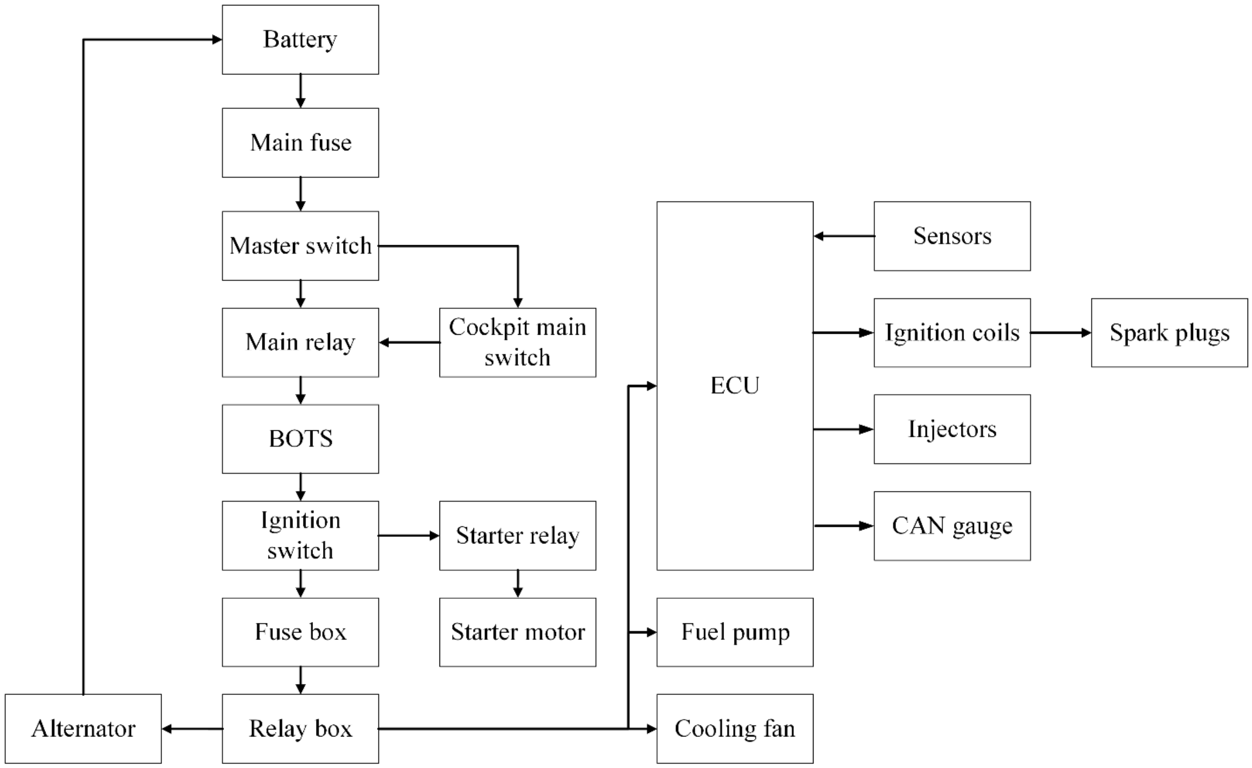

Figure 4.9. Block diagram for the electrical cluster of the racing car.

4.3.8. Suspension system configuration

The first system to be presented is the suspension system for the racing car. As established previously in the conceptual development stage, the suspension system acts in the car through the use of elements including the spring, the damper or even the tire, as outlined in Figure 3.3. Considering the quarter-car SMD model, the configuration of both the spring and the damper for the racing car are determined as follows.

The ride frequency is a parameter that must be related to the vehicle's suspension system application. As mentioned in the findings of Rajeev [65], ride frequency of the suspension system plays a major role in the design of the vehicle and the determination of ride frequency is largely based on assumptions. The ride frequency is computed with the equation (4.91) that related the frequency (f) to the spring stiffness (K) and the sprung mass (m). This equation is used to estimate spring rate (K_s) for the car using a ride frequency focused on handling, although this may compromise comfort.

$$f = \frac{1}{2\pi}\sqrt{\frac{K}{m}} \tag{4.91}$$

The spring rate is then calculated for the front and rear axle of the racing car using the corresponding sprung mass for each axle in relation to the initial mass distribution approximated in the IVDS. After the spring rates are computed, the springs for the car can be adjusted to commercial values in order to select these parts later on.

As the spring rates were adjusted previously, the damping coefficient can be calculated as well. Solving the second-order differential equation (3.3) for the single degree of freedom mass-spring-damper system using the damped harmonic motion theory results in the equation (4.92). At the equation (4.92) the damping ratio (ζ) is calculated in relation to the damping coefficient (C), the spring rate and the sprung mass for the front and the rear axle of the racing car.

$$\zeta = \frac{C}{2\sqrt{Km}} \tag{4.92}$$

Once the damping coefficient are computed, this damping coefficient is used to determine the shock absorbers for the racing car. It is important to determine some conditions to select the shock absorbers, such as the geometry, type and dimensions of the coil-over shock absorber, the effective travel of the shock absorber and the computed damping ratio range in which the shock absorber can enable the damping coefficient. Considering the data reported by the shock absorber manufacturer, the dynamometer graph is used to choose an adequate option for the shock absorbers of the racing car. As a matter of fact, the selected coil-over shock absorbers are nitrogen-actuated twin-tube that allow independent tuning of compression and rebound.

With the shock absorber selected, the springs for the racing car are analyzed to determine if the commercial springs may support the exerted force in the suspension with an elastic behavior. To verify this condition, a pair of commercial springs are selected using the dimensions of the shock absorbers and the estimated spring rate. Hence, the equations (4.93), (4.94) and (4.95) are used to calculate the total number of coils (N_t), the number of active coils (N_a) and the spring pitch (p) based on the data of the springs including free length (L_0), solid length (L_s) and the wire diameter (d).

$$N_t = N_a + 2 \tag{4.93}$$

$$L_0 = pN_a + 2d \tag{4.94}$$

$$L_s = N_t d \tag{4.95}$$

Considering the computed data of the springs and the material from which those are made, parameters such as the wire's yield shear stress (S_{sy}), the static load at yield point (F) and the deflection under the static load at yield point (y) can be determined. First, the equation (4.96) is used to estimate the ultimate tensile strength of the material used for the wire of the spring in relation to constants available in the literature [45]. In addition, the shear yield strength is computed using equation (4.97) based on the maximum-shear stress theory.

$$S_{ut} = \frac{A}{d^m} \tag{4.96}$$

$$S_{sy} = 0.5(S_y) \tag{4.97}$$

Later on, the spring index (C) is calculated with equation (4.98) as a relation between the mean coil diameter (D) and the wire diameter. Once the spring index is computed, the Bergsträsser factor can be estimated with equation (4.99) to include the curvature effect in the spring.

$$C = \frac{D}{d} \tag{4.98}$$

$$K_B = \frac{4C + 2}{4C - 3} \tag{4.99}$$

Finally, the corresponding static load (F) and deflection (y) at yield point are calculated using equation (4.100) and (4.101) respectively.

$$F = \frac{\pi d^3 S_{sy}}{8 K_B D} \tag{4.100}$$

$$y = \frac{F}{K_s} \tag{4.101}$$

At this point, the computed static load at yield point may be used as a failure condition to estimate a safety factor for use of the helical springs at the suspension system of the racing car. After checking the viability of the springs for the suspension system, the next step is to determine the geometry of the system for both the front and rear axle.

As conducted in the conceptual development stage, the suspension system for the front axle is meant to be a pullrod suspension geometry, meanwhile the rear axle incorporates a pushrod suspension geometry. Therefore, the corresponding geometries are defined through the parameters and dimensions that relate the suspension system to the wheel assembly and the chassis. The front view of the geometry for the pullrod suspension at the front axle and the geometry for the pushrod suspension at the rear axle are shown in Figure 4.10. It is important to note that the front view does not consider the complete mounting points for the chassis, as the geometry requires more information to define those points.

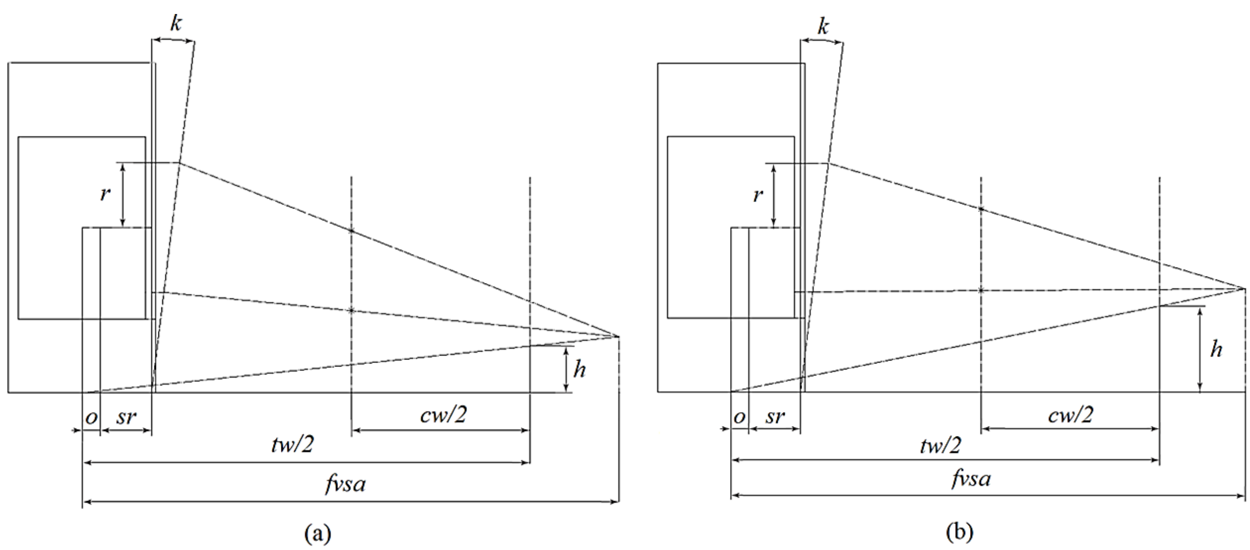

Figure 4.10. Front view of the suspension geometry for the (a) front axle and (b) rear axle.

Hence, the front view presents several relevant data for the definition of the suspension geometry in both cases. For instance, the chassis width (cw) and the track width (tw) of the racing car at the front and rear axle are used as reference to determine the behavior of the suspension system by the proposition of a front view swing arm (*fvsa*) and the roll center height (*h*). In addition, the wheel must consider the offset (*o*), the kingpin inclination angle (*k*) and the scrub radius (*sr*), which is an important parameter to define the steering axis and the tire's contact patch, or the radius of the knuckle's joints (*r*). In fact, parameters such as the front view swing arm and the kingpin inclination angle are proposed for the geometry of the suspension for the car.

The location of the mounting points for the suspension system to the chassis must consider some other factors. As reported in the findings of Azman et al. [66], the anti-dive and anti-squat geometries have a great influence on the handling and the dynamics of the car, specifically towards the plane of the car that causes the pitch rotation. This leads to associating the anti-dive and anti-squat geometries with the acceleration and braking behavior of the racing car. However, the implementation of both anti-dive and anti-squat geometries into the suspension system of the racing car requires iterative design to achieve the benefits of the geometry and reduce the disadvantages that can appear from it.

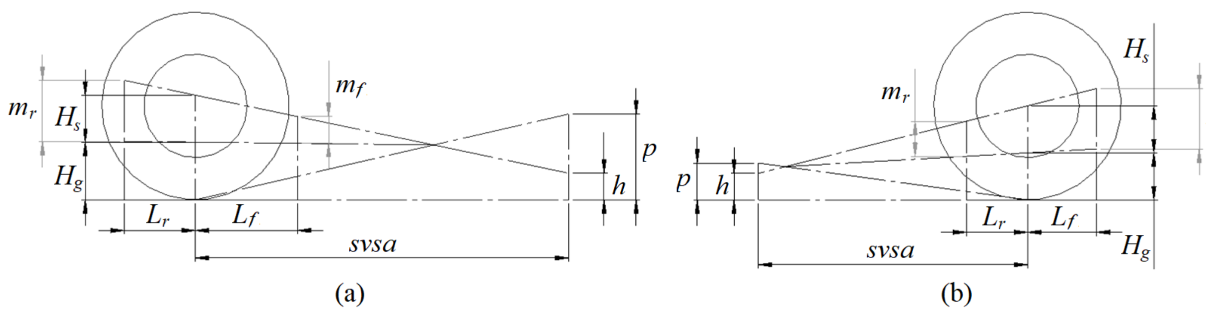

Figure 4.11. Side view of the suspension mounting points for the (a) rear axle and the (b) front axle.

The anti-dive and anti-squat geometries for the mounting points of the suspension system are determined with the assistance of the side view and parameters shown in Figure 4.11. In fact, the geometry consists of the side view swing arm (*svsa*) length for both front and rear axle, which is estimated towards the location of the center of gravity. In addition, the percentage (*p*) of either anti-dive or anti-squat are proposed into the geometry and some other parameters such as the ride height (*h*) for the racing car, the corresponding ground (H_g) and suspension (H_s) heights from the front view in Figure 4.10., or the front and rear lengths (*L*) considering the near structural members of the chassis. Finally, the rear and front mounting points heights (*m*) are established to define the geometry of the suspension system for the racing car.

Once the suspension geometry is defined, the motion ratio for the suspension and the element forces can be calculated by different means such as simulation tools and the elements of the suspension system including the control arms and the bell crank can be designed. As a matter of a fact, the suspension control arms of the double wishbone suspension system are subjected to several stresses consisting mainly of axial tension and compression stress or bending stress. These stress conditions are taken into account to define the control arms cross-section. Effects such as torsional stress and other shear stress can be accounted for the suspension design in joints but still are neglected to determine the cross-section of the control arms.

As noted previously, the control arms are subjected to compression axial forces that may cause the arms to act as a column. Therefore, the design of the control arms, even the pushrod and pullrod, must consider the buckling criterion. Firstly, the buckling criterion demands the determination of the slenderness ratio (λ) for the column to classify the element as either a short or medium column. The equation (4.102) relates the effective length (L_e) of the member to the radius of gyration (r) to compute the slenderness ratio. After the member is classified, the primary failure concern is established for the control arms and rods as either the yielding or buckling criterion. For those members that require the analysis by means of buckling criterion, the equation (4.103) and (4.104) may be used to estimate the critical load (P_{cr}) and the allowable normal stress (σ_{allow}) within the length, the elasticity modulus and the moment of inertia of the member, using a hollow circular cross-section for the suspension members.

$$\lambda = \frac{L_e}{r} \tag{4.102}$$

$$P_{cr} = \frac{\pi^2 EI}{(L_e)^2} \tag{4.103}$$

$$\sigma_{allow} = \frac{4P_{cr}}{\pi(D^2 - d^2)} \tag{4.104}$$

It is important to note that the selection of the inner and outer diameters for the hollow circular cross-section of the members needs to consider commercial rod-end bearings for the suspension joints. Hence, both the suspension members and the rod-end bearings are selected in this procedure.

Ultimately, the characteristics of rockers for both pushrod and pullrod suspension geometries are defined to ensure adequate motion for the system. In accordance with Chauhan et al. [67], the rocker geometry must be designed in relation to the maximum compression of the spring. Considering this and other design conditions, the geometry of the rocker is defined for the suspension based on the motion ratio of the system. The motion ratio (mr) is obtained as a relation between the spring travel (t_s) and the wheel travel (t_w) for the suspension geometry, as shown in equation (4.105).

$$mr = \frac{t_w}{t_s} \tag{4.105}$$

4.3.9. Steering system configuration

Furthermore, the steering system for the racing car involves the selection of several components that may serve as the cornerstone for the design of the system. To begin with, the steering rack for the system is established among the limited but adequate alternatives for the racing car in relation to the corresponding application. Other relevant components to be determined at this point are the steering wheel and the quick-release mechanism, which are mandatory for the racing car in accordance with the rules of the competition. For instance, the steering wheel provides not only the appropriate mechanical advantage or leverage for the system but also the steering sensitivity and feedback for the driver.

As a matter of fact, the steering rack is one of the most crucial components for the steering system. The steering rack allows the translation of the rotational motion from the steering wheel into linear motion for the tie-rods to be connected with the wheel assembly, yet it defines some other parameters in relation to the geometry of the steering system or the steering ratio as well. Once the steering rack is determined, the required joints can also be defined for this component. This includes the universal joints to be used in order to link the motion from the steering wheel to the steering rack by means of the steering column.

Therefore, the steering column is designed in relation to the universal joint's dimensions. Nevertheless, the proposed design for the steering column is an alternative collapsible steering column, which is intended to be a passive safety feature for the car that is able to telescope under impact in order to reduce the risk of injury for the driver of the racing car. The first step to determine the geometry of the steering column is to define both the material for the column and the allowable torque to be considered as a design parameter.

The material to be used for the steering column is proposed as a SAE-AISI 4140 alloy steel. However, the torque (*T*) may be computed with the equation (4.106) in respect of the allowable shear stress and the desired nominal diameter (*D*) for the column. To be established as a reference, relevant data for the allowable torque to be exerted on the steering column for the vehicle are reported in the literature [68]. Still, the torque exerted on the steering column may vary from driver to driver as the response on the steering wheel is different.

$$\tau_{allowable} = \frac{16T}{\pi D^3} \tag{4.106}$$

With the torque computed for the column, the equation (4.46) is used to calculate the desired inner diameter (*d*) for the steering column, as it is going to be part of a telescopic shaft coupling. Following the determination of the steering column, the telescopic coupling for the column requires a shear pin to be designed specifically to break under certain conditions upon impact. This places the shear pin as a critical part for the assembly. The proposed shear pin for the column is a circular cross-section pin made from a cast aluminum alloy that enables an adequate assembly under normal operation of the column yet disposed to break after impact. The equation (4.107) is derived from the shear stress due to a shear force (*V*) that may act in different directions, but always towards the same two cross-sections of the shear pin with the same pin diameter (*d*). The corresponding shear force is estimated to be acting in a radius of the steering column to which the telescopic assembly may act. In a similar way to equation (4.97), the shear yield strength is computed using equation (4.108) based on the distortion energy theory.

$$\tau = \frac{2V}{\pi d^2} \tag{4.107}$$

$$S_{sy} = 0.577\left(S_y\right) \tag{4.108}$$

Both equations (4.107) and (4.108) are used to calculate the pin diameter for the shear pin. After the geometry and dimensions for the steering column assembly are determined, the required axial compressive force to break the shear pin is calculated in relation to parameters such as the testing g-force reported in the guidelines of the competition, the impact force due to the acceleration of the mass of the driver and the estimation of the assembly angle towards the mounting of the column in respect of other components.

With the shear pin established, the steering column telescopic shaft assembly must be analyzed to determine the feasibility in relation to the torque transfer from splined couplings to the universal joints, the buckling of the column or fatigue. To determine the feasibility of the torque transmission to the universal joints, the corresponding splined section for the steering column is designed towards the geometry of the universal joints and both the shear and normal stress are calculated with equations (4.20) and (4.21). On the other hand, the buckling for the steering column must consider the classification of the column and critical stress calculated by means of equations (4.102), (4.103) and (4.104).

Notwithstanding, the fatigue analysis for the steering column is conducted for the two shafts of the steering column assembly, specifically at the hole designed for the position of the shear pin of the collapsible mechanism. First, the Marin equation for the endurance limit approximation in equation (4.51) is established for the Marin factors for both shafts of the steering column. With the designed shear pin geometry and the information of the shafts, the data reported in the literature is used to determine the stress-concentration factor (K_t) is approximated in order to establish the fatigue stress-concentration factor with equation (4.56), as the load exerted on the shaft is the torque applied. After the fatigue stress-concentration factor is calculated, the maximum shear stress is computed with equation (4.59) using the shear stress that can be determined with equation (4.109). The shear stress in equation (4.109) involves that the applied torque for the analysis is at certain radius (r) of the shaft and that the pin diameter (d) defines the double shear.

$$\tau = \frac{4T}{\pi d^2 r} \tag{4.109}$$

After this, the alternating stress (σ_a, τ_a) and the midrange stress (σ_m, τ_m) are all determined with the equations (4.58), (4.59), (4.60), (4.61), (4.62), and (4.63) respectively. Finally, the von Mises stress is calculated for alternating and midrange stress conditions to immediately apply the design equation for modified Goodman line at equation (4.64) and the Langer first cycle yielding at equation (4.65), the fatigue factor of safety (n_f) and the yield factor of safety (n_y) for this analysis are determined.

Once the viability of the steering column is verified, the next step is to define the steering geometry for the system. As noted in the study of Drakulić et al. [52], the anti-Ackermann steering geometry and behavior is defined by a series of equations. Some of these equations are used in the analysis of the proposed geometry for the steering system of the racing car. The equation (4.110) is used to determine the length of the tie rod (t) with respect to the track width (tw), the length of the steering rack (r), the length of the steering arm to the wheel hub (b), the distance between the rack and the front axle of the vehicle (d) and the angle of the steering arm (β) in relation to the longitudinal axis of the car.

$$t = \sqrt{\left[\frac{tw}{2} - \frac{r}{2} + b \cdot sin(\beta)\right]^2 + (d - b)^2} \tag{4.110}$$

In addition, the equation (4.111) involves the angle of the tie rod (α) in relation to a horizontal line, the distance between the rack and the front axle of the vehicle (d), the length of the steering arm to the wheel hub (b), the length of the tie rod (t) and the angle of the steering arm (β) in relation to the longitudinal axis of the car.

$$\alpha = \sin^{-1}\left(\frac{d - (b)\cos(\beta)}{t}\right) \tag{4.111}$$

With the equations (4.110) and (4.111), the anti-Ackermann steering geometry for the racing car is established. Following the configuration of the steering system, the force applied to the toe rods is estimated with the aim of designing these parts. To begin with, the steering rack ratio (r_r) of the system is calculated with the rack distance travel for a certain angle (t_r) and the length of the steering rack in equation (4.112).

$$r_r = \frac{t_r}{r} \tag{4.112}$$

The equation (4.112) is used as an approximation of the steering ratio. Still, it is an estimate of the total possible travel of the rack towards the angle of the pinion. This equation is applied with the information reported by the manufacturer of the selected steering rack. It is with the estimated steering rack ratio that the torque of the steering column (T_c) can be related to the force applied to the steering rack (F_r) at equation (4.113) considering the pinion radius (r_p).

$$F_r = (r_r)T_c r_p \tag{4.113}$$

Therefore, the force applied to the steering rack is the force transmitted to the tie rod. As this is supposed for the design of the tie rods and the stress is conducted as only normal axial stress, the cross-section of the tie rod can be designed with the distortion energy theory using equation (4.114). This equation considers the safety factor as a trade-off to select a commercial cross-section for the tie rod in relation to the available tie rod ends to be adjusted for the assembly.

$$\sigma_v = \frac{S_y}{n} \tag{4.114}$$

Nevertheless, the tie rod must be checked for viability within the buckling criterion, as it may act as a column with the applied stress conditions. Hence, the designed tie rods are analyzed with equations (4.102), (4.103) and (4.104) with respect to buckling criteria considering the selected material for these parts.

Finally, the corresponding bearings to support the assembly of the steering column to the chassis are defined using the equations (4.15) and (4.16) to determine the multiple of rating life and the catalog load rating for the bearings.

4.3.10. Braking system configuration

The braking system of the racing car is configured as part of the dynamic control cluster. In the first instance, the braking system configuration consider the top speed that a Formula SAE racing car may achieve during competition as a parameter for the design. Although this parameter is taken into account for the configuration, there are still several parameters such as the tire pressure, the friction coefficient at contact patch, or the brake friction elements that may affect the braking distance, as noted in the literature [69].

In accordance with the principle of conservation of energy, the vehicle parameters including the mass (m), linear velocity (v), moment of inertia (I) and the angular frequency of the wheels (ω) to the translational kinetic energy (E_{kt}) and rotational kinetic energy (E_{kr}) at the following equations (4.115) and (4.116).

$$E_{kt} = \frac{1}{2}m\left(v_f^2 - v_0^2\right) \tag{4.115}$$

$$E_{kr} = \frac{1}{2}I\left(\omega_f^2 - \omega_0^2\right) \tag{4.116}$$

With the aim of computing the required braking torque at the wheels, an equivalent moment of inertia (I_{eq}) is estimated within the equations (4.115) and (4.116) considering that the linear and angular parameters may be related with the equations (4.117) and (4.118) to establish the equivalence at the motion of the car.

$$v = \omega r \tag{4.117}$$

$$a = \alpha r \tag{4.118}$$

At this point, both the equivalent moment of inertia for the car and the angular acceleration at the wheels (α) can be used to calculate the braking torque (T) with equation (4.119).

$$T = I_{eq}\alpha \tag{4.119}$$

Upon completion of the analysis of the braking torque, the configuration of the braking system is continued with the alternatives of the brake discs for the racing car. As a matter of fact, the key factor to check feasibility of an alternative for the brake discs is the diameter of this part, as it must incorporate into the wheel assembly and leave some space for the assembly of the caliper. Within this specification, the alternatives for the brake disc are analyzed. To perform the analysis for the brake disc, a uniform condition of the brake friction elements is established as the corresponding caliper and brake pads are selected for the system.

First, the brake pad material is searched in order to determine the approximated value of the friction coefficient for the analysis. After this, the previously obtained torque for every wheel is defined as the analysis condition and the geometry for the assembly of the brake disc, brake pad and caliper is fixed for every alternative. The geometry of the contact area for the brake pad with the disc is then established in accordance with the parameters found in the literature for the analysis if the disc brake system [45]. The equation (4.120) calculates the equivalent radius (r_e) to specify the location of an equivalent infinitesimal shoe in relation to the outer radius (r_o) and inner radius (r_i) of the brake pad contact area.

$$r_e = \frac{r_o + r_i}{2} \tag{4.120}$$

Hence, the equations (4.121), (4.122) and (4.123) are applied to the analysis in order to compute the normal pressure (P_a), the applied acting force (F) and the required hydraulic pressure (P_h) with respect of parameters including shoe friction coefficient (μ), the locating angles of the shoe (θ) and the cross-section for the caliper piston (A_p).

$$P_a = \frac{2T}{(\theta_2 - \theta_1)\mu r_i (r_o^2 - r_i^2)} \tag{4.121}$$

$$F = (\theta_2 - \theta_1) P_a r_i (r_o - r_i) \tag{4.122}$$

$$P_h = \frac{F}{A_p} \tag{4.123}$$

In relation to the brake bias estimated in the conceptual development stage, the requirement of the brake pressure and fluid control is fulfilled with an array of two master cylinders, which are designated for the front and rear brake lines respectively. According to the brake bias, the inner diameter of the master cylinders is searched to propose a natural brake bias for the system by means of the internal cross-section of these components. From another standpoint, the brake force distribution (BFD) can be calculated as a relation between the pressure at front and rear master cylinders (P_{hf}, P_{hr}) in equation (4.124).

$$BFD = \frac{P_{hf}}{P_{hf} + P_{hr}} \tag{4.124}$$

Another element to be included into the assembly of the master cylinders is a balance bar, to be able to modify or adjust the brake balance with this mechanical linkage. Furthermore, the brake lines for the system are specified after considering the brake fluid to be used in the racing car, as well as the volume required for the reservoir at each master cylinder. The brake lines consist of appropriate hoses for the required application in terms of materials and operation conditions with fittings to connect the hydraulic lines for leak-proof and compact design. When the flow of the brake lines is defined, it can be used to either estimate the length of the lines for physical layout or the required height of the reservoir for the master cylinders for this system.

4.3.11. Cockpit and driver controls configuration

As a first step, the parts for the cockpit and the driver controls are defined. Parts such as the steering wheel and the quick-release mechanism for the steering system were defined previously as those served as a dimensional reference for the steering system layout. Presented as another relevant case, the gauge and display for the cockpit were determined and included in the configuration of the electrical cluster.

Still, there are some cases that may require the selection and adjustment of other parts to complete the configuration. For instance, the gear shift mechanism may be adjusted for the selected ICE and transmission group. Nevertheless, this mechanism can be implemented with commercial kits, which include the lever and fulcrum to be mounted in relation to the actual mechanism of the engine without major modifications. Other item to be selected is the pedal box.

Even though the pedal box can be designed specifically for the racing car, acceptable alternatives for the pedal box may be found in the aftermarket. In fact, the proposed pedal box for the racing car is one designed specifically to assembly the master cylinders that were selected for the braking system. The suggested pedal box includes a three-pedal assembly, with the ability to use the pedals for the throttle, brake and clutch action. As this pedal box design requires to be fixed by means of fasteners, this issue must be taken into advantage to enable the adjustment of the position of the pedals for each driver to have a seat at the cockpit of the racing car.

To establish a safe and ergonomic environment for the driver during the stints at the competition, the cockpit must contemplate several elements that can be classified as mandatory in most cases. Those elements include the crash protection, harness mounting and head restraint as a direct influence of the cockpit with the chassis of the racing car, and other elements that may serve as driver accommodation such as the seat. To simplify the development of the seat for driver accommodation, the seat is selected for the application among a list of suitable seats. The selected seat allows the adjustment of the position in relation to the cockpit, which is an important detail to be compliant with the guidelines of the competition for driver accommodation.

Another element to be included in the cockpit is the driver's harnessing, which must be compliant with the rules of the competition and requires a specific mounting to the chassis. The guidelines of the competition establish the characteristics, the mounting point location and the arrangement of the harness. First, the harness for the racing car is selected in order to be adequate for the competition. Once it is selected, the harness mounting holes are used as a design constraint to evaluate the shear force exerted in the fasteners for the harness. Considering this mounting as critical fasteners, the allowable shear force (V) for the fasteners of the harness mounting is obtained with equations (4.125) and (4.107). The equation (4.125) integrates the distortion energy theory to compute the shear stress in relation to the minimum proof strength for the fasteners (S_p) and the design factor.

$$\tau = 0.577 \frac{S_p}{n_d} \tag{4.125}$$

After checking the viability of the harness mounting, the mounting points for the harness at the chassis are located in relation to the driver's template in a similar manner to the illustration referenced in Figure 3.2.

4.3.12. Chassis and bodywork configuration

Following the configuration of the enclosure cluster components, the tubular spaceframe geometry for the chassis that was previously proposed at conceptual development stage of the design process is analyzed to determine the viability of the geometry in terms of performance. The analysis that is performed is a finite element analysis (FEA) considering the model as the geometry presented in

Figure 3.5. As a matter of fact, the tubular spaceframe geometry shown in Figure 3.5. introduced as the conceptual chassis geometry has already been modeled as BEAM elements using ANSYS Mechanical APDL. The corresponding model requires the set of mechanical properties and cross-section characteristics for every member of the chassis, in accordance with the conditions stipulated by the Formula SAE rules.

To ensure that the FEA is conducted for accurate and reliable results, a mesh convergence study is carried out for the modeled chassis. As a result of multiple runs and mesh size control, the results of the mesh convergence study are plotted in Figure 4.12. using APDL considering a simplified load condition for the chassis, only applying the acceleration due to gravity to compute the weight of the tubular spaceframe.

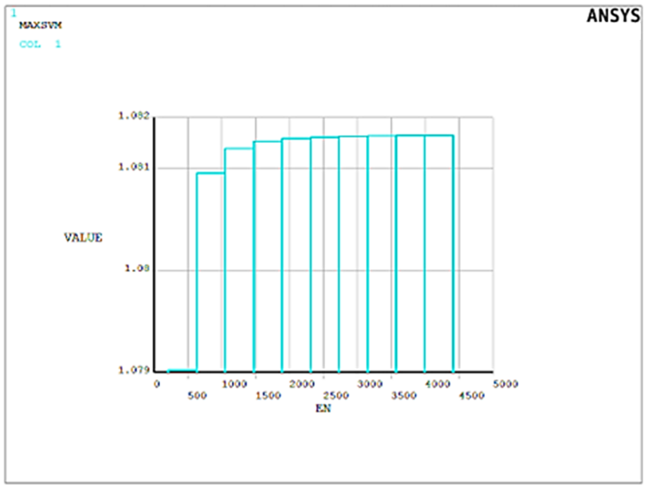

Figure 4.12. Mesh convergence study for the conceptual chassis geometry.

As shown in Figure 4.12., the plot evaluates the maximum von Mises stress for the load condition of the weight of the chassis for a certain range of the number of elements on the model. Hence, the value of the von Mises stress reaches convergence and the mesh convergence study is established as satisfied for the model. After this, the next step for the FEA of the conceptual chassis geometry is to evaluate certain loads applied to the structure of the chassis. The main deformation modes for an automotive chassis are longitudinal torsion, vertical bending, lateral bending and horizontal lozenging; as reported in the literature [70], [71], [72]. Considering these deformation modes, the boundary conditions for the FEA of the model for the chassis geometry are defined in relation to the data obtained from the IVDS with respect to acceleration under different driving circumstances.

Once the analysis is conducted, the results for the boundary conditions for every deformation mode proposed previously are presented at Table 4.8. It is important to note that the safety factor presented at Table 4.8. is calculated with the distortion energy theory at equation (4.114) as the maximum von Mises stress is highlighted for each boundary condition applied and the yield strength of the material for every structural member is known. As a reference, the plotted results for von Mises stress for the longitudinal torsion deformation mode boundary conditions submitted to the FEA of the conceptual chassis geometry are illustrated in Figure 4.13.

Table 4.8. Results of the FEA for the conceptual chassis geometry.

Deformation mode	Safety factor
Longitudinal torsion	2.39
Vertical bending	11.04
Lateral bending	2.09
Horizontal lozenging	2.89

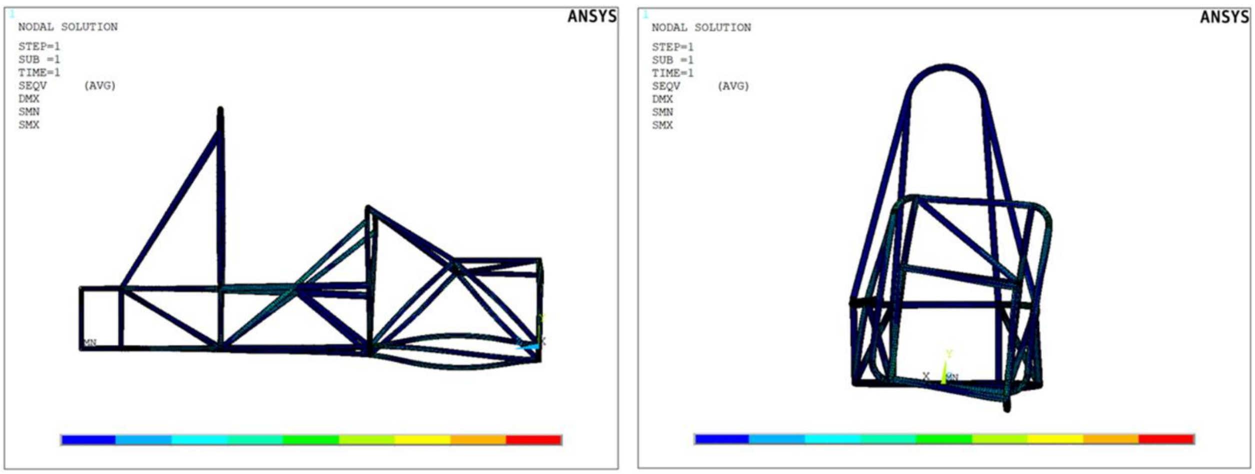

Figure 4.13. FEA of the conceptual chassis geometry submitted to longitudinal torsion.

Notwithstanding, the results are used to compute torsional stiffness for the chassis. As defined by Arifin et al. [73], the torsional stiffness is a measure of the frame flex under loads at front wheels while the rear of the frame is held and usually occurs during cornering. Mathematically, the expression to estimate the torsional stiffness (K_c) of the frame is shown at equation (4.126), which is a relation between the torque (T) applied to the frame and the angular deflection (θ) due to the applied torque. Using the data directly from the results of the FEA of the chassis geometry, the corresponding torsional stiffness is obtained.

$$K_c = \frac{T}{\theta} \tag{4.126}$$

The torsional stiffness of the chassis is a key parameter for the behavior of the racing car. This is because of the influence of the chassis' resistance to twisting loads on handling, suspension acting and even driving feedback. Therefore, a simplified model for the stiffness of the racing car is implemented on the analysis, in a similar manner to other models presented in the literature [71], [72]. The simplified model involves frame stiffness (K_c) and suspension spring stiffness (K_s) with respect to the racing car stiffness (K_v) in the equation (4.127).

$$\frac{1}{K_v} = \frac{1}{K_c} + \sum \frac{1}{K_s} \tag{4.127}$$

To be able to relate the torsional stiffness of the chassis to the racing car stiffness, the relative stiffness of the car is computed using the equation (4.128). Hence, the plot at Figure 4.14. presents the relation between the stiffness of the car and the chassis in a graphical manner. Using as reference the data reported in the findings of Costa [72], the dash lines in Figure 4.13. represent the threshold of the torsional stiffness for a common FSAE racing car.

$$K_r = \frac{K_{vehicle}}{K_{suspension}} \tag{4.128}$$

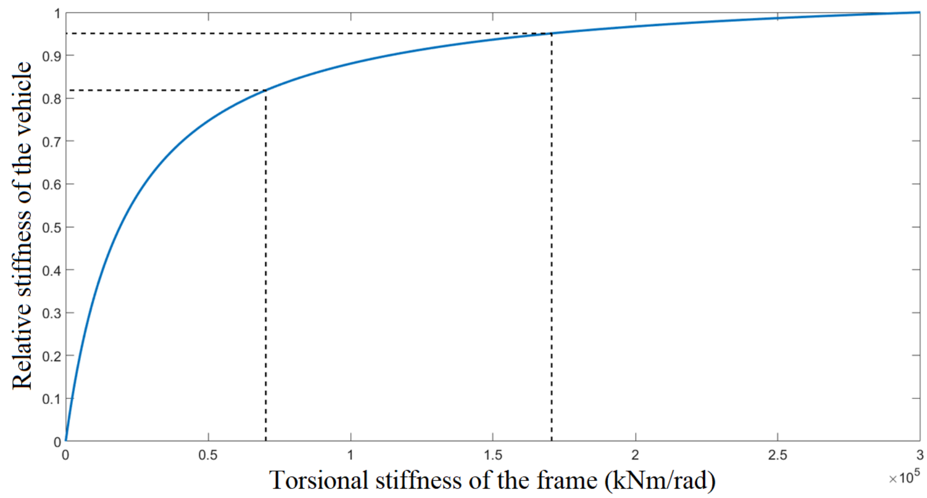

Figure 4.14. Relative vehicle stiffness as a function of chassis stiffness.

The plot at Figure 4.14. may be used to locate the torsional stiffness of the proposed chassis. Still, this stage of the analysis must be considered as the first iteration to design the tubular spaceframe for the racing car. After the analysis of the conceptual chassis geometry, the chassis geometry is modified to incorporate the complete structural members and to fit the geometry for specific functions at the racing car including the ICE mounting, the mounting points for the suspension at front and rear axle of the vehicle, the location of cockpit and driver controls, etc.

For instance, the cockpit design must consider the elements selected previously and the chassis geometry is then adjusted to fulfill the requirements for the design. The driving posture and the effects of the position of the driver at the cockpit is the topic studied by Marques et al. [74], reporting the most ergonomic positions for an ideal driver. However, the selected seat for the racing car is not manufactured for the angle proposed as an ergonomic position. The way to overcome this issue is to provide the ergonomic position by aligning the chassis geometry at the cockpit to better suit the posture of the driver.

Once the chassis geometry is modified to complete the functions of this part, this structural assembly requires to mount an anti-intrusion plate and impact attenuator at the front of the tubular spaceframe. First, the anti-intrusion plate is determined in accordance with minimum dimensions reported in at the rules of the competition. It is important to note that the front bulkhead of the chassis and the anti-intrusion plate are made out from different materials, but both are compatible for welding. The welding joint type and welding process are determined mainly in relation to the materials to be joined and the thickness of both the front bulkhead and the anti-intrusion plate.

Hence, the welding parameters for this operation are defined including the welding current, the electrode to be used, shielding gas and filler metal.

The welded joints for fixing the anti-intrusion plate to the front bulkhead are proposed as intermittent weld joints. In order to determine the total length of the throat geometry for these joints, the equation (4.129) relates the normal stress calculation with the axial force (F) exerted to the joint, the throat (h) and the length (L).

$$\sigma = \frac{F}{hL} \tag{4.129}$$

With the anti-intrusion plate fixed in position, the next step is to set in position the impact attenuator. Proposing the standard impact attenuator suggested by the competition and in accordance with the guidelines emitted by the organizers, the way to link the impact attenuator with the anti-intrusion plate is to bond these two parts. To bond the impact attenuator, the feasible adhesives are limited and must be compared in order to select a specific adhesive. To determine the effective area to hold in place the adhesive to bond these parts, the equation (4.27) is used considering the limit force in accordance with the rules of the competition [8] and the allowable shear stress with the information available in the literature [45]. At the end, the substrate for the bonding requires adequate cleaning, preparation and application, as well as controlling some conditions such as the temperature. With all the information gathered, the bonding process is defined for this assembly.

Notwithstanding, the final geometry for the chassis requires fitting different tabs for mounting and fixing brackets for the racing car assembly. For that reason, the tabs are analyzed. Considering the mechanical properties of the filler metal for the weld joint and the information available in the literature [45], the weld joint for the anti-intrusion plate is presented with a determined throat area (A) and the loads applied may generate vertical shear stress (τ_v) and horizontal shear stress (τ_h) due to bending. To begin with, the throat area and the second moment of area (I) are computed for the corresponding weld joint geometry. These parameters may serve as the basis for the calculation of both the vertical and horizontal shear stress at the throat. The vertical shear stress can be obtained with equation (4.27), while the horizontal shear stress is calculated with equation (4.130). Therefore, the vertical and horizontal shear stress are combined as vectors with equation (4.131).

$$\tau_h = \frac{Mc}{I} \tag{4.130}$$

$$\tau = \sqrt{((\tau_v)^2 + (\tau_h)^2)} \tag{4.131}$$

The computed shear stress magnitude from the vector addition with equation (4.131) is established as the allowable stress to determine the factor of safety based on the distortion-energy criterion in equation (4.132).

$$n = \frac{S_{sy}}{\tau} \tag{4.132}$$

As a result, the maximum force that can be supported by each single tab for the chassis is obtained and established as the design constraint for any element to be mounted to the tabs. It is with this maximum force that the fatigue analysis for the mounting tabs is conducted. For this fatigue analysis, the loads applied are assumed to be completely reversible and the Marin equation for the endurance limit approximation for the filler metal is obtained with equation (4.51).

Once again, the information available in the literature [45] is used to determine the corresponding the fatigue stress-concentration factor for shear stress for the filler material of the welded joint. Taking into account that the loads are assumed as fully reversible, only the alternating shear stress is calculated with the equation (4.133). Consequently, the fatigue factor of safety is obtained by relating the alternating shear stress to the estimated endurance limit in equation (4.134).

$$\tau_a = K_{fs}\tau \tag{4.133}$$

$$n_f = \frac{S_e}{\tau_a} \tag{4.134}$$

Hence, the analysis of the specific tab geometry is conducted, and the fatigue factor of safety is obtained. After completion, the configuration of the chassis may be considered as concluded with the layout of the assembly with other components.

In addition, the configuration of the chassis may be considered as the cornerstone of the configuration for the bodywork. Continuing with the configuration of the bodywork for the racing car from the conceptual development stage and the selection of materials, the bodywork is proposed to be formed by sheet metal. The bodywork for the racing car consists of several parts to be manufactured including the nose cone, the sidepods and panels and the floor of the vehicle. The corresponding geometry for these parts is defined with the layout of the rest of the car. As these parts are going to be fixed to the chassis, the implementation of quick-release fasteners to link the bodywork to the chassis is an easier, faster and practical proposition for the racing car.

Finally, the configuration of the racing car is concluded, and the design process continues to the next stage: the detailed design stage.

Chapter 5: Detail design of the racing car

The detailed design stage of the design process of the formula-style racing car is the preamble to the manufacturing phase. Hence, this stage is deemed to be the conclusion of the design process of the racing car. At this point, the configuration of the racing car is used as a basis to define the technical details regarding the performance of the vehicle, as well as evaluating the proposed abstract embodiment for the parts of the racing car with respect to the ability to withstand critical load conditions.

5.1. Technical specifications and documentation

As of this moment, the systems and components of the formula-style racing car are configured in relation to the desired application of the car: the Formula SAE competition. Nevertheless, the parts of the car must be designed carefully in order to be able to develop their functions, adapt to the assembly, be capable of manufacturing and even be lightweight. Therefore, useful methods, concepts and philosophies can be applied into the design process to ensure that the designed parts, specially the special purpose parts, are adequately developed for the racing car. One of the most used strategies is to incorporate the DFX concepts into the design.

The DFX are implemented into the special purpose parts configuration and provide valuable tools to reach a satisfactory design for the racing car. Still, this implementation may only be fruitful until a careful consideration of the overcomes is taken into account, as stated by Chiu and Okudan [75]. Before an extensive analysis is performed to validate the design of those special purpose parts, the DFX methods are incorporated to refine the geometry and the integration of these parts into the assembly of their corresponding systems or the racing car as a whole.

To be able to visualize the subassemblies of the systems, the arrangement of the components and the overall layout of the vehicle, the 3D CAD models of every part and the assemblies are developed. In a similar manner, the interface and fit up of the systems of the car is performed in order to ensure that packaging constraints are met, and the assembly is compliant with the guidelines of the competition. As a reference, the technical drawings related to the parts and assemblies mentioned previously are presented in appendix B.

The detail design stage considers the CAD modeling, the system integration, the overall satisfaction of the rules of the competition, the FEA and CFD simulations, and the documentation of technical specifications of the racing car. The documentation for the designed racing car is strictly dependent on the requirements of the competition, as the files and information to be submitted may change over the course of time, more likely if it is either a Formula SAE competition or another spin-off competition.

It is important to note that for the sake of simplicity, several procedures in the design stages including the detailed design stage are neglected in this thesis project. However, the most relevant aspects of the design process are presented in this document. Those mentioned relevant aspects include the simulations of final geometries for special purpose parts, which are presented below.

5.2. Numerical simulations

In order to complete the information delivered by the design process, some key components of the racing car are submitted to numerical simulations. Those numerical simulations include finite element analysis (FEA) and computational fluid dynamics (CFD). The FEA simulations for the structural parts of the racing car are important to provide failure predictions due to stress concentration and previous design results validation, as well as to ensure that those components meet the rules and even to identify opportunity areas to optimize the design to reduce weight. Meanwhile, the CFD simulations are used to evaluate the aerodynamic response of specific parts and define the trade-off between downforce and drag. Hence, the corresponding numerical simulations for key parts are developed below.

The numerical simulations are conducted using a determined methodology and are going to be presented in relation to this workflow for the sake of clearance. The aim is to define the steps to provide enough and useful data for the analysis via numerical simulations even if the boundary conditions change or the conducted simulations vary from one to another. The proposed methodology is illustrated in Figure 5.1.

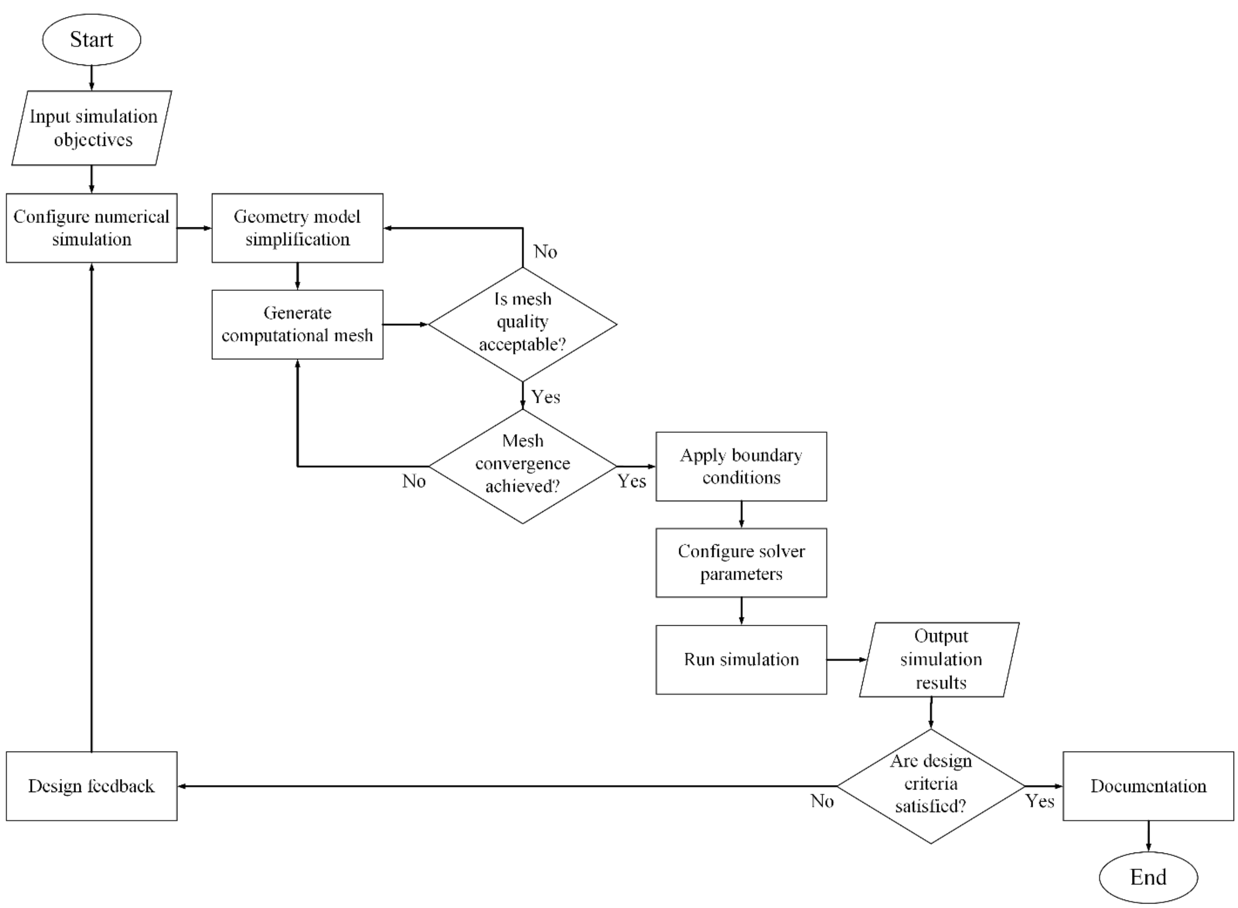

Figure 5.1. Numerical simulation methodology flowchart.

As illustrated above in Figure 5.1., numerical simulations are performed taking into account several conditions, including mesh quality, mesh convergence study and design criteria to verify if the results obtained by the means of those simulations are useful for validation and decision-making. Following this procedure, the numerical simulations for the racing car are conducted and consist of both FEA and CFD simulations. The parts to analyze by numerical simulations are special purpose parts, which for this thesis project are only integrated by the nosecone of the bodywork, the wheel hub, the wheel knuckle, the chassis and the suspension.

5.2.1. Numerical simulation of the nosecone

As the aerodynamics of the racing car stands as one of the key factors to differentiate a participant vehicle from another at the student design competitions, it is important to analyze the shape of the bodywork in order to predict the performance of the car during dynamic events. For instance, the nosecone is a crucial part of the bodywork when the car is related to the aerodynamic response. This is because of several factors, including the fact that the nosecone is the first surface to get in contact with the oncoming airflow. Therefore, the nosecone is analyzed using CFD tools to simulate the conditions of the racing car during a straight-line path.

The geometry of the nosecone for a Formula SAE racing car has a significant influence on the drag force of the car and fuel efficiency, as noted by Hoque et al. [76]. For those reasons, the proposed geometry for the nosecone of the formula-style racing car is analyzed as presented below. The CFD simulation is based on other similar study cases reported in the literature [53], [54], [76]. Considering the flowchart of the methodology for numerical simulations presented in Figure 5.1., the corresponding data for the numerical simulation of the nosecone for the racing car is listed at Table 5.1.

Table 5.1. Simulation data for the CFD analysis of the nosecone.

Simulation parameters	Simulation data
Objective	Coefficient of drag and drag force
Configuration	Steady-state, pressure based with constant density k-omega SST model
Governing equations	Continuity equation, Navier-Stokes equations, drag force equation, Reynolds number equation
Boundary conditions	Domain inlet uniform velocity of 60 kph, output static gauge pressure set to zero
Assumptions	Incompressible fluid flow, no-slip condition at walls and nosecone

The geometry of the nosecone to begin the analysis is determined using a CAD model with the dimensions of chassis and other components, as well as with the constraints marked by the rules of the competition. On the other hand, the inlet velocity for the analysis is defined within the usual speed of the racing car during dynamic events and the range of other similar study cases reported in the literature [76]. Hence, this CFD analysis is developed using ANSYS Fluent.

With the geometry set and with the aim of convergence check, the mesh convergence study is performed considering the boundary conditions, the number of elements and the results obtained for the coefficient of drag. The mesh convergence study results for the nosecone CFD analysis are gathered, plotted using MATLAB and presented in Figure 5.2.

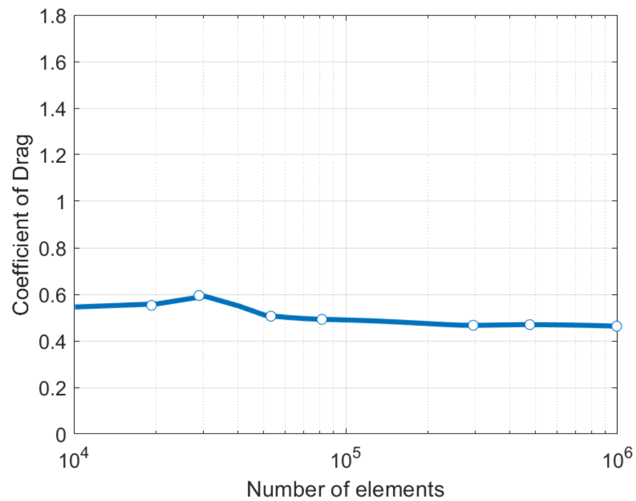

Figure 5.2. Mesh convergence study results for the CFD simulation of the nosecone.

After the grid independence is ensured, the simulation results are considered useful. In the case of the CFD simulation for the nosecone, it provides significant data related to the aerodynamics of the racing car, mainly based on the proposed geometry for the nosecone. The simulation results are shown in the graphs taken from the ANSYS Fluent interface and presented in Figure 5.3.

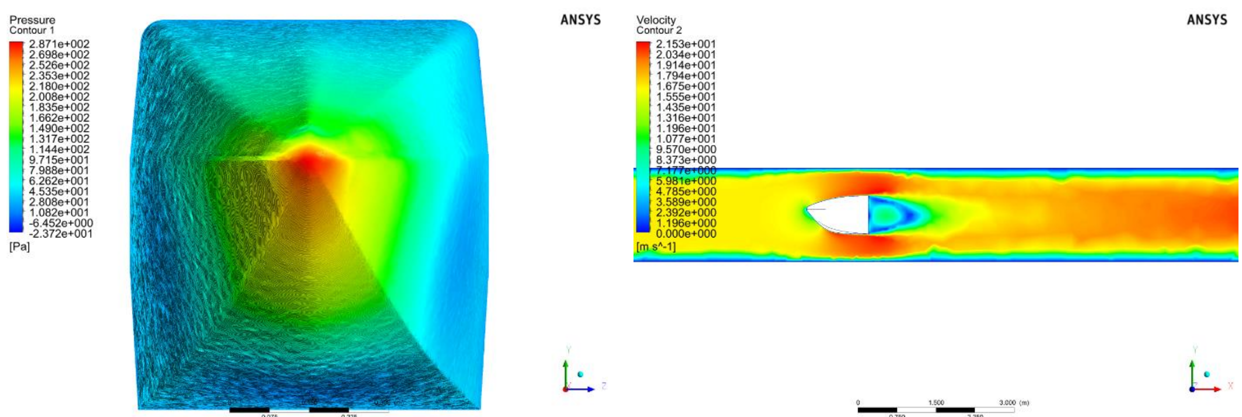

(a) (b)

Figure 5.3. Results of the CFD simulation of the nosecone for (a) pressure distribution and (b) velocity field.

The coefficient of drag obtained via CFD simulation is later compared with other relevant data in the literature for similar racing car nosecone geometries. The computed coefficient of drag is about forty percent higher than other designed nosecones for formula-style racing cars. This is mainly due to the selection of a standard seat for the racing car for this first design.

The findings of Craig and Passmore [77] demonstrate with simulations that a simple aerodynamic package can suppose a relevant advantage for the vehicle in both the events and fuel economy at student competitions. As a result, the aerodynamics of the nosecone for the racing car are marked as an opportunity area for optimization for later iterations and evolutions of the design.

5.2.2. Numerical simulation of the wheel hub

As a matter of fact, the desired wheel hub geometry for the racing car does not require major simplification. Instead, the geometry to be implemented into the analysis is based on the approach illustrated at the configuration stage of the design process without the splines or threads at the model. Nevertheless, the wheel hub geometry is submitted to the loads in a simulation in order to confirm the expected strength of the selected material for both the yielding criteria and the fatigue criteria. Hence, the FEA of the wheel hub is performed to ensure the previous calculations are validated for the design of this special-purpose part.

The main interest on the numerical simulation for the wheel hub of the racing car relies in the factor of safety for yield criteria and the factor of safety for fatigue criteria, as other similar FEA simulations have reported in the literature [78], [79]. The FEA simulation of the wheel hub is performed using the information listed at Table 5.2. below. It is important to note that the boundary conditions are defined by the geometry and assembly of the wheel parts, considering that the wheel hub acquires the motion by means of the CV joint splines and is attached to the wheel rim and brake disc using the selected fasteners.

Table 5.2. Simulation data for the FEA of the wheel hub.

Simulation parameters	Simulation data
Objective	Equivalent von Mises stress, factor of safety for yield criteria, factor of safety for fatigue criteria
Configuration	Static structural analysis, fatigue tool for stress conditions and material properties
Governing equations	Equilibrium equation, strain-displacement relation, linear-elastic constitutive equation, discretized system equation
Boundary conditions	Torsion moment at the splined surface of the wheel hub and fixed supports at bearings
Assumptions	Isotropic and homogeneous material, inertial effects negligible, no modeling of friction, no residual stress

The geometry model of the wheel hub is developed using CAD tools and the proposed geometry is imported into ANSYS Mechanical to begin with the analysis. With the geometry set and with the aim of convergence check, the mesh convergence study is performed considering the boundary conditions, the number of elements and the results obtained for the equivalent von Mises stress. The mesh convergence study results for the FEA simulation of the wheel hub are gathered, plotted using MATLAB and presented in Figure 5.4.

Once grid independence is ensured, the numerical simulation results are considered useful. The corresponding results of the simulation are plotted by ANSYS Mechanical interface and presented below in Figure 5.5. for the computed equivalent von Mises stress and for the factor of safety towards the fatigue criteria respectively. The factor of safety for the yield criteria is computed using the equation 4.22.

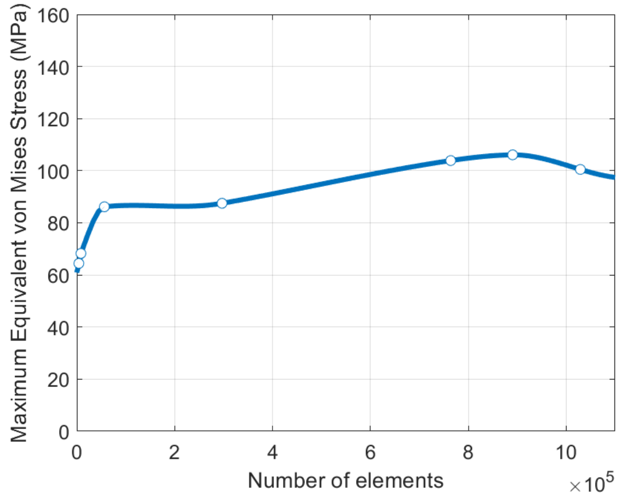

Figure 5.4. Mesh convergence study results for the FEA simulation of the wheel hub.

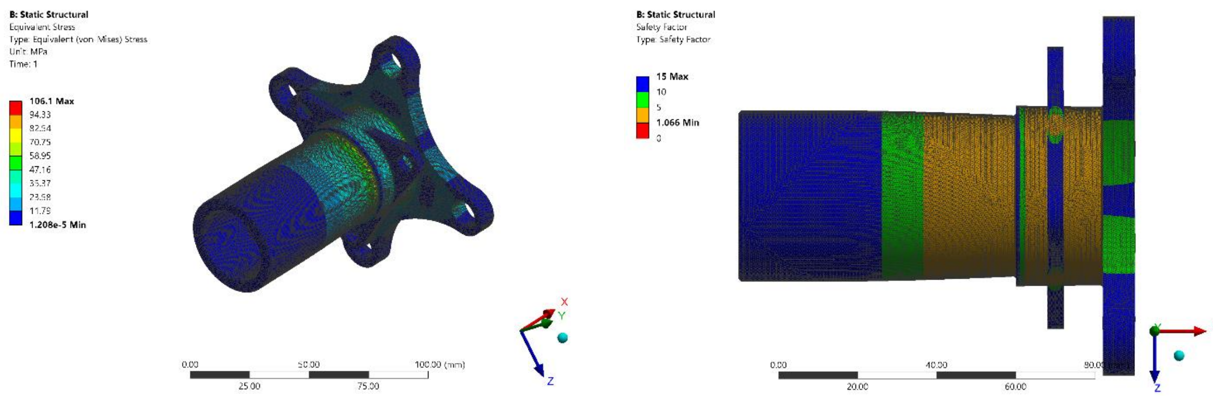

(a) (b)

Figure 5.5. Results of FEA simulation of the wheel hub for (a) equivalent stress and (b) fatigue safety factor.

The results obtained in the FEA simulation, shown in Figure 5.5., are significantly similar to those expected in the configuration stage of the design process for the formula-style racing car. In addition, both the yield criteria and fatigue criteria are met and validated with the results of the numerical simulation performed. Consequently, the proposed geometry for the wheel hub of the racing car is defined.

5.2.3. Numerical simulation of the wheel knuckle

In a similar manner, the proposed geometry of the wheel knuckle does not require major simplification and is only adjusted to neglect any thread available in the geometry. In the case of the wheel knuckle, the geometry is defined towards the available space at the wheel assembly, the geometry of other assembly parts and the loads to be applied, as detailed in the configuration stage of the design process at Chapter four. The aim of the FEA simulation of the wheel knuckle is to validate the expected behavior of this part under critical conditions towards both the yield criteria and the fatigue criteria.

As mentioned previously, the main objective of the numerical simulation is to verify if the proposed geometry for this special-purpose part meets the expected factor of safety for yield criteria and the computed fatigue life is acceptable for this particular case. The knuckle or uprights for FSAE racing cars are parts of interest in many cases for numerical simulations [30], [60], [79], [80]. Based on similar numerical simulations and the configuration of those, the corresponding FEA simulation for the wheel knuckle is performed using the data listed in Table 5.3. The boundary conditions are simpler for the geometry of the knuckle as it is fixed at the center in relation to the wheel assembly and the loads are applied at the mounting points for either the suspension elements or the steering elements.

Table 5.3. Simulation data for the FEA of the wheel knuckle.

Simulation parameters	**Simulation data**
Objective	Equivalent von Mises stress, factor of safety for yield criteria, expected life for fatigue criteria
Configuration	Static structural analysis, fatigue tool for stress conditions and material properties
Governing equations	Equilibrium equation, strain-displacement relation, linear-elastic constitutive equation, discretized system equation
Boundary conditions	Bearing loads applied at mounting holes due to suspension action, load applied at the surface of mounting plate due to steering action and fixed support at the center
Assumptions	Isotropic and homogeneous material, inertial effects negligible, no modeling of friction, no residual stress

The model of the wheel knuckle is developed using CAD tools and the proposed geometry is imported into ANSYS Mechanical to start the analysis. With the geometry set and with the aim of convergence check, the mesh convergence study is performed considering the boundary conditions, the number of elements and the results obtained for the equivalent von Mises stress. The mesh convergence study results for the FEA simulation of the wheel knuckle are gathered, plotted using MATLAB and presented in Figure 5.6.

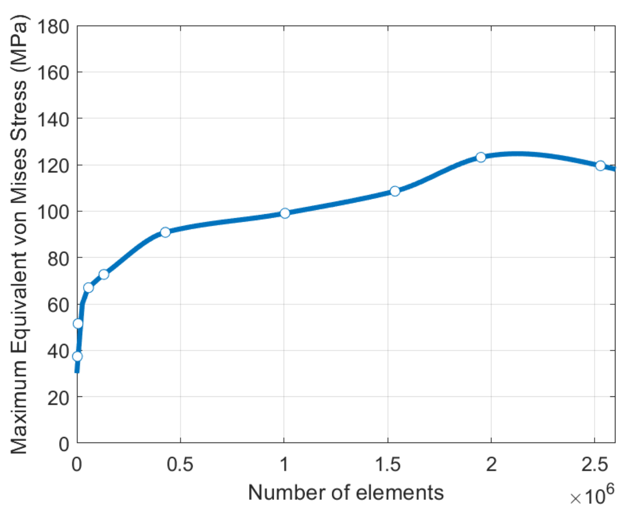

Figure 5.6. Mesh convergence study results for the FEA simulation of the wheel knuckle.

After the mesh convergence study, the grid independence is ensured, and the results of the simulation are established. The corresponding results of the simulation are plotted by ANSYS Mechanical interface and presented below in Figure 5.7. for the computed equivalent von Mises stress and for the expected life towards the fatigue criteria respectively.

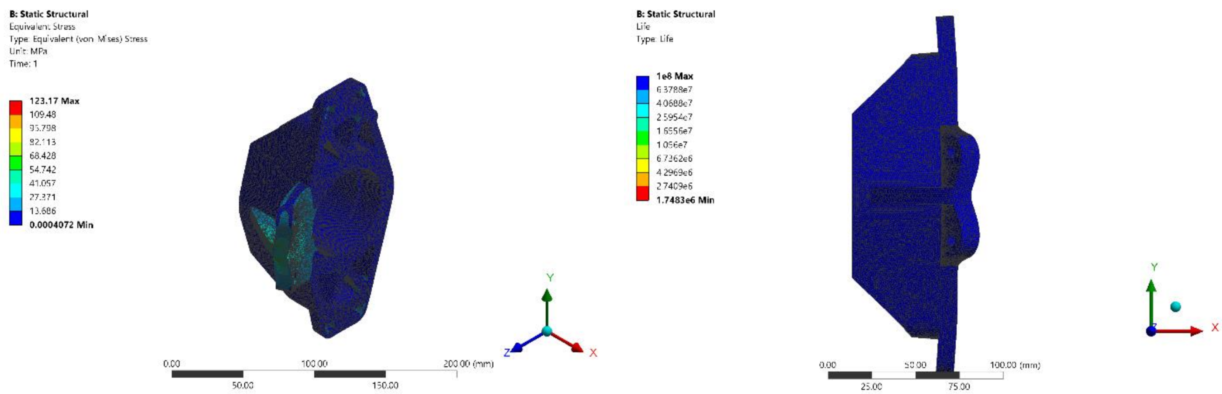

(a) (b)

Figure 5.7. Results of FEA simulation of the wheel knuckle for (a) equivalent stress and (b) fatigue life.

Considering the results shown in Figure 5.7. above, both the yield criteria and fatigue criteria are validated with the numerical simulation performed for the wheel knuckle. Even though the safety factor is slightly below one, the expected life is acceptable for the application of the racing car. Therefore, the proposed geometry for the wheel knuckle is established as the selected alternative.

5.2.4. Numerical simulation of the chassis and suspension

Finally, the geometry of both the chassis and the suspension is analyzed to verify the viability of these parts in relation to specific deformation modes. After the configuration stage of the design process for the racing car, the chassis geometry is modified considering several factors including cockpit, driver position, layout of the powertrain assembly and the rules of the competition to deliver a complete version of the proposed design. Other relevant definition for the behavior of the chassis is the suspension geometry and the mounting points. Gathering the information for the chassis and the suspension members, the numerical simulation to be performed considers the assembly of these elements integrated with a simplified action of the springs and the wheel knuckles.

The aim of the numerical simulation of the assembly of chassis and suspension is to define the threshold of the combined stress at the structural members of those two proposed geometries under different load conditions. The load conditions to verify the feasibility of a chassis geometry include deformation modes such as longitudinal torsion, vertical bending and lateral bending, as noted in the literature [70], [71]. Although, there are studies that analyze the relation between chassis and suspension geometries with a similar scope [81]. Taking into account this information, the numerical simulation for FEA of the chassis and suspension is developed according to the data listed in Table 5.4. Another relevant note is that this FEA simulation is once again performed using beam elements, similar to previous simulations at the configuration stage for the chassis.

Table 5.4. Simulation data for the FEA of the chassis and suspension.

Simulation parameters	Simulation data
Objective	Combined stress and total displacement in structural members, safety factor for yield criterion
Configuration	Static structural analysis, cross-section parameters and material properties
Governing equations	Equilibrium equation, strain-displacement relation, linear-elastic constitutive equation, discretized system equation, Timoshenko beam theory
Boundary conditions	Supports at selected structural members or wheel knuckles, vertical loads at wheel knuckles for longitudinal torsion, gravity and acceleration applied
Assumptions	Isotropic and homogeneous material, ideal springs, rigid joints, aerodynamic and road surface interaction neglected, weld failure neglected

For the sake of clearance, the combined stress computes the total stress at a certain point due to simultaneous effects of multiple types of loads. The maximum combined stress at the corresponding load conditions is then used to calculate the safety factor for yield criteria with equation 4.22. In addition, the numerical simulation for the chassis and suspension considers three different load scenarios: longitudinal torsion, acceleration test and cornering test. The corresponding loads and accelerations for the boundary conditions are based on either configuration stage calculations or IVDS data.

In the case of the chassis and suspension model, the chassis geometry is developed using CAD tools and the proposed geometry is imported into ANSYS Mechanical to start the analysis. The corresponding model is complete when the assembly parts of the suspension geometry is integrated using the mounting points for the suspension. With the geometry set and with the aim of convergence check, the mesh convergence study is performed considering the boundary conditions, the number of elements and the results obtained for the combined stress. The mesh convergence study results for the FEA simulation of the chassis and suspension are gathered from the cornering load condition, plotted using MATLAB and presented in Figure 5.8.

Once the mesh convergence study is performed, the numerical simulations for the load conditions are computed. The longitudinal torsion simulation considers torsional stiffness of the chassis and suspension while applying critical loads at the front wheel knuckles. The results for combined stress and total displacement of longitudinal torsion simulation are presented in Figure 5.9. On the other hand, the acceleration test simulation and cornering test simulation correspond to critical accelerations expected during dynamic events at the competition. In a similar manner, the results for combined stress and total displacement of acceleration and cornering test simulations are presented in Figure 5.10. and Figure 5.11., respectively.

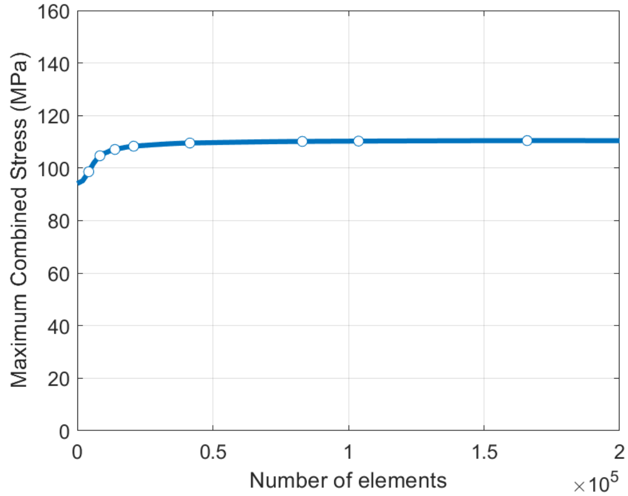

Figure 5.8. Mesh convergence study results for the FEA simulation of the chassis and suspension.

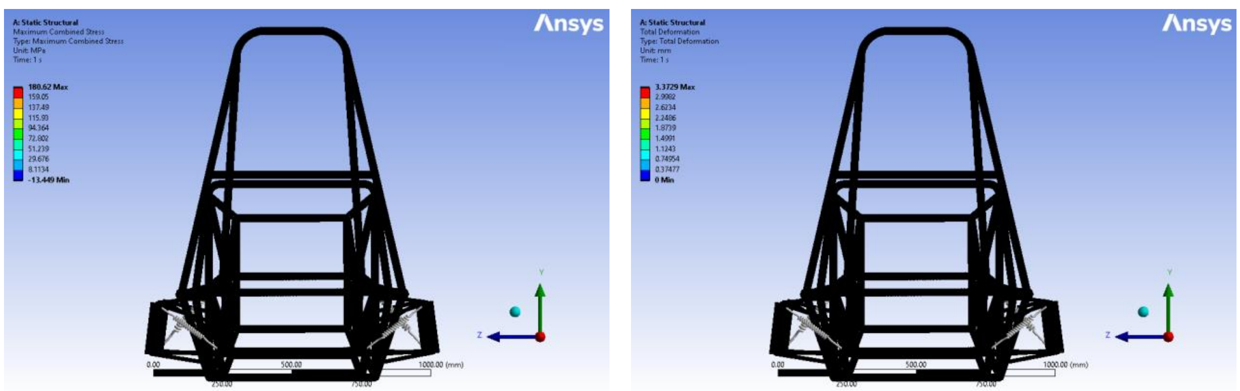

(a) (b)

Figure 5.9. Results of FEA longitudinal torsion simulation of chassis and suspension for (a) combined stress and (b) total displacement.

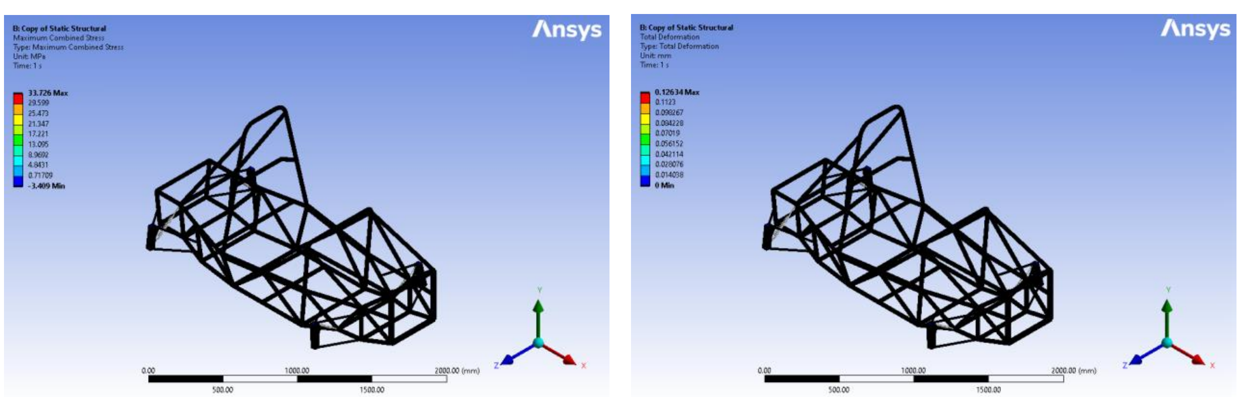

(a) (b)

Figure 5.10. Results of FEA acceleration test simulation of chassis and suspension for (a) combined stress and (b) total displacement.

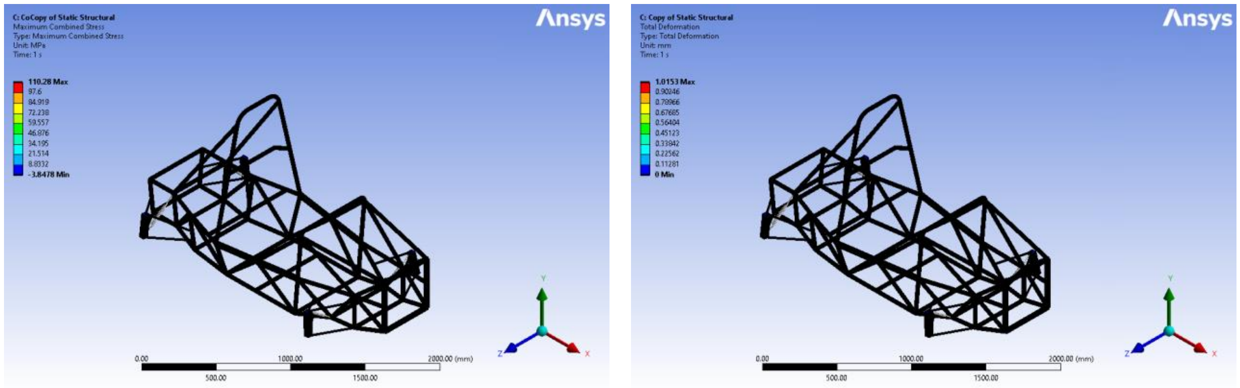

(a) (b)

Figure 5.11. Results of FEA cornering test simulation of chassis and suspension for (a) combined stress and (b) total displacement.

In fact, the numerical simulations results presented in Figure 5.9., 5.10. and 5.11., respectively, are similar in magnitude to the results obtained at the configuration stage numerical simulations performed to the chassis. The results are slightly different due to geometry modification mainly, as the proposed geometry is based on the selected concept exposed in Chapter three of this thesis project. Consequently, the geometry for the chassis and suspension system is determined and validated with the results of the numerical simulations.

Hence, as the special-purpose parts for the formula-style racing car are defined and the design process reaches the detail design stage, the next step is to gather all the information of the designed racing car and perform a final simulation in order to compare the brief expected initial simulation of the vehicle dynamics results computed by the IVDS to a significantly substantive simulation of the designed vehicle. Below, the development of the final simulation of the racing car is presented in Chapter six of this thesis document.

Chapter 6: Final simulation and testing of the racing car

Once the detailed design of the formula-style racing car is completed, the resulting specifications, geometries and characteristics can be established as the designed vehicle. Even though the racing car is defined at this point in the design process, this thesis project does not cover any physical prototypes or the manufacturing of the vehicle. For this reason, the aim of this chapter is to provide a wide perspective of the designed racing car performance in relation to the dynamic events of the student competition with the help of virtual prototyping. In a similar way to the model developed in Chapter two, vehicle dynamics are the key tool to obtain useful information about the performance of the racing car.

The final simulation and testing of the racing car consists of using the designed vehicle data to model a virtual prototype of the car into a simulation environment in order to run a vehicle dynamics simulation. Several studies have already used simulation software tools to provide a virtual prototype of a formula-style racing car [17], [82]. The virtual prototypes generated by those simulation software tools are employed to either determine the behavior of selected subsystem of the car or determine the overall performance of the racing car. In the case of the designed car, the main purpose of the vehicle dynamics simulation is to define the performance of the car under driving conditions similar to the ones the vehicle is going to experience during the dynamic events of the competition.

6.1. Simscape vehicle virtual prototype model

Simscape is a toolbox based on block diagrams that allow model and simulation of multidomain physical systems [83]. The modeling of physical components at the Simscape toolbox is developed by creating physical connections between schematic blocks and adding data that allow precise modeling of the analysis components and their interaction. Specifically, the driveline toolbox complement adds useful rotational and translational mechanical systems that may help to simulate the racing car. Using blocks available at Simscape, the designed racing car is recreated into the simulation environment with the aim to conduct a vehicle dynamics simulation.

Every block at Simscape has input and output ports that can be identified by capital letters around the block. Additionally, each block incorporates information that can be modified in order to approximate the behavior of the physical component to the actual part of the assembly. Below, the virtual prototype of the racing car is developed by separating the complete prototype into three main sections: the engine model, the powertrain model and the vehicle model. For the sake of practicality, the data introduced into the blocks at Simscape is filled using variables reported in MATLAB to facilitate the modification of modeling parameters.

6.1.1. Engine model using Simscape

The engine model is a subsystem centered on a generic engine block, which is used to model an internal combustion engine (ICE) and that is connected with other features to provide the desired behavior for the simulation of longitudinal dynamics of the racing car. The generic engine block and the rest of the elements of the engine model are presented in Figure 6.1. As shown in Figure 6.1., the generic engine block counts with five ports: throttle, base, power, fuel consumption and follower. The throttle port of the generic engine block allows to input a signal to represent the throttle response over time. For the racing car, the throttle response for the simulation can be approximated with a ramp block that use a slope to adjust a normalized function of the pedal from an initial value of zero to a final value of one. The power and fuel consumption ports are output ports that may be used to scope the data of mechanical power and used fuel of the engine among the simulation time. The base of the engine block is connected to a reference and the follower port connects to the next block, which in this case is a simple gear block.

Even though the engine block transmits the mechanical power by means of the follower port, the engine must be connected to a torque converter or a simple gear to allow the engine to idle without stalling. As a practical way to achieve this, a simple gear block is added to provide a smooth transmission of power, similar to the use of a mechanical clutch. The simple gear block is physically connected to a rotational motion sensor block that enables the scope of the angular frequency at the output shaft of the engine. The other line represents the interaction of the engine model with the powertrain model.

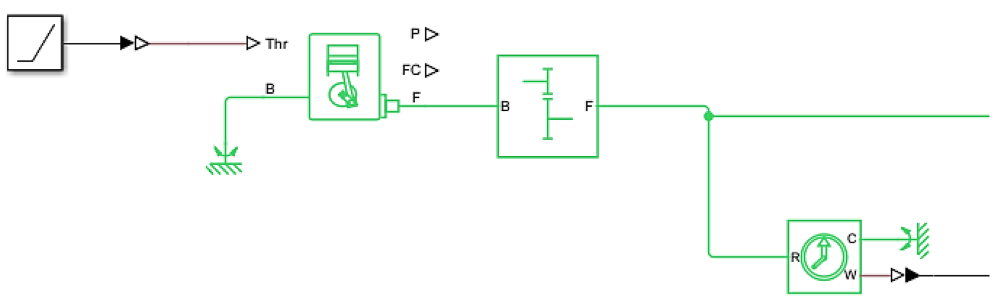

Figure 6.1. Engine model subsystem at Simscape.

The main block to adjust with the designed racing car data is the generic engine block, which enables model parameterization by three different means: normalized three-order polynomial, tabulated torque data and tabulated power data. For the designed racing car, the desired model is the tabulated torque data. Hence, the parameters and units used for the engine model at Simscape are listed in Table 6.1.

Table 6.1. Engine model subsystem simulation parameters.

Block	Parameter	Units	Description
Generic engine	Speed vector	rpm	Angular frequency tabulated data
	Torque vector	Nm	Torque tabulated data
	Stall speed threshold	rpm	Minimum speed without stalling
	Engine inertia	kgm^2	Rotational inertia of engine components
	Fuel consumption	mg/rev	Consumption per revolution

6.1.2. Powertrain model using Simscape

In a similar way, the powertrain model is a subsystem that receives the input mechanical power with certain torque and speed and transmits the mechanical power with adjusted torque and speed to the wheels of the vehicle. The powertrain of a formula-style racing car may vary for every car, but mainly consists of the gearbox, chain drive and differential. These components and other powertrain model blocks are shown in Figure 6.2.

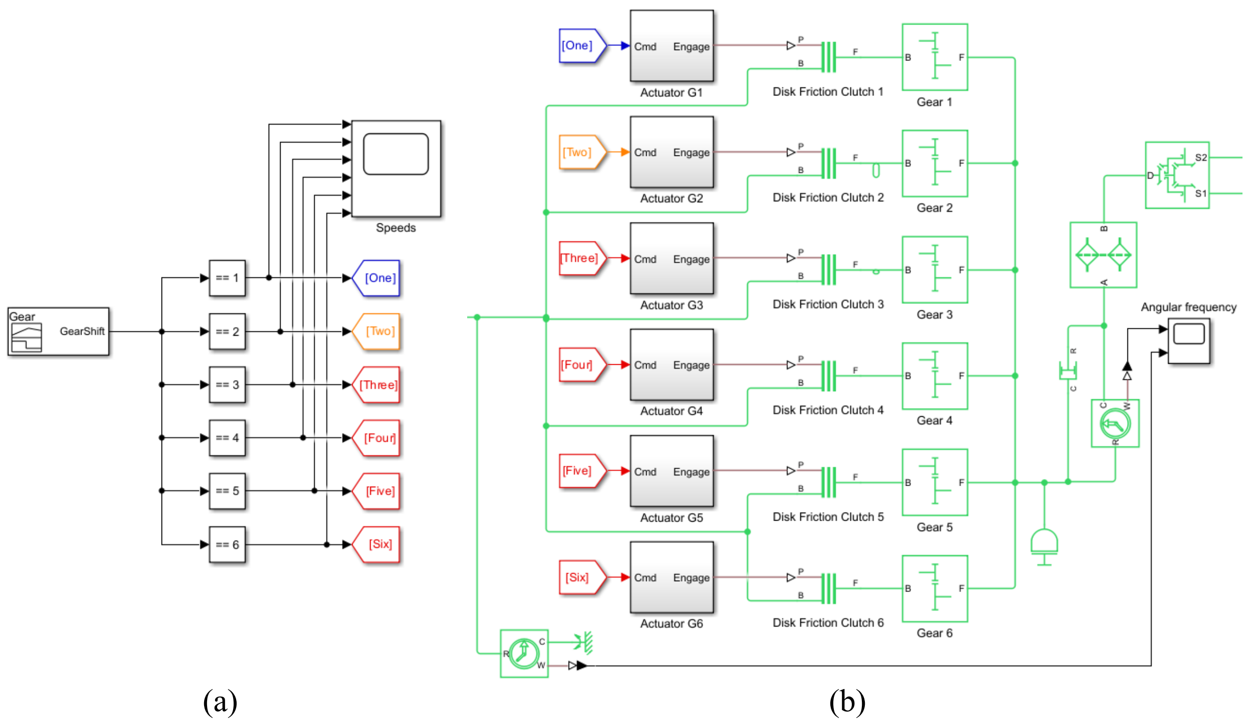

Figure 6.2. Powertrain model at Simscape for (a) gearshift control unit and (b) powertrain unit.

To begin with, the gearbox of the powertrain model is separated into two complements: the gearshift control unit and the gearbox unit. The gearshift control unit is integrated into the model to provide a control of the selected engaged gear over time during the simulation. First, a signal builder block is placed to deliver data of selected gear during the simulation using a signal value, which should fit under a set list of values that are positive integers. These numbers correspond to the available gears at the gearbox. The signal builder block is connected to constant comparison blocks that switch the signal searching for the values that match the gearshifts with the actuators. Each comparison block connects to a go-to block, which later communicates the signal to the activation of the physical actuators at the gearbox unit.

The gearbox unit incorporates an actuator subsystem, that controls the required applied pressure to engage the disc friction clutch blocks that lock the selected gear. The power transmission is adjusted for torque and speed by connecting the disc friction clutch block to the corresponding simple gear block that modifies the follower to base teeth ratio. Each of the available gears requires a physical connection to the next step of the powertrain model: the chain drive and the differential. Before the physical connection to the chain drive, an inertia block and a rotational damper block are employed.

The inertia block represents rotational body resistance to changes in angular frequency and the rotational damper block models energy dissipation due to rotational friction. The chain drive enables power transmission in relation to sprocket A as an input and sprocket B as output. At the end of the powertrain model, the differential block is used to split the torque for the left and right rear wheels of the RWD racing car. However, the differential block may vary to an LSD differential block depending on the racing car to be modeled.

The scoped variables to be measured at the powertrain model are the selected gear over time and the output angular frequency of the gearbox. The powertrain model subsystem required parameters and units to be implemented at Simscape are listed in Table 6.2.

Table 6.2. Powertrain model subsystem simulation parameters.

Block	Parameter	Units	Description
Signal builder	Gearshift function	-	Selected engaged gear over time
Disc friction clutch	Friction coefficient	-	Clutch frictional resistance
	Number of friction surfaces	-	Contact faces for clutch friction
	Engagement piston area	mm^2	Surface area of hydraulic piston
Simple gear	Teeth ratio	-	Follower to base teeth ratio
	Effective torque radius	mm	Effective engage geometry
Chain drive	Sprocket pitch radius	mm	Radius of the input and output sprocket pitch circle
Differential	Teeth ratio	-	Follower to base teeth ratio

6.1.3. Vehicle model using Simscape

The vehicle model of the virtual prototype consists of three main blocks, which are the vehicle body, tire and disc brake blocks. The vehicle model including these blocks and physical interactions are shown in Figure 6.3. The vehicle body block counts with six ports: a mechanical translational conserving port, two normal force output ports, a velocity output port and two input ports for headwind speed and the road inclination angle respectively. The vehicle body block requires a physical connection to the tire blocks to modify the normal forces at front and rear axle tires. The parameters required to adjust the vehicle body are listed in Table 6.3. Those parameters include mass, technical dimensions, aerodynamic and pitch dynamics data. Pitch dynamics data can be activated into the vehicle body block and allows the modeling of suspension parameters related to stiffness and damping.

One of the most critical elements to be modeled are the tires. At Simscape, the magic formula tire block is the most suitable block to model a high-performance tire. The magic formula tire block is based on a semi-empirical model that describes the tire behavior in relation to the forces and moments acting on tires under various slip conditions, such as longitudinal, lateral and camber slip; as reported by Pacejka and Besselink [84]. Consequently, the required parameters to model the tires include four different magic formula coefficients, as described in Table 6.3. However, other parameters to be introduced into the tire model are rolling radius, rolling resistance coefficient, tire stiffness and tire inertia. The magic formula tire block has four ports: a mechanical rotational conserving port, a mechanical translational conserving port, input port for normal force acting on the tire and output port for the tire slip. Hence, the inputs to be communicated to the tire block are the normal forces due to vehicle body motion and the rotational motion that may be affected by acceleration or braking maneuvers at the simulation. Meanwhile, the output port for tire slip is closed for the simulation using a physical signal terminal.

The vehicle model is completed with disc brake block addition. The disc brake block requires an input of cylinder pressure, and the output is set at the mechanical rotational conserving port to be linked to the tire blocks at the model. For the racing car, the cylindrical pressure input is provided by a ramp block that acts as the brake pedal and is separated for front and rear axle tires in order to model the brake distribution. The corresponding parameters to adjust the disc brake block are listed in Table 6.3.

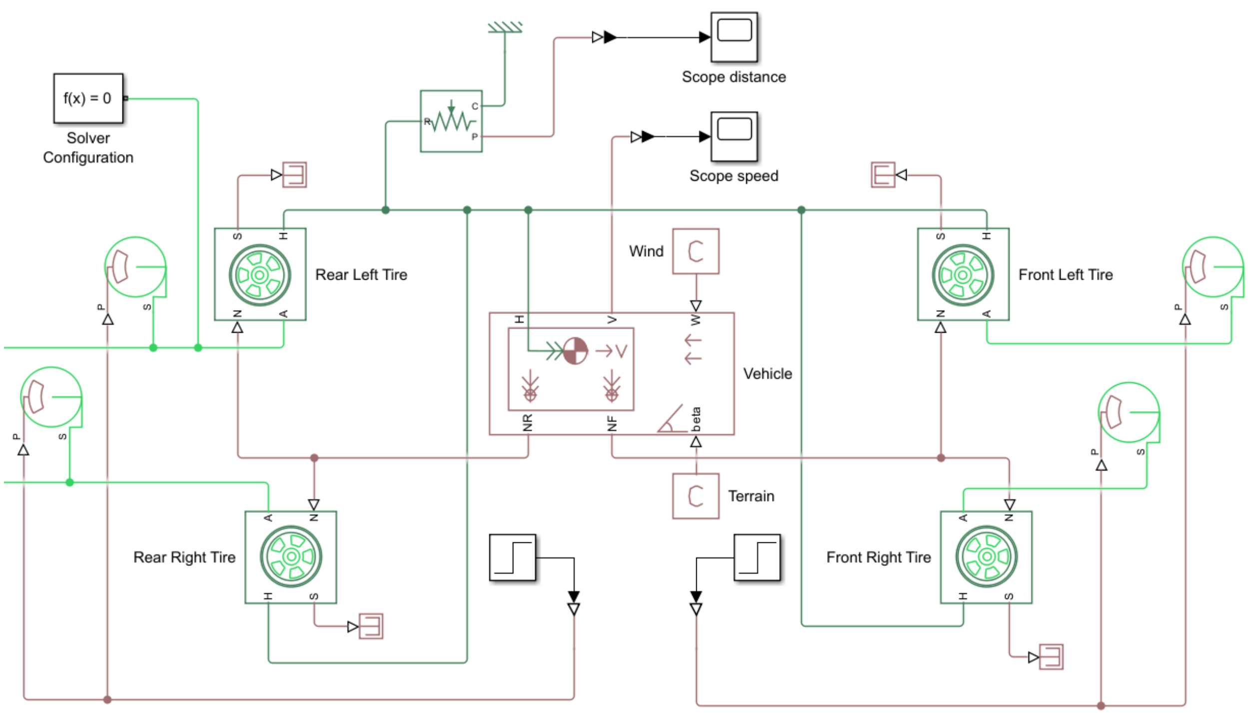

Figure 6.3. Vehicle model subsystem at Simscape.

As shown in Figure 6.3., the vehicle also includes the scope of the speed of the car by means of the vehicle body block and the displacement of the racing car using a translational motion sensor. To complete the virtual prototype of the racing car, a solver configuration block is connected to the model and the simulation is ready to be performed.

Table 6.3. Vehicle model subsystem simulation parameters.

Block	Parameter	Units	Description
Vehicle body block	Mass	kg	Vehicle total mass, including driver mass
	Horizontal distance from CG to front axle	mm	Distance computed for front axle in relation to the wheelbase
	Horizontal distance from CG to rear axle	mm	Distance computed for rear axle in relation to the wheelbase
	CG height	mm	Vertical distance the location for the center of gravity
	Frontal area	m^2	Projected frontal area of the vehicle in the direction of motion
	Drag coefficient	-	Fluid resistance quantification
	Pitch moment of inertia	kgm^2	Rotational acceleration resistance
	Front suspension stiffness	N/m	Frontal compression resistance under load
	Front suspension damping	Ns/m	Frontal motion resistance by dissipation of energy
	Rear suspension stiffness	N/m	Rear compression resistance under load
	Rear suspension damping	Ns/m	Rear motion resistance by dissipation of energy
Tire (Magical formula)	Magic formula coefficient B	-	Tire stiffness response to slip
	Magic formula coefficient C	-	Tire force versus slip overall shape
	Magic formula coefficient D	-	Peak value of tire force
	Magic formula coefficient E	-	Tire force curve sharpness
	Rolling radius	mm	Effective tire radius rolling under load
	Rolling resistance coefficient	-	Tire resistance to roll over a surface
	Tire stiffness	N/m	Tire deformation resistance
	Tire inertia	kgm^2	Rotational inertia of the tire
Disc brake	Mean pad radius	mm	Brake pad force application average radius
	Cylinder bore	mm	Diameter of piston cylinder within the disc brake caliper
	Pad friction coefficient	-	Static and Coulomb constant friction coefficient between brake pad and disc surface
	Cylinder pressure	bar	Hydraulic pressure inside cylinder

6.2. Vehicle virtual prototype simulation

With the virtual prototype of the racing car completed, the next step is to run the vehicle dynamics simulation using the Simscape environment. The parameters to be introduced into the virtual prototype are the same parameters used in Chapter two for the IVDS of the RC modeled vehicle. This decision is taken in order to be able to compare the simulation results obtained previously at Chapter two with the Simscape simulation results.

6.2.1. Simscape simulation results

The RC vehicle data is incorporated into the virtual prototype developed using the parameters listed in Table 6.1., 6.2. and 6.3. However, the main objective of the Simscape simulation is to perform a vehicle dynamics simulation based on the acceleration event, a test for participant vehicles at student competitions for Formula SAE and other spin-offs.

To simulate the acceleration event and obtain relevant data about the performance of the virtual prototype, the throttle input data for the generic engine block and the brake cylinder pressure input data for the front and rear axle disc brakes are all adjusted. In this case, the throttle pedal starts from a normalized value of zero and reaches a full-throttle condition after one second, similar to a driver response at the event. On the other hand, the brake pedal commands both the pressure for front and rear axle disc brakes, but the pedal is only applied after reaching the mark of the checkered line. Therefore, only the throttle response is modified on a first iteration; once the time to reach the 75 meters mark is known, it can be used for a second iteration with the time to apply the brake pedal input.

The results for the Simscape simulation are presented below. The vehicle speed plot for the acceleration test and the displacement of the vehicle plot for the acceleration plus braking test are presented in Figure 6.4. in relation to the elapsed time.

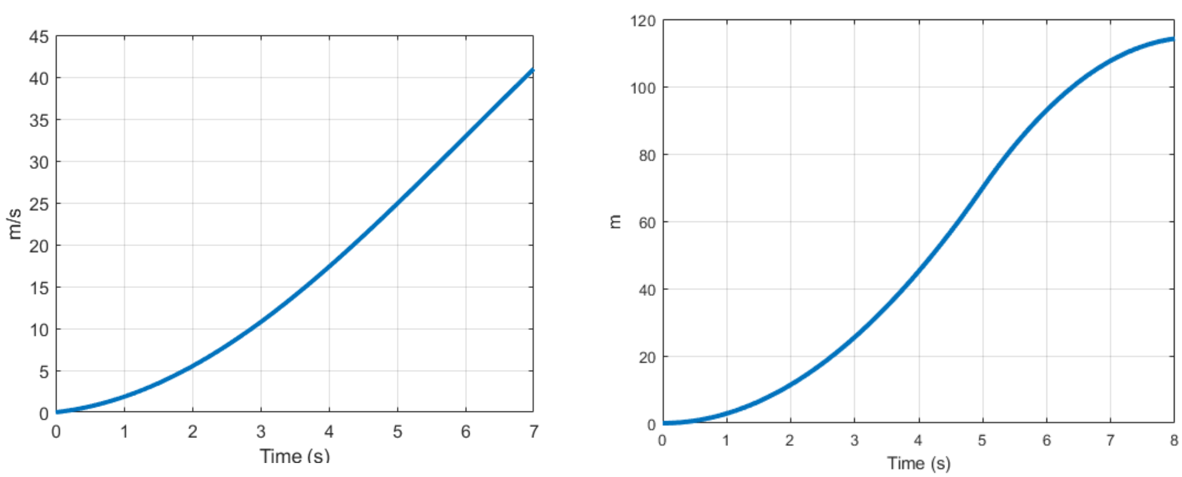

(a) (b)

Figure 6.4. Results of Simscape simulation for (a) acceleration test and (b) acceleration and braking test.

6.2.2. Benchmark and validation of simulation results

After completing the virtual prototype simulation, the results obtained are compared with the IVDS results and with the reported results of the RC vehicle at the student competition acceleration test. The acceleration event time is proposed as an important performance metric, as it reflects the cumulative effects of several vehicle dynamic effects, specifically for longitudinal dynamics of the car. The comparison of the acceleration event times for the IVDS, virtual prototype simulation and reported competition results is presented in Table 6.4.

Table 6.4. Acceleration event simulation results benchmark.

Metric	IVDS	Virtual prototype simulation
Simulated acceleration event lap time	5.06 s	5.19 s
Absolute error (s)	0.22 s	0.09 s
Relative error (%)	4.34%	1.73%
Accuracy (%)	95.65%	98.26%

Considering the computed accuracy of the acceleration event results for both conducted simulations shown in Table 6.4., the developed IVDS and the virtual prototype of the formula-style racing car are validated as reliable simulation tools that may be used to obtain relevant data regarding the performance of racing cars.

As a matter of fact, the longitudinal performance of the racing car is a standard and widely used benchmark for early-stage performance measurement or even for the overall performance of cars on track. Notwithstanding, there are some limitations of this scope. For example, the longitudinal dynamics only test the straight-line acceleration under ideal conditions and the launch conditions of the powertrain and other environment variables may affect the scoped result. However, the comparison of the results obtained with vehicle dynamics simulations at different design process stages gives a clue of how powerful and helpful an initial vehicle dynamics simulation can be for the complex design process of a high-performance car.

Conclusion

In this thesis, the conceptual development and the design of a formula-style racing car based on the rules, guidelines and constraints of the Formula SAE competition, has been presented. An early-stage vehicle dynamics simulation model was developed, validated and applied to the design process of the racing car. The findings demonstrate that the implemented methodology during the design process facilitated a streamlined design process and enhanced the efficiency and clarity of decision-making during the project.

Moreover, the outcomes of this study have led to the following conclusions:

- Vehicle dynamics analysis is proposed as a guideline through the design process when it is implemented at an early stage, as defined in the methodology employed in this thesis. The results of the analysis may serve as a basis for decision making during the following phases of the design process for the racing car.
- Developing a vehicle dynamics analysis for the design of the racing car is not only practical in the overall product development, but also quite indispensable for student competition cars and many other high-performance cars. The vehicle dynamics analysis provide certainty of the car to be designed.
- The conceptual development stage of the design process for the racing car is a crucial phase that defines the direction of the entire project. An ideal conceptualization of the racing car ensures that the vehicle will meet strategic objectives and stand out over other participants. In addition, conceptual development allows the alignment of aesthetics with practical requirements and to foresee potential design challenges.
- One of the most exhausting and complex stages of the design process of a racing car is undoubtedly the system-level phase. This is because the design moves from isolated concepts to an interconnected system that demands comprehensive integration and configuration of the subsystems of the car with concurrent engineering.
- Numerical simulations based on FEA and CFD are key at validating the configuration of isolated parts and even interaction between subsystems in the car. The results of the numerical simulations serve as a reference point to determine if the proposed configuration of the parts and subsystems are going to withstand the most critical operating conditions of the expected performance of the racing car or to determine opportunity areas for future work.
- Several simulation software focused on vehicle dynamics are available from different providers. Many of those pack software ages include diverse and versatile tools that allow robust and complex modeling and simulation of cars. Still, most of that software remain unreachable for many student teams, especially for novice teams willing to participate in the competition. However, simplified models of vehicle dynamics analysis may serve as the starting point for any team, and they can be implemented regardless of the experience in the competition.
- Even though the accuracy of the performed simulations is considerably higher than expected, it is important to use the results obtained with caution. Numerical simulations always have an implicit approximation error that directly impacts the accuracy, reliability,

and usefulness of the results. If these errors are ignored, the scoped parameters at simulations may deviate from the actual behavior, leading to wrong decision-making at any stage of the design process.

- The Ulrich and Eppinger product development methodology remains as a well-structured approach for design in either academic or industrial applications. However, it is clear that this methodology dismiss some iterative procedures over the design process and may require adaptations or additional steps in order to fit the needs of some specific applications, such as automotive design.

Contributions of the study

The main contributions of this thesis project are outlined below.

- A first-approach concept development was developed, and it is intended to be the basis for the launch of the student team of UASLP (Autonomous University of San Luis Potosi), a project that can be used as a platform for innovation and continuous improvement in the future.
- The design process documentation of the designed racing car was prepared during the execution of the project, and it was based on the requirements to be presented at the Formula SAE competition regarding static events.
- A modification to the product development methodology was proposed as a specific framework for automotive design applied to high-performance cars.
- Simulation models for early-stage vehicle dynamics analysis and virtual prototype were developed for different phases of the design process of the racing car. After a comparison of the computed results, the models provide high accuracy in relation to reported results of a vehicle designed for a formula-style racing car competition.

Future work

The prospective work for the project is detailed in the following.

- Expand the range of involved variables and scoped relevant data in the initial vehicle dynamics simulation, such as an extended list of parameters that model tire behavior, environmental factors that affect the performance of the racing car and data reporting the available torque calculation for the vehicle modeled.
- Document the information of the designed racing car with significant numerical simulations, including frontal and lateral crash test simulations, multibody suspension simulations or rendered driving simulations of the virtual prototype.
- Rearrange the configuration of the virtual prototype to be able to simulate constant radius cornering test protocol and be able to compare the data with the IVDS results for skidpad.
- Optimize the design of special purpose parts for desired goals, such as weight reduction or stiffness maximization.
- Optimize the performance of the racing car with data obtained from telemetry once the car is manufactured and tested.

References

[1] "2023 statistics | www.oica.net," www.oica.net. Accessed: Aug. 09, 2024. [Online]. Available: https://www.oica.net/category/production-statistics/2023-statistics/

[2] A. Mayyas, A. Qattawi, M. Omar, and D. Shan, "Design for sustainability in automotive industry: A comprehensive review," *Renew. Sustain. Energy Rev.*, vol. 16, no. 4, pp. 1845–1862, May 2012, doi: 10.1016/j.rser.2012.01.012.

[3] M. Gadola and D. Chindamo, "Experiential learning in engineering education: The role of student design competitions and a case study," *Int. J. Mech. Eng. Educ.*, vol. 47, no. 1, pp. 3–22, Jan. 2019, doi: 10.1177/0306419017749580.

[4] C. S. Abhinav and K. S. Prasad, "Role of Motorsports Club In Engineering Education," *J. Eng. Educ. Transform.*, vol. 36, no. S1, pp. 161–168, Dec. 2022, doi: 10.16920/jeet/2022/v36is1/22188.

[5] P. Hylton and D. J. Russomanno, "Motorsports Engineering: Bridging the Divide between Engineering and Engineering Technology with an Industry-Focused Curriculum," *J. Eng. Technol.*, 2014.

[6] K. T. Ulrich and S. D. Eppinger, *Product design and development*, Sixth edition. New York, NY: McGraw-Hill Education, 2016.

[7] "Formua SAE | www.sae.org," www.sae.org. Accessed: Aug. 15, 2024. [Online]. Available: https://www.sae.org/attend/student-events/formula-sae-michigan/awards-results

[8] "Formula SAE Rules." 2023.

[9] "Formua Student | imeche.org," imeche.org. Accessed: Aug. 18, 2024. [Online]. Available: https://osf.imeche.org/events/formula-student/previous-events

[10] T. Ayres, K. Hayward, and F. Guzzomi, "Design of a Custom FSAE Engine," *SAE- Veh. Technol. Eng. - J.*, vol. 3, no. 1, pp. 1–15, Sep. 2017, doi: 10.26474/vte-j.v3i1.2.

[11] J. P. Srivastava, G. G. Readdy, M. Moizuddin, K. S. Theja, and N. Sambasiva Rao, "Case Study on Different Go Kart Engine Transmission Systems," *IOP Conf. Ser. Mater. Sci. Eng.*, vol. 981, no. 4, p. 042026, Dec. 2020, doi: 10.1088/1757-899X/981/4/042026.

[12] D. Kennedy, G. Woods, and D. Forrest, "Development of a new Air Intake and Exhaust System for a Single Seat Race Car," *Proc. ITRN 2011*, 2011.

[13] E. Gupta, D. K. S. Bora, and R. A, "Design and analysis of brake system for FSAE race car," *Eng. Res. Express*, vol. 4, no. 2, p. 025039, Jun. 2022, doi: 10.1088/2631-8695/ac6ecd.

[14] J. W. Melvin and T. Gideon, "Biomechanical Principles of Racecar Seat Design for Side Impact Protection," presented at the Motorsports Engineering Conference & Exposition, Nov. 2004, pp. 2004-01–3515. doi: 10.4271/2004-01-3515.

[15] D. Kaya and E. Özyurt, "Design and optimization of impact attenuator for a Formula SAE racing car," *Sigma J. Eng. Nat. Sci. – Sigma Mühendis. Ve Fen Bilim. Derg.*, 2022, doi: 10.14744/sigma.2022.00041.

[16] R. Anbazhagan, B. Satheesh, and K. Gopalakrishnan, "Mathematical Modeling and Simulation of Modern Cars in the Role of Stability Analysis," *Indian J. Sci. Technol.*, vol. 6, no. 5, pp. 1–9, Dec. 2013, doi: 10.17485/ijst/2013/v6isp5.9.

[17] M. Balena, G. Mantriota, and G. Reina, "Dynamic Handling Characterization and Set-Up Optimization for a Formula SAE Race Car via Multi-Body Simulation," *Machines*, vol. 9, no. 6, p. 126, Jun. 2021, doi: 10.3390/machines9060126.

[18] E. F. Gaffney and A. R. Salinas, "lntroduction to Formula SAE Suspension and Frame Design," p. 13, 1997, doi: https://doi.org/10.4271/971584.

[19] M. Meywerk, *Vehicle Dynamics*. in Automotive series. John Wiley & Sons, 2015.
[20] R. W. Allen, H. T. Szostak, T. J. Rosenthal, D. H. Klyde, and K. J. Owens, “Characteristics Influencing Ground Vehicle LateralIDirectional Dynamic Stability,” *SAE Trans.*, pp. 336–361, 1991.
[21] P. Paramita Pattanaik and V. Balu, “Plus size tire: Effect on the performance of the vehicle,” *Mater. Today Proc.*, vol. 81, pp. 423–426, 2023, doi: 10.1016/j.matpr.2021.03.431.
[22] R. Rajamani, D. Piyabongkarn, J. Y. Lew, and J. A. Grogg, “Algorithms for Real-Time Estimation of Individual Wheel Tire-Road Friction Coefficients,” *IEEEASME Trans. Mechatron.*, vol. 17, no. 6, pp. 1183–1195.
[23] C. Smith, *Tune to Win: The art and science of race car development and tuning*. Aero Publishers, 1978.
[24] A. Deakin and D. Crolla, “Fundamental Parameter Design Issues Which Determine Race Car Performance,” presented at the Motorsports Engineering Conference & Exposition, Michigan, Nov. 2000. doi: 10.4271/2000-01-3537.
[25] S. Wordley and J. Saunders, “Aerodynamics for Formula SAE: Initial Design and Performance Prediction,” presented at the SAE 2006 World Congress & Exhibition, Apr. 2006, pp. 2006-01–0806. doi: 10.4271/2006-01-0806.
[26] C. West and D. Cao, “Defining Critical Speed in Driver-Vehicle Systems,” in *2013 IEEE International Conference on Systems, Man, and Cybernetics*, Manchester: IEEE, Oct. 2013, pp. 4155–4160. doi: 10.1109/SMC.2013.708.
[27] M. Ni, “Study on Mechanical Effect of the Vehicle at Corners,” presented at the 4th International Conference on Mechatronics, Materials, Chemistry and Computer Engineering, Atlantis press, 2015, pp. 614–617.
[28] Z. S. Filipi and D. N. Assanis, “The effect of the stroke-to-bore ratio on combustion, heat transfer and efficiency of a homogeneous charge spark ignition engine of given displacement,” *Int. J. Engine Res.*, vol. 1, no. 2, pp. 191–208, 2000, doi: 10.1243/1468087001545137.
[29] “Motorcycle News,” Motorcycle News. Accessed: Aug. 16, 2024. [Online]. Available: https://www.motorcyclenews.com/
[30] G. Wheatley and M. Zaeimi, “On the design of a wheel assembly for a race car,” *Results Eng.*, vol. 11, Sep. 2021, doi: 10.1016/j.rineng.2021.100244.
[31] N. D. Smith, “Understanding Parameters Influencing Tire Modeling,” 2004.
[32] E. M. Kasprzak and D. Gentz, “The Formula SAE Tire Test Consortium-Tire Testing and Data Handling,” presented at the Motorsports Engineering Conference & Exposition, Dec. 2006. doi: 10.4271/2006-01-3606.
[33] P. Marciano, G. Wheatley, and A. Ali, “Differential designing for FSAE motor sports vehicle JCU,” *Sci. J. Silesian Univ. Technol. Ser. Transp.*, 2022.
[34] A. Bhatt, “Kinematic Analysis of Formula SAE suspension”.
[35] C. H. Suh, “Synthesis and Analysis of Suspension Mechanisms with Use of Displacement Matrices,” presented at the Autotechnologies Conference and Exposition, Apr. 1989, p. 890098. doi: 10.4271/890098.
[36] P. A. Simionescu, “A unified approach to the kinematic synthesis of five-link, four-link, and double-wishbone suspension mechanisms with rack-and-pinion steering control,” *Proc. Inst. Mech. Eng. Part J. Automob. Eng.*, vol. 231, no. 10, pp. 1374–1387, Sep. 2017, doi: 10.1177/0954407016672775.
[37] Y. S. Saurabh *et al.*, “Design of Suspension System for Formula Student Race Car,” *Procedia Eng.*, vol. 144, pp. 1138–1149, 2016, doi: 10.1016/j.proeng.2016.05.081.

[38] V. S. Swamy, H. G. Karan Shivayogi, and N. Rajesh Mathivanan, “Selection of Optimal Tire and Design Optimisation of Steering System for a Formula Student Race Car through Tire Data Treatment,” *J. Phys. Conf. Ser.*, vol. 1478, no. 1, p. 012032, Apr. 2020, doi: 10.1088/1742-6596/1478/1/012032.

[39] M. Veneri and M. Massaro, “The effect of Ackermann steering on the performance of race cars,” *Veh. Syst. Dyn.*, vol. 59, no. 6, pp. 907–927, Jun. 2021, doi: 10.1080/00423114.2020.1730917.

[40] A. Bulsara, D. Lakhani, Y. Agarwal, and Y. Agiwal, “Design and Testing of an Adjustable Braking System for an FSAE vehicle,” *Int. J. Res. Eng. Technol.*, vol. 6, no. 10, pp. 25–29, Oct. 2017, doi: 10.15623/ijret.2017.0610005.

[41] M. Usama and G. Singhal, “Design and Analysis of Braking System for FSAE,” *Int. J. Sci. Res. Dev.*, vol. 6, no. 2, 2018, doi: 10.13140/RG.2.2.26149.65760.

[42] F. J. Sanchez-Alejo, M. A. Alvarez, N. F. Holgado, and J. M. Lopez, “Defining the ergonomic parameters of the driver’s seat in a competition single-seater,” *Int. J. Veh. Des.*, vol. 55, no. 2/3/4, p. 139, 2011, doi: 10.1504/IJVD.2011.040580.

[43] S. Mačužić, J. Lukić, J. Glišović, and D. Miloradović, “Pedal force determination respect to ride comfort,” *IOP Conf. Ser. Mater. Sci. Eng.*, vol. 252, p. 012010, Oct. 2017, doi: 10.1088/1757-899X/252/1/012010.

[44] S. B. Mishra and A. A. S. Khokar, “Design and Analysis of Bodyworks of a Formula Style Racecar,” *Int. J. Res. Eng. Technol.*, vol. 04, no. 10, pp. 141–148, Oct. 2015, doi: 10.15623/ijret.2015.0410025.

[45] R. G. Budynas and J. K. Nisbett, *Shigley’s mechanical engineering design*, 9. ed. in McGraw-Hill series in mechanical engineering. New York, NY: McGraw-Hill, 2011.

[46] M. Gadola, D. Chindamo, and B. Lenzo, “Revisiting the Mechanical Limited-Slip Differential for High-Performance and Race Car Applications,” vol. 29, no. 3, 2021.

[47] T. Saraçyakupoğlu, “Manufacturing and Maintenance Operations for Bladder-Type Aircraft Fuel Tanks,” in *Materials, Structures and Manufacturing for Aircraft*, M. C. Kuşhan, S. Gürgen, and M. A. Sofuoğlu, Eds., in Sustainable Aviation. , Cham: Springer International Publishing, 2022, pp. 181–210. doi: 10.1007/978-3-030-91873-6_8.

[48] A. Sethi, “Wet Sump Design for a FSAE Racing Car,” *Appl. Mech. Mater.*, vol. 165, pp. 175–181, Apr. 2012, doi: 10.4028/www.scientific.net/AMM.165.175.

[49] J. Segers, *Analysis Techniques for Racecar Data Acquisition - Second Edition*. Warrendale, PA: SAE International, 2014. doi: 10.4271/R-408.

[50] W. F. Milliken and D. L. Milliken, *Race car vehicle dynamics*. Warrendale, PA, U.S.A: SAE International, 1995.

[51] H. Wang, B. Wu, X. Cheng, and Y. Mao, “Analysis and Majorization of FSAE Racing Car Steering Trapezoid Based on Ackerman Principle,” *Acad. J. Eng. Technol. Sci.*, vol. 1, no. 1, 2018, doi: 10.25236/AJETS.920007.

[52] M. Drakulić, L. Stojnić, I. Blagojević, A. Đurić, and S. Perić, “Development of mathematical model for design of vehicle steering system,” *IOP Conf. Ser. Mater. Sci. Eng.*, vol. 1271, no. 1, p. 012009, Dec. 2022, doi: 10.1088/1757-899X/1271/1/012009.

[53] S. Hetawal, M. Gophane, B. K. Ajay, and Y. Mukkamala, “Aerodynamic Study of Formula SAE Car,” *Procedia Eng.*, vol. 97, pp. 1198–1207, 2014, doi: 10.1016/j.proeng.2014.12.398.

[54] F. Mariani, C. Poggiani, F. Risi, and L. Scappaticci, “Formula-SAE Racing Car: Experimental and Numerical Analysis of the External Aerodynamics,” *Energy Procedia*, vol. 81, pp. 1013–1029, Dec. 2015, doi: 10.1016/j.egypro.2015.12.111.

[55] J. Iljaž, L. Škerget, M. Štrakl, and J. Marn, "Optimization of SAE Formula Rear Wing," *Stroj. Vestn. - J. Mech. Eng.*, vol. 62, no. 5, pp. 263–272, May 2016, doi: 10.5545/sv-jme.2016.3240.
[56] H. Wang, Q. Bai, X. Hao, L. Hua, and Z. Meng, "Genetic algorithm-based optimization design method of the Formula SAE racing car's rear wing," *Proc. Inst. Mech. Eng. Part C J. Mech. Eng. Sci.*, vol. 232, no. 7, pp. 1255–1269, Apr. 2018, doi: 10.1177/0954406217700181.
[57] O. H. Ehirim, K. Knowles, and A. J. Saddington, "A Review of Ground-Effect Diffuser Aerodynamics," *J. Fluids Eng.*, vol. 141, no. 2, p. 020801, Feb. 2019, doi: 10.1115/1.4040501.
[58] X. Zhang, W. Toet, and J. Zerihan, "Ground Effect Aerodynamics of Race Cars," *Appl. Mech. Rev.*, vol. 59, no. 1, pp. 33–49, Jan. 2006, doi: 10.1115/1.2110263.
[59] M. A. Fentahun and D. M. A. Savaş, "Materials Used in Automotive Manufacture and Material Selection Using Ashby Charts," *Int. J. Mater. Eng.*, 2018.
[60] J. Mesicek, M. Richtar, J. Petru, M. Pagac, and K. Kutiova, "Complex View to Racing Car Upright Design and Manufacturing," *Manuf. Technol.*, vol. 18, no. 3, pp. 449–456, Jun. 2018, doi: 10.21062/ujep/120.2018/a/1213-2489/MT/18/3/449.
[61] B. A. Jawad and B. D. Polega, "Design of Formula SAE Suspension Components," presented at the Motorsports Engineering Conference & Exhibition, Dec. 2002, pp. 2002-01–3308. doi: 10.4271/2002-01-3308.
[62] L. Sun, Z. Deng, and Q. Zhang, "Design and Strength Analysis of FSAE Suspension," *Open Mech. Eng. J.*, vol. 8, no. 1, pp. 414–418, Dec. 2014, doi: 10.2174/1874155X01408010414.
[63] V. Sharma, S. Dhauni, and V. K. Chawla, "Design and manufacturing of air intake assembly for formula SAE vehicle," *Mater. Today Proc.*, vol. 43, pp. 58–64, 2021, doi: 10.1016/j.matpr.2020.11.209.
[64] S. Padmaraman, N. R. Mathivanan, and B. R. Ponangi, "Heat Dissipation Characteristics of a FSAE Racecar Radiator," *Int. J. Heat Technol.*, vol. 39, no. 5, pp. 1667–1672, Oct. 2021, doi: 10.18280/ijht.390531.
[65] N. Rajeev, "Natural Frequency, Ride Frequency and their Influence in Suspension System Design," *J. Eng. Res. Appl.*, vol. 9, no. 3, pp. 60–64, 2019, doi: 10.9790/9622- 0903036064.
[66] M. Azman, H. Rahnejat, P. D. King, and T. J. Gordon, "Influence of anti-dive and anti-squat geometry in combined vehicle bounce and pitch dynamics," *Proc. Inst. Mech. Eng. Part K J. Multi-Body Dyn.*, vol. 218, no. 4, pp. 231–242, Dec. 2004, doi: 10.1243/1464419043541464.
[67] P. Chauhan, K. Sah, and R. Kaushal, "Design, modeling and simulation of suspension geometry for formula student vehicles," *Mater. Today Proc.*, vol. 43, pp. 17–27, 2021, doi: 10.1016/j.matpr.2020.11.200.
[68] A. Price, "Electric Vehicle Steering System Optimization," p. 866, 2024.
[69] S. Allam, F. Nader, and K. Abdelwahed, "Vehicle Braking Distance Characterization using Different Brake Types," vol. 09, no. 03, 2022.
[70] W. B. Riley and A. R. George, "Design, Analysis and Testing of a Formula SAE Car Chassis," presented at the Motorsports Engineering Conference & Exhibition, Dec. 2002, pp. 2002-01–3300. doi: 10.4271/2002-01-3300.
[71] R. Desai, "Formula SAE Chassis System," *Int. J. Innov. Sci. Res. Technol.*, vol. 5, no. 5, 2020.
[72] P. M. Costa, "Modelling and structural analysis based on numerical simulation of a car chassis," Universidad de Aveiro, 2020. [Online]. Available: http://hdl.handle.net/10773/31450
[73] Z. Arifin, I. N. Yoga, and J. F. Zain, "Design and Torsional Rigidity Analysis on Frame of Formula Garuda 17 Based on Student Formula Japan 2017 Rules," *J. Phys. Conf. Ser.*, vol. 1700, no. 1, p. 012060, Dec. 2020, doi: 10.1088/1742-6596/1700/1/012060.

[74] M. E. Marques, G. Oliveira, and G. C. Silva, "Estudo de Ergonomia para Construção do Chassi de Um Protótipo de Fórmula SAE," in *Blucher Engineering Proceedings*, São Paulo: Editora Blucher, Mar. 2021, pp. 184–190. doi: 10.5151/simea2021-PAP44.

[75] M.-C. Chiu and G. E. Okudan, "Evolution of Design for X Tools Applicable to Design Stages: A Literature Review," in *Volume 6: 15th Design for Manufacturing and the Lifecycle Conference; 7th Symposium on International Design and Design Education*, Montreal, Quebec, Canada: ASMEDC, Jan. 2010, pp. 171–182. doi: 10.1115/DETC2010-29091.

[76] M. A. Hoque, M. S. Rahman, K. N. Rimi, A. R. Alif, and M. R. Haque, "Enhancing formula student car performance: Nose shape optimization via adjoint method," *Results Eng.*, vol. 20, p. 101636, Dec. 2023, doi: 10.1016/j.rineng.2023.101636.

[77] C. Craig and M. A. Passmore, "Methodology for the Design of an Aerodynamic Package for a Formula SAE Vehicle," *SAE Int. J. Passeng. Cars - Mech. Syst.*, vol. 7, no. 2, pp. 575–585, Apr. 2014, doi: 10.4271/2014-01-0596.

[78] V. Gowtham, A. S. Ranganathan, S. Satish, S. John Alexis, and S. Siva Kumar, "Fatigue based design and analysis of wheel hub for Student formula car by Simulation Approach," *IOP Conf. Ser. Mater. Sci. Eng.*, vol. 149, p. 012128, Sep. 2016, doi: 10.1088/1757-899X/149/1/012128.

[79] R. Kaushal, P. Chauhan, K. Sah, and V. K. Chawla, "Design and analysis of wheel assembly and anti-roll bar for formula SAE vehicle," *Mater. Today Proc.*, vol. 43, pp. 169–174, 2021, doi: 10.1016/j.matpr.2020.11.610.

[80] I. H. A. Razak, M. Y. M. Yusop, M. S. M. Yusop, and M. F. Hashim, "Modeling, Simulation and Optimization Analysis of Steering Knuckle Component for race car," *Int. J. Res. Eng. Technol.*, vol. 03, no. 11, pp. 221–225, Nov. 2014, doi: 10.15623/ijret.2014.0311037.

[81] L. I. Bortoluzzi, A. Schommer, M. Martins, and A. A. Buenos, "Formula SAE Chassis Design to Improve Suspension Tuning," presented at the 25th SAE BRASIL International Congress and Display, Oct. 2016, pp. 2016-36–0239. doi: 10.4271/2016-36-0239.

[82] A. Madhu and J. R. Aravind, "Software tool development for estimating forces acting on a formula student racing vehicle using simple vehicle dynamics models," *Transp. Eng.*, vol. 2, p. 100016, Dec. 2020, doi: 10.1016/j.treng.2020.100016.

[83] "Mathworks Simscape." 2025. [Online]. Available: https://www.mathworks.com/products/simscape.html

[84] H. B. Pacejka and I. J. M. Besselink, "Magic Formula Tyre Model with Transient Properties," *Veh. Syst. Dyn.*, vol. 27, no. sup001, pp. 234–249, Jan. 1997, doi: 10.1080/00423119708969658.

Appendix A

A1. Initial vehicle dynamics simulation model flowchart

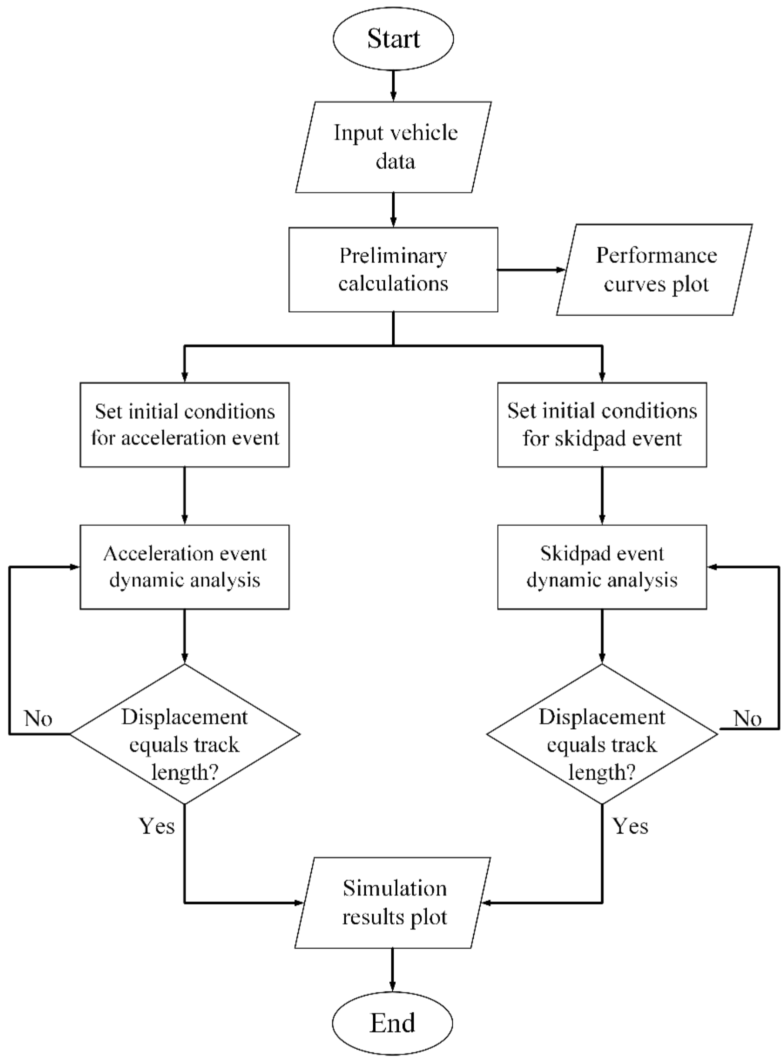

Appendix B

B1. Material properties of selected materials for special-purpose parts

Material	Density (g/cm^3)	Elastic modulus (GPa)	Poisson's ratio	Yield strength (MPa)	Ultimate tensile strength (MPa)	Brinell hardness	Fatigue strength (MPa)	Thermal conductivity (W/m-K)	Thermal expansion (μm/m-K)
AISI 1018 HR carbon steel	7.9	190	0.29	240	430	130	180	52	12
SAE-AISI 4140 alloy steel	7.8	190	0.29	590	690	210	360	43	13
A513 Structural steel	7.8	200	0.29	310	450	160	230	50	12
3000-series aluminum alloy	2.8	70	0.33	130	160	42	60	180	23
5000-series aluminum alloy	2.7	68	0.33	180	230	60	120	140	24
6000-series aluminum alloy	2.7	69	0.33	270	310	93	96	170	24
7000-series aluminum alloy	3.0	70	0.32	480	560	150	160	130	23
43300 cast aluminum alloy	2.5	71	0.33	230	290	94	76	140	22

Appendix C

C1. Chassis technical drawing

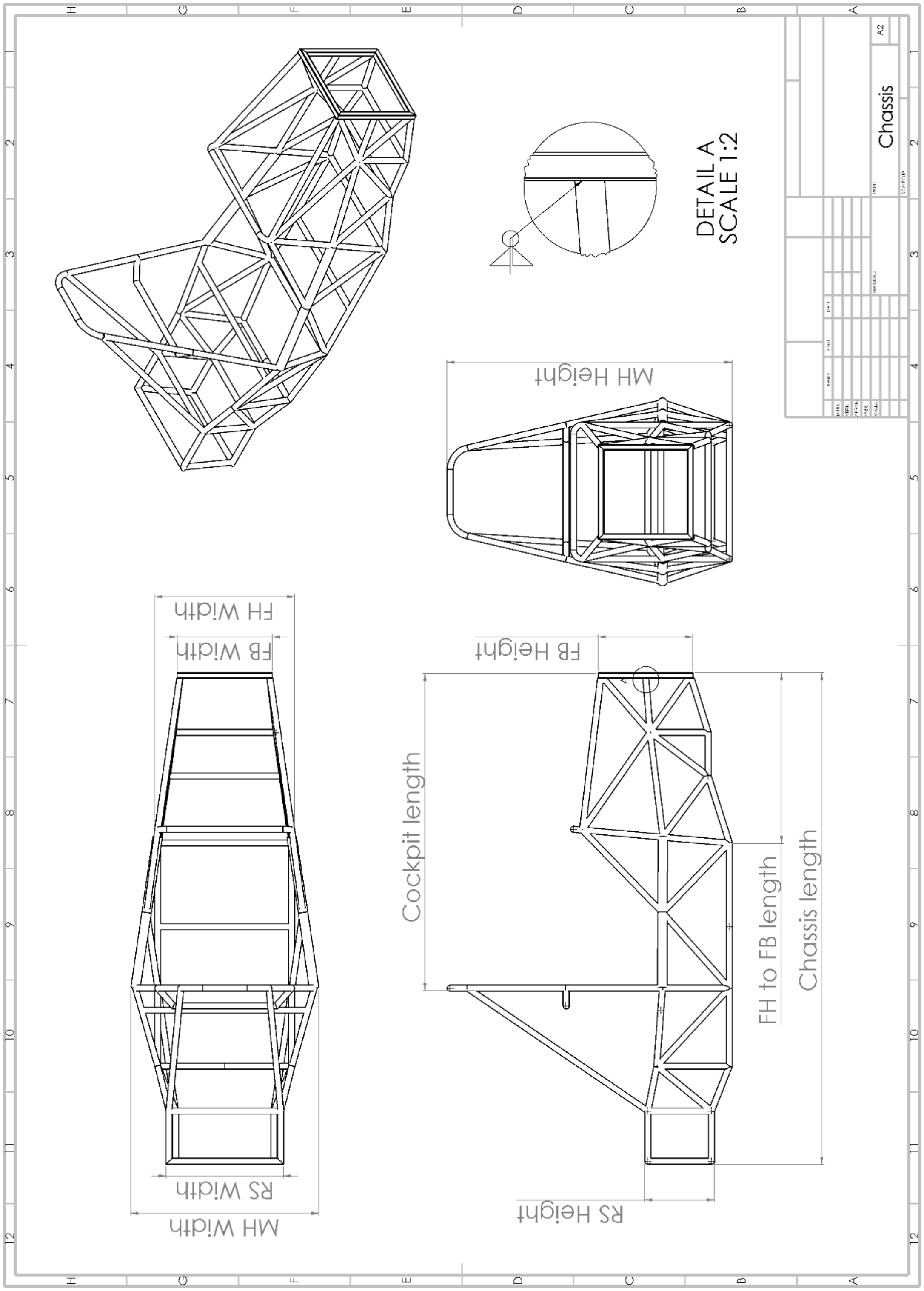

C2. Wheel hub technical drawing

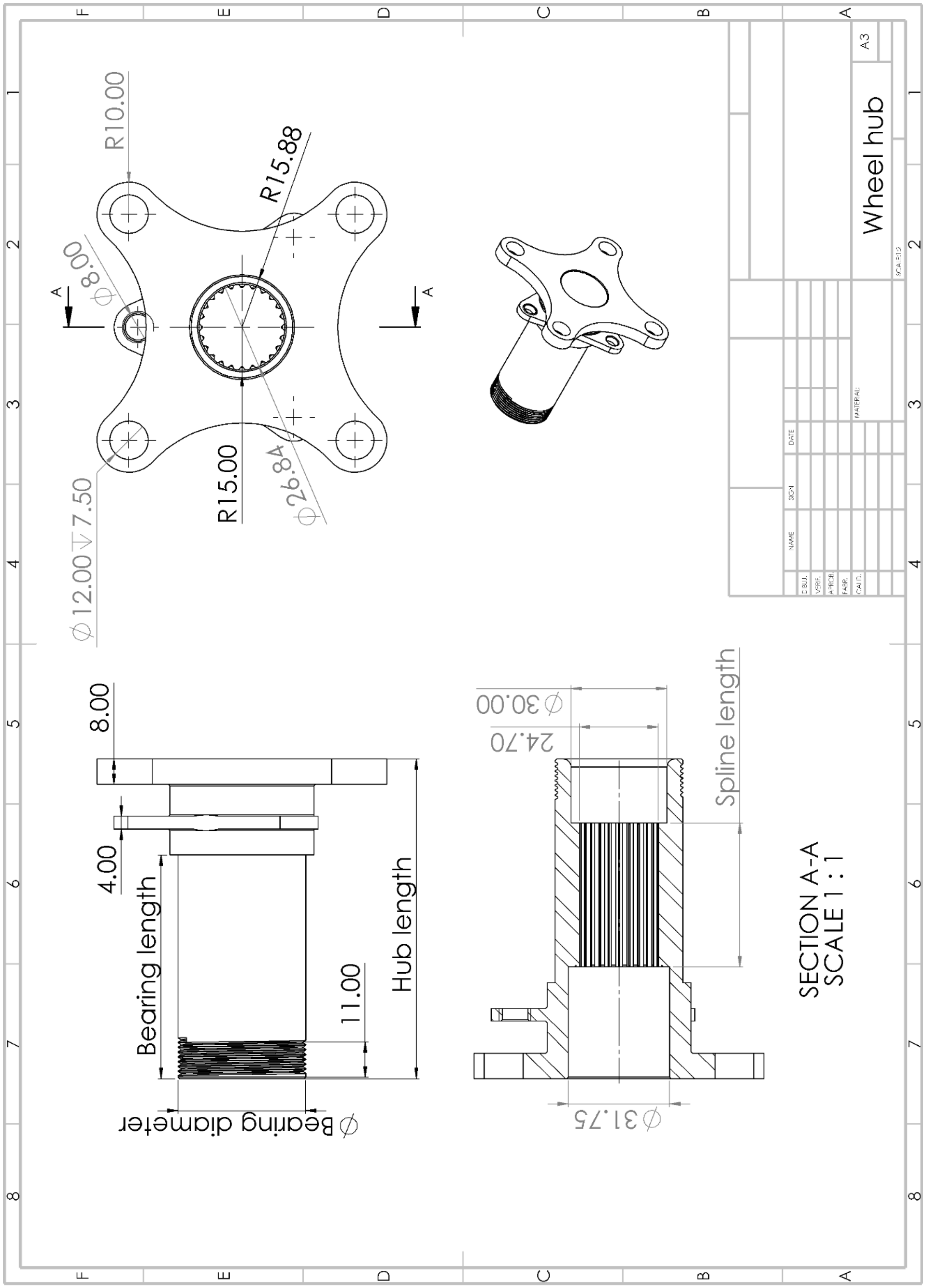

C3. Wheel knuckle technical drawing